

Mathematisch-Naturwissenschaftliche Fakultät  
Wegelerstr. 10  
53115 Bonn

**The Effect of S1P-lyase Deficiency on the Metabolism of  
the Alzheimer's related Amyloid Precursor Protein.**

Dissertation

Zur

Erlangung des Doktorgrades (Dr. rer. nat.)

der

Mathematisch-Naturwissenschaftlichen Fakultät

der

Rheinischen-Friedrich-Wilhelms-Universität Bonn

Vorgelegt von

**Ilker Karaca**

aus

**Viersen**

- Bonn, Juli 2014 -

Angefertigt mit Genehmigung der Mathematisch-Naturwissenschaftlichen  
Fakultät der Rheinischen Friedrich-Wilhelms-Universität Bonn.

**Gutachter**

1. Prof. Dr. rer. nat. Jochen Walter
2. Prof. Dr. rer. nat. Jörg Höfeld

Eingereicht am: 07.07.2014

**In der Dissertation eingebunden:**

Zusammenfassung/Abstract

Lebenslauf

An Eides statt versichere ich, dass ich die Dissertation "*The Effect of SIP-lyase Deficiency on the Metabolism of the Alzheimer's related Amyloid Precursor Protein.*" selbst und ohne jede unerlaubte Hilfe angefertigt habe und dass diese oder eine ähnliche Arbeit noch an keiner anderen Stelle als Dissertation eingereicht worden ist.

Auszüge aus dieser Arbeit wurden in „*The Journal of Biological Chemistry*, 2014 289: 16761 – 16772“ unter dem folgendem Titel publiziert:

„*Deficiency of Sphingosine-1-phosphate Lyase Impairs Lysosomal Metabolism of the Amyloid Precursor Protein*“

Die vorliegende Arbeit wurde in der Zeit von September 2010 bis März 2014 in der Klinik und Poliklinik für Neurologie, Molekulare Zellbiologie, Universitätsklinikum Bonn, Sigmund-Freud-Str. 25, Bonn unter Leitung von Prof. Dr. Jochen Walter durchgeführt.

Promotionsordnung vom 17. Juni 2011

---

Ilker Karaca

*Sizin için...*



# Contents

List of Figures.....	I
List of Tables.....	II
Abbreviations.....	III
Amino Acids.....	VI
Summary/Abstract.....	VII
<b>1. Introduction.....</b>	<b>1</b>
1.1. Alzheimer's disease and the neuropathological hallmarks.....	1
1.1.1. Genetics of AD.....	3
1.1.2. Metabolism of the Amyloid Precursor Protein.....	4
1.1.3. Physiological relevance of APP.....	12
1.2. Sphingolipids.....	13
1.2.1. Topology and metabolism of sphingolipids.....	15
1.2.2. S1P and metabolizing enzymes.....	17
1.2.3. Pathological effects of altered Sphingolipid metabolism.....	20
1.2.4. Sphingolipids in Alzheimer's disease.....	21
1.3. Rationale.....	25
<b>2. Material and Methods.....</b>	<b>26</b>
2.1. Cell biological techniques.....	27
2.1.1. Cell culture.....	27
2.1.2. Pharmacological treatment.....	28
2.1.3. Immunocytochemistry.....	29
2.1.4. Transient transfection.....	30
2.1.5. Viral transduction.....	30
2.1.6. RNAi transfection.....	31
2.1.7. Calcium measurement.....	31
2.2. Protein biochemical techniques.....	32
2.2.1. Protein extraction.....	32
2.2.2. Extraction of membrane proteins.....	32
2.2.3. Cell fractionation.....	33
2.2.4. Protein extraction from mouse brain.....	34
2.2.5. Immunoprecipitation.....	35
2.2.6. Protein estimation.....	36
2.2.7. Sodium dodecyl sulfate polyacrylamide gel electrophoresis (SDS-PAGE).....	36

2.2.8. Western immunoblotting. ....	38
2.2.9. Measurement of A $\beta$ . ....	40
2.3. Molecular biological techniques. ....	41
2.3.1. mRNA extraction and reverse transcription polymerase chain reaction (rt-PCR).....	41
2.3.2. Quantitative real time PCR (q-PCR).....	41
2.4. Secretase activity measurements. ....	42
2.4.1. $\beta$ - and $\gamma$ -secretase assay in living cells. ....	43
2.4.2. $\beta$ - and $\gamma$ -secretase assay in purified membranes.....	43
2.4.3. <i>In vitro</i> $\gamma$ -secretase assay. ....	44
2.5. Lipid analysis. ....	44
2.5.1. Lipid extraction and thin-layer-chromatography. ....	44
2.5.2. Mass spectrometry analysis. ....	45
2.6. Statistical analysis. ....	46
<b>3. Results .....</b>	<b>47</b>
3.1. Modulation of intracellular S1P concentration affect the metabolism of APP. ....	47
3.1.1. Accumulation of S1P in S1P-lyase deficient cells. ....	47
3.1.2. Genetic deletion of S1P-lyase results in increased levels of APP-FL and APP-CTFs.....	48
3.1.3. Pharmacological inhibition of sphingosine kinases decreases APP-FL and APP-CTFs.....	49
3.1.4. Overexpression of S1P-lyase increases APP-FL and APP-CTFs. ....	51
3.2. Modulation of S1P-receptor activity has no effect on APP. ....	52
3.3. S1P-lyase deficiency affects proteolytic processing of APP. ....	54
3.3.1. Lack of S1P-lyase modulates the generation of A $\beta$ in APP695 <sub>swe</sub> overexpressing cells. ....	54
3.3.2. Elevation of S1P concentration decreases the activity of $\gamma$ - and $\beta$ -secretase.....	55
3.3.2.1. Direct modulation of $\beta$ -secretase BACE1 through S1P.....	55
3.3.2.2. S1P impairs $\gamma$ -secretase activity.....	58
3.4. S1P-lyase deficiency impairs lysosomal function. ....	62
3.4.1. Accumulation of APP-CTFs in lysosomal compartments. ....	62
3.4.2. Increased stability in S1P-lyase deficient cells. ....	63
3.4.3. Deletion of the S1P-lyase impairs the maturation of cathepsin D. ....	64
3.4.4. Impaired autophagic turnover in S1P-lyase deficient cells. ....	66
3.5. Distribution of subcellular compartments is altered in S1PL-KO cells. ....	68
3.6. Alteration in lipid metabolism in S1P-lysase deficient cells. ....	70
3.7. Immediate elevation of intra.cellular Ca <sup>2+</sup> reduces APP-FL and APP-CTF levels. ....	72
3.8. Alteration in protein kinase C signaling in S1P-lyase deficient cells. ....	73
3.8.1. Lack of S1P-lyase affects the localization of activated PKC. ....	73
3.8.2. Inhibition of PKC causes its translocation into membrane fractions and increases APP.....	74

3.8.3. Sphingosine causes PKC translocation and increases APP levels.....	76
<b>4. Discussion.....</b>	<b>78</b>
4.1. The role of S1P metabolism in the proteolytic processing of APP. ....	78
4.2. Deficiency of the S1P-lyase impairs the lysosomal turnover. ....	82
4.3. Potential role of S1P-lyase in vesicular trafficking. ....	85
4.4. Role of PKC in the Processing of APP. ....	87
<b>5. Outlook. ....</b>	<b>92</b>
<b>6. References. ....</b>	<b>93</b>
<b>7. Acknowledgment. ....</b>	<b>117</b>
<b>8. Curriculum vitae. ....</b>	<b>118</b>



## List of Figures

- Fig. 1: A $\beta$  positive plaques and tau positive NFTs in human AD brains.
- Fig. 2: Proteolytic processing pathways of APP.
- Fig. 3:  $\gamma$ -secretase complex and A $\beta$  producing sequential cleavage lines.
- Fig. 4: Intracellular trafficking of APP and subcellular sites for processing.
- Fig. 5: Inter-conversion of the sphingoid bases ceramide, sphingosine and sphingosine-1-phosphate.
- Fig. 6: Topological biosynthesis of sphingolipids in the de novo and the recycling pathway. .
- Fig. 7: Similarities between trafficking and localization of APP and GSLs.
- Fig. 8: Effect of S1P-lyase knock-out on S1P concentration.
- Fig. 9: Genetic deletion of the S1P-lyase gene results in accumulation of APP-FL and APP-CTFs.
- Fig. 10: Pharmacological inhibition of sphingosine-kinases.
- Fig. 11: Reconstitution of S1P-lyase variants elevates the levels of APP-FL and APP-CTF.
- Fig. 12: Inhibition of S1PR1 and S1PR2 using potent antagonists.
- Fig. 13: Decreased secretion of A $\beta$  in S1P-lyase KO cells.
- Fig. 14: S1P reduces BACE1 activity.
- Fig. 15: Determination of the sAPP $\beta$ /sAPP $\alpha$  ratio using APP695<sub>swe</sub> -overexpressing cells.
- Fig. 16: Immunoprecipitation of APP-FL and APP-CTFs.
- Fig. 17: Presence of high S1P concentrations selectively affects the  $\gamma$ -secretase activity in living cells.
- Fig. 18: In vitro  $\gamma$ -secretase assay revealed a reduced generation of AICD in S1P-lyase deficient cells.
- Fig. 19: Sphingosine kinase inhibition reduces PS1-CTFs.
- Fig. 20: Accumulation of APP-CTFs in lysosomal compartments.
- Fig. 21: APP-FL is more stable in S1P-lyase deficient cells than in WT cells.
- Fig. 22: S1P-lyase affects the maturation of cathepsin D.
- Fig. 23: Accumulation of Lamp2 and Gm2a in S1P-lyase deficient cells.
- Fig. 24: Impaired turnover of radiolabeled proteins during shorter chasing times in S1P-lyase KO cells.
- Fig. 25: Impaired autophagic turnover in S1P-lyase deficient cells.
- Fig. 26: Co-staining of endoplasmic reticulum reveals increased reactivity for calnexin in S1P-lyase deficient cells.
- Fig. 27: Co-immunostaining of early and late golgi marker.
- Fig. 28: Co-immuno staining revealed strong differences in EEA1 and cathepsin D between WT and S1P-lyase deficient cells.
- Fig. 29: S1P-lyase deficient cells show several alterations in lipid homeostasis in comparison to WT.

- Fig. 300: Increase of intracellular  $\text{Ca}^{2+}$  affects the metabolism of APP-FL and APP-CTFs.
- Fig. 311: Selective release of lysosomal  $\text{Ca}^{2+}$  affects the APP metabolism.
- Fig. 32: Analysis of PKC localization in WT and S1PL-KO cells.
- Fig. 33: Analysis of PKC localization and APP metabolism in WT and S1P-lyase deficient cells upon PKC inhibition.
- Fig. 34: Time-dependent treatment of WT and S1P-lyase deficient cells with 10  $\mu\text{M}$  sphingosine causes APP-FL elevation.
- Fig. 35: Hypothetical scheme of the effects induced by S1P-lyase deficiency.

## List of Tables

- Table 1: Equipment and Material.
- Table 2: Cell lines.
- Table 3: List of pharmacological compounds.
- Table 4: Dilution scheme for the Optiprep (iodixanol) gradient.
- Table 5: Composition of the SDS gels for protein separation.
- Table 6: List of the primary antibodies used for western immunoblotting, immunocytochemistry and immunoprecipitation.
- Table 7: List of secondary antibodies used for western immunoblotting and immunocytochemistry.
- Table 8: List of primers used for rt-PCR and q-PCR.

## Abbreviations

<b>AB</b>	Antibody
<b>ACSF</b>	Artificial Cerebrospinal Fluid
<b>AD</b>	Alzheimer's Disease
<b>ADAM</b>	A Disintegrin And Metallo Proteinase
<b>AICD</b>	Amyloid Intracellular Domain
<b>Aph1</b>	anterior pharynx defective 1
<b>APLP 1/2</b>	APP like Protein 1/2
<b>ApoE</b>	Apolipoprotein E
<b>APP</b>	Amyloid Precursor Protein
<b>APP-FL</b>	Amyloid Precursor Protein - Full Length
<b>APP<sup>swe</sup></b>	APP - Swedish Variant
<b>APS</b>	Ammoniumpersulfate
<b>A<math>\beta</math></b>	Amyloid $\beta$
<b>BACE 1/2</b>	$\beta$ -site APP Cleaving Enzyme 1/2
<b>BIM I</b>	Bisindolylmaleimide I
<b>BSA</b>	Bovine Serum Albumin
<b>Cat.D</b>	Cathepsin D
<b>Cer</b>	Ceramide
<b>CERT</b>	Ceramide Transfer Protein
<b>Chx</b>	Cycloheximid
<b>COPI</b>	Coat Protein Complex I
<b>CTF</b>	C-Terminal Fragments
<b>DAG</b>	Diaglycerol
<b>DEAE</b>	Diethylaminoethylcellulose
<b>DHS</b>	Dihydrospingosine
<b>DMEM</b>	Dulbecco's Modified Eagle's Medium
<b>DMSO</b>	Dimethylsulfoxide
<b>DNA</b>	Desoxyribonucleic Acid
<b>DTT</b>	Dithiothreitol
<b>EBSS</b>	Earle's Balanced Salt Solution
<b>ECL</b>	Enhanced Chemiluminescence Solution
<b>EDTA</b>	Ethylendiaminetetraacetat
<b>EEA1</b>	Early Endosomal Adaptor Protein 1
<b>EOAD</b>	Early Onset Alzheimer's Disease

<b>ER</b>	Endoplasmic Reticulum
<b>ERK 1/2</b>	Extracellular Signal-Regulated Kinases 1/2
<b>FACS</b>	Fluorescence-Activated Cell Sorting
<b>FCS</b>	Fetal Calf Serum
<b>FTLD</b>	Fronto-Temporal Lobe Dementia
<b>FTY720</b>	Fingolimod
<b>GFP</b>	Green Fluorescent Protein
<b>GGA</b>	Golgi associated, $\gamma$ -adaptin ear containing, ARF binding protein
<b>GluCer</b>	Glucosyl-Ceramide
<b>GM2a</b>	GM2 activator Protein
<b>GPN</b>	Gly-Phe $\beta$ -naphthylamide
<b>GSK3<math>\beta</math></b>	Glycogen Synthase Kinase 3 $\beta$
<b>GSL</b>	Glycosphingolipids
<b>HEK</b>	Human Embryonic Kidney Cells
<b>Hex A/B</b>	Hexosaminidase A/B
<b>HRP</b>	Horseradish peroxidase
<b>ICC</b>	Immunocytochemistry
<b>IR</b>	Infrared
<b>IRES</b>	Internal Ribosomal Entry Site
<b>KO</b>	Knockout
<b>KPI</b>	Kunitz Protease Inhibitor Domain
<b>LC/MS/MS</b>	Liquid chromatography coupled to triple-quadruple mass spectrometry
<b>LOAD</b>	Late Onset Alzheimer's Disease
<b>LRP1</b>	Low density lipid protein receptor related protein
<b>LSD</b>	Lysosomal Lipid Storage Disorders
<b>MAM</b>	Mitochondria Associated Membranes
<b>MAPK</b>	Mitogen Activated Protein Kinase
<b>MEF</b>	Mouse Embryonic Fibroblasts
<b>mRNA</b>	messenger Ribonucleic Acid
<b>mTOR</b>	mammalian Target
<b>MTT</b>	4,5-dimethylthiazol-2-yl)-2,5-diphenyltetrazolium
<b>MW</b>	Molecular Weight
<b>N9</b>	Murine Microglial Cells
<b>NCT</b>	Nicastrin
<b>NFT</b>	Neurofibrillary Tangles

<b>NP A/B/C</b>	Niemann Pick A/B/C Disease
<b>NPC 1/2</b>	Niemann Pick C Cholesterol Transporter 1/2
<b>NRG-1</b>	Neuregulin 1
<b>NTF</b>	N-Terminal Fragment
<b>PBS</b>	Phosphate Buffered Saline
<b>PCR</b>	Polymerase Chain Reaction
<b>PEN2</b>	Presenilin Enhancer 2
<b>PFA</b>	Paraformaldehyde
<b>PHF</b>	Paired Helical Filaments
<b>PIP2</b>	Phosphatidylinositol 4,5-Bisphosphate
<b>PKA</b>	Protein Kinase A
<b>PKC</b>	Protein Kinase C
<b>PLC</b>	Phospholipase C
<b>PM</b>	Plasma Membrane
<b>PS 1/2</b>	Presenilin 1/2
<b>qPCR</b>	quantitative-real-time-Polymerase Chain Reaction
<b>RACK</b>	receptor for activated c-kinases
<b>RNAi</b>	RNA interference
<b>rt-PCR</b>	reverse-transcriptase-Polymerase Chain Reaction
<b>S1P</b>	Sphingosine-1-Phosphate
<b>S1PL</b>	S1P-lyase
<b>S1PR 1 - 5</b>	S1P Receptor 1 - 5
<b>sAPP</b>	soluble APP
<b>SDS</b>	Sodiumdodecylsulfate
<b>SDS-PAGE</b>	Sodiumdodecylsulfate Polyacrylamide Gel Electrophoresis
<b>siRNA</b>	small interfering Ribonucleic Acid
<b>SM</b>	Sphingomyelin
<b>Sph</b>	Sphingosine
<b>SphK 1/2</b>	Sphingosine Kinase 1/2
<b>SPP 1/2</b>	S1P-Phosphatase 1/2
<b>TBE</b>	TRIS-Borat-EDTA
<b>TEMED</b>	Tetramethylethylenediamine
<b>TGN</b>	Trans Golgi Network
<b>TM</b>	Transmembrane
<b>TNF<math>\alpha</math></b>	Tumor Necrosis Factor $\alpha$
<b>TREM2</b>	Triggering Receptor On Myeloid Cells 2

<b>TRPML 1 -3</b>	TRP-mucopolidosis type IV associated 1 - 3
<b>WB</b>	Westernblot
<b>WT</b>	Wild type

### **Amino Acids, Abbreviation and Single Letter Code**

<u><i>Aminno Acid</i></u>	<u><i>3-Letter code</i></u>	<u><i>1-Letter Code</i></u>
<b>Alanine</b>	Ala	A
<b>Arginine</b>	Arg	R
<b>Asparagine</b>	Asn	N
<b>Aspartic acid</b>	Asp	D
<b>Cysteine</b>	Cys	C
<b>Glutamic acid</b>	Glu	E
<b>Glutamine</b>	Gln	Q
<b>Glycine</b>	Gly	G
<b>Histidine</b>	His	H
<b>Isoleucine</b>	Ile	I
<b>Leucine</b>	Leu	L
<b>Lysine</b>	Lys	K
<b>Methionine</b>	Met	M
<b>Phenylalanine</b>	Phe	F
<b>Proline</b>	Pro	P
<b>Serine</b>	Ser	S
<b>Threonine</b>	Thr	T
<b>Tryptophan</b>	Trp	W
<b>Tyrosine</b>	Tyr	Y
<b>Valine</b>	Val	V

### *Summary/Abstract*

Alzheimer's disease is neuropathologically characterized by intracellularly accumulated tau protein and by extracellular plaques, mainly composed of the small hydrophobic peptide amyloid  $\beta$  ( $A\beta$ ). Sequential cleavage of the amyloid precursor protein (APP) by the transmembrane enzymes  $\beta$ - and  $\gamma$ -secretase generates  $A\beta$ . In addition to the proteolytic processing, APP can further undergo metabolic processing by acidic hydrolases in lysosomal compartments.

Membrane lipid composition is of great importance for the proper function of secretases, as well as for lysosomal activity. Disturbances in the lipid homeostasis can cause severe accumulations of different lipids and thereby also impair the metabolism of APP. Several lysosomal lipid storage disorders (LSDs) show pathological accumulation of lipids and share similarities to the pathological features of AD.

Here it is shown that accumulation of intracellular sphingosine-1-phosphate (S1P) impairs the metabolism of APP. Lack of the S1P cleaving enzyme S1P-lyase induces a LSD-like phenotype and causes an accumulation of full-length APP and its potentially pathogenic C-terminal fragments (CTFs) which was partially rescued by the inhibition of sphingosine phosphorylation. Genetic deletion of S1P-lyase impairs the  $\beta$ - and  $\gamma$ -secretase dependent processing of APP on one hand, but also decreased the lysosomal degradation of APP and its CTFs on the other hand. The increase of lysosomal marker proteins like cathepsin D or lamp2 indicated a general impairment of the lysosomal activity. Accumulation of APP and CTFs was also partially reversed when  $Ca^{2+}$  was selectively mobilized from endoplasmic reticulum or lysosomes. Additional results further indicate an involvement of protein kinase C in the altered lysosomal metabolism upon inhibition of S1P lyase.

Taken together, the data demonstrate that S1P-lyase plays a critical role in the regulation of lysosomal activity and the processing of APP. S1P and other sphingolipid metabolizing enzymes could therefore be further explored to dissect molecular pathways underlying the pathogenesis of AD and represent potential targets in disease progression or prevention.

## 1. Introduction

### 1.1 Alzheimer's disease and the neuropathological hallmarks.

When Alois Alzheimer presented his discoveries on “A peculiar disease of the brain cortex.” in 1906, the overall interest at the south-west-German conference for psychiatrists was very low (Maurer and Maurer, 2010). However, nearly 110 years later Alzheimer's disease (AD) has become the most common cause of dementia. AD is a progressive neurodegenerative disorder characterized by severe brain atrophy. Patients suffer from cognitive and functional impairments in their brain activity, and show a loss of memory and language skills (Arnaiz & Almkvist, 2003; Forstl & Kurz, 1999). Aging is a major risk factor for developing AD and with the continuous increase in life expectancy, the number of affected people will rise. Currently more than 24 million people are diagnosed with dementia, from which about 60% are affected by AD. According to predictions, the numbers will double every 20 year (Ferri et al, 2005). This makes AD the sixth most leading cause of death in the United States of America and represents a major liability on medical care ([www.alz.org/facts](http://www.alz.org/facts)).

AD is characterized by two distinct neuropathological hallmarks presented as intracellular neurofibrillary tangles (NFT) that contain hyper phosphorylated tau protein, and extracellular amyloid plaques mainly composed of the A $\beta$  peptide (*Fig. 1*) (Masters & Beyreuther, 1991; Selkoe, 2001a). The relationship of these two independent protein accumulations is poorly understood and under extensive investigation.

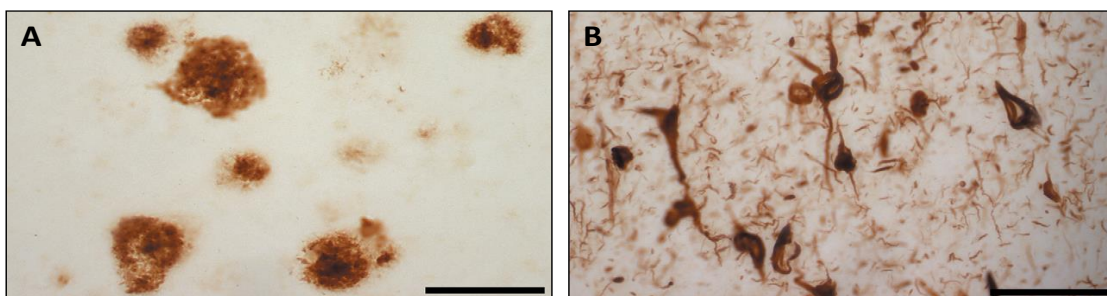


**Fig. 1: A $\beta$  positive plaques and tau positive NFTs in human AD brains.** (A) Immuno histochemical staining of plaques using an anti-A $\beta$ 42 specific antibody. Scale bar represents 125  $\mu$ m. (B) Immuno histochemical staining of neurofibrillary tangles using an anti-tau PHF-1 antibody. Scale bar represents 62.5  $\mu$ m. (LaFerla & Oddo, 2005).



Tau is a microtubule associated protein that stabilizes polymerized microtubules by binding to the  $\alpha$ - and  $\beta$ -tubulin subunits via its 3-repeat or 4-repeat binding domains. Hyper-phosphorylation of tau in these domains due to increased kinase activity or lowered phosphatase activity, leads to its detachment from the microtubule and the formation of so-called paired helical filaments (PHFs) with a diameter of ~20 nm (Goedert et al, 2006). Continuous formation of PHFs leads to the accumulation of NFTs within neurons. The decreased binding of tau results in destabilization of the microtubule network, causing an impaired retrograde transport in neuronal cells. As a result, tau accumulates and aggregates in somatodentric compartments (Grundke-Iqbal et al, 1986). The formation of PHFs and NFTs could induce retrograde degeneration of neurons and cell death. The tau hypothesis assumes that formation of NFTs initiates and promotes the pathogenesis of AD.

The second distinct neuropathological hallmark of AD brains are A $\beta$  plaques that show a heterogeneous appearance with a diameter of up to 20 - 50  $\mu$ m. Plaques are spherical extracellular multi-protein aggregates that are mainly composed of the peptides A $\beta$ 40 or A $\beta$ 42 and surrounded by abnormal neuronal processes. Plaques can be classified into diffuse and neuritic (senile) types. The involvement of diffuse plaques in early stages of AD is discussed controversially. They lack association with altered neurites and glial cells when compared to neuritic plaques (Joachim et al, 1989). Diffuse plaques are not necessarily indicative for AD patients, since they are also detected in cognitively normal individuals as well (Hardy & Selkoe, 2002). They are mainly composed of non-fibrillar A $\beta$  and can be found in most brain regions (Tagliavini et al, 1988; Yamaguchi et al, 1988). Neuritic or senile plaques, on the other hand occur in a brain region specific sequence and increasing number during disease progression (Thal et al, 2002). The cortex and the hippocampus are mainly affected by neuritic plaques. In later stages, neuritic plaques can also be found to a lesser extent in the brainstem and the molecular layer of the cerebellum (Thal et al, 2002). Neuritic plaques are more heterogeneous and dense than diffuse plaques, and consist of fibrillar and non-fibrillar A $\beta$  variants as well as degenerated neurites (Braak & Braak, 1996). Further components of neuritic plaques are complement factors, glucosaminoglycans, ApoE, cholesterol or cytoskeletal proteins (Liao et al, 2004).

The amyloid-hypothesis states that the accumulation of A $\beta$  triggers the pathological development of AD, including neuronal dysfunction and neuroinflammation. A $\beta$  induced damage of neuronal cells and alterations in phosphatase or kinase activities are suspected to induce hyper-phosphorylation of tau and the formation of NFTs (Hardy & Selkoe, 2002). Interestingly, mutations that are associated with early onset AD have been identified in three different genes directly involved in A $\beta$  generation, strongly supporting the amyloid hypothesis. In contrast no mutations in tau have been identified so far to cause AD. However, tau mutations are associated with other neurodegenerative diseases, including frontotemporal dementia (Goedert & Spillantini, 2000) or progressive supranuclear palsy (Stanford et al, 2000)suggesting an important role of tau in neurodegeneration.

### 1.1.1 Genetics of AD.

The majority of AD cases occur sporadically at a higher age (>65 years) without a known causative gene mutation. This form is known as late onset AD (LOAD). The genetic factors underlying the pathogenesis of LOAD are not fully understood. However, the apolipoprotein allele  $\epsilon$ 4 (ApoE4) was discovered as the major genetic risk factor for developing LOAD (Strittmatter et al, 1993). The chance to develop AD is increased by threefold in the presence of one ApoE4 allele and approximately by 12-fold when two alleles are present, as compared to individuals with no  $\epsilon$ 4 allele ([www.alzgene.org](http://www.alzgene.org)). While the exact molecular mechanism remains elusive, several studies indicated a decreased ability of ApoE4 for the clearance of A $\beta$  (Bu, 2009) or an impaired endocytosis of A $\beta$  by microglial cells (Carter, 2005). A recent study has furthermore identified TREM2 (triggering receptor expressed on myeloid cells 2) as an additional risk factor for the pathogenesis of AD (Guerreiro et al, 2013; Jonsson et al, 2013). Loss of a single TREM2 copy had no effects on the A $\beta$  deposition, but altered the morphology of plaque-associated microglial cells, which highlights its role in microglial response (Ulrich et al, 2014). In genome wide association studies a number of further genes like PICALM or CLU have been shown to be associated with the AD risk (Harold et al, 2009). However, all of these risk factors have much lower impact on the AD development compared to ApoE.

A minor percentage of all AD cases are linked to mutations in *PS1*, *PS2* and *APP*, and cause an early onset of AD (EOAD). A high number of different mutations in these genes were identified (>25 *APP*;

>10 PS2; >150 PS1) and shown to cause either a misbalance in the processing of APP or to promote the aggregation propensity of A $\beta$  (Cai et al, 1993; Citron et al, 1992; Goate et al, 1991). Commonly, these mutations lead to elevated generation of total A $\beta$  or a change in the relative ratio of A $\beta$ 40 to A $\beta$ 42, and thus, could promote plaque formation (Tanzi & Bertram, 2001). The so-called Swedish mutations of APP at position 670 and 671 (KM $\rightarrow$ NL) favors processing by the  $\beta$ -secretase and increases generation of A $\beta$ 40 and A $\beta$ 42 (Citron et al, 1992). Further mutations such as the Austrian (T714A), German (V715A) or Florida (I716V), lie within the trans-membrane domain and cause an increased production of the longer A $\beta$ 42 species that are more hydrophobic and more neurotoxic (Suzuki et al, 1994). All APP mutations identified so far, are mainly located close or within the A $\beta$  domain.

Mutations in the presenilin genes on the other hand occur in different regions of the encoded proteins, but are enriched in hydrophobic trans-membrane or membrane associated domains (Tanzi & Bertram, 2005). Most mutations in the *PS1* and *PS2* genes are missense mutations and affect their endo-proteolytic cleavage (see 1.1.2), the generation of different splice variants and also the overall enzymatic activity. A missense mutation in the splice acceptor site of exon 9 causes a deletion of this exon ( $\Delta$ exon9) and results in the loss of the endo proteolytic cleavage site of PS1 (De Strooper, 2007). A double transgenic mouse model expressing PS1  $\Delta$ exon9 and the human variant of APP<sup>swe</sup>, also known as APP/PS1, is a commonly used mouse model for AD. These mice show severe plaque load with increasing age, as well as cognitive and behavioral deficits (Dewachter et al, 2001).

Interestingly, even though more than 60 mutations for tau have been identified, none is associated with the pathogenesis of AD. Most of the tau mutations are mainly associated with fronto-temporal lobe dementia (FTLD). An interactive diagram with all mutations in APP, PS1, PS2 and tau can be found at <http://www.alzforum.org/mutations>.

### 1.1.2 Metabolism of the Amyloid Precursor Protein.

A $\beta$  peptides derive from the sequential cleavage of the amyloid precursor protein (APP). APP is a 100 – 140 kDa, ubiquitously expressed type I transmembrane protein. The molecular weight varies due to

differences in maturation states, alternative splicing and post-translational modifications. Alternative splicing of the 19 different exons generates three predominant length variants that show tissue specific distribution. APP695, also known as the neuronal APP, consists of exons 1 – 6 and 9 – 18, whereas APP751 (exon 1 – 7, 9 – 13) and APP770 (exons 1 – 18) are predominately expressed in peripheral tissues (Selkoe, 2001b). Heterogeneity in APP is further caused by co- and posttranslational modifications (Hung & Selkoe, 1994; Tomita et al, 1998; Walter et al, 1997a; Walter & Haass, 2000). First, immature full-length APP (APP-FL<sub>im</sub>) undergoes co-translational *N*-glycosylation in the endoplasmic reticulum and is then transported to *cis*-Golgi compartments. During transport in the Golgi, APP undergoes further maturation by *O*-glycosylation, sulfation and phosphorylation. Mature APP (APP-FL<sub>m</sub>) is then transported via secretory vesicles to the plasma membrane for proteolytic cleavage or re-internalization into endocytic vesicles (Weidemann et al, 1989). APP can undergo sequential cleavage mediated by three distinct intramembranous proteases, called  $\alpha$ -,  $\beta$ - and  $\gamma$ -secretases. Processing of APP can take place in two principal cleavage pathways: the non-amyloidogenic and the amyloidogenic pathway (Fig. 2).

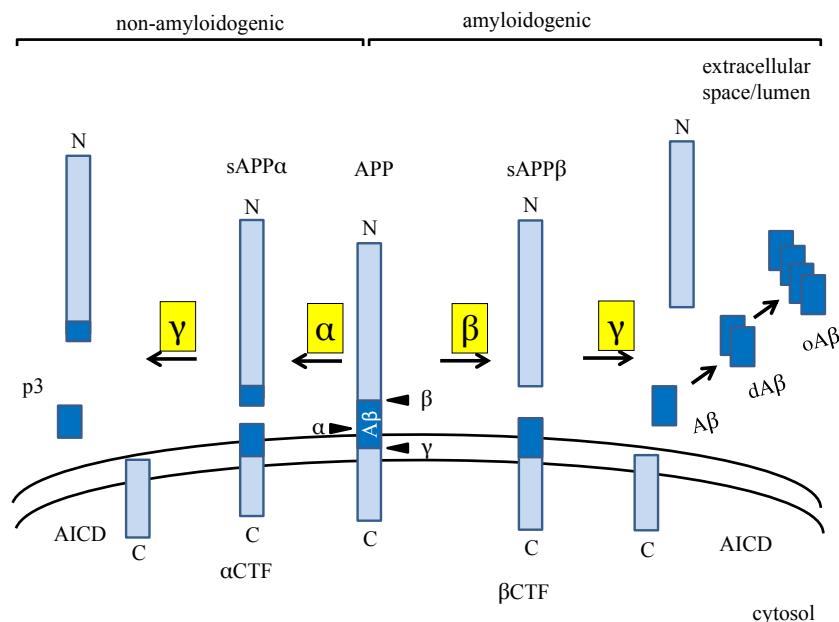


**Fig. 2: Proteolytic processing pathways of APP.** Initial cleavage of APP by  $\alpha$ -secretase in the non-amyloidogenic pathway precludes the generation of A $\beta$ , but liberates sAPP $\alpha$  into extracellular fluids. Membrane associated  $\alpha$ CTFs are further processed by the  $\gamma$ -secretase complex producing the amyloid-intracellular domain (AICD) and p3. Alzheimer's associated A $\beta$  variants are generated in the amyloidogenic pathway by  $\beta$ -secretase (BACE1) cleavage. Initial  $\beta$ -secretase cleavage leads to secretion of sAPP $\beta$  into the extracellular milieu.  $\beta$ CTFs are then further processed by the  $\gamma$ -secretase complex, resulting in the generation of A $\beta$  and the AICD. Secreted A $\beta$  can undergo dimerization (dA $\beta$ ) or moreover oligomerization (oA $\beta$ ), which might result in the formation of amyloid plaques.

### *$\alpha$ -Secretase*

The predominant cleavage of APP is initiated by the  $\alpha$ -secretase in the non-amyloidogenic pathway between Lys16 and Leu17 within the A $\beta$  domain.  $\alpha$ -secretase cleavage precludes the generation of A $\beta$  and results in the secretion of soluble APP $\alpha$  (sAPP $\alpha$ ) and the generation of the membrane-tethered C-terminal fragment ( $\alpha$ CTF) (Esch et al, 1990; Sisodia et al, 1990; Wang et al, 1991) (*Fig. 2*). This cleavage occurs predominantly at the cell surface and suggests a plasma-membrane localization of the  $\alpha$ -secretases (Sisodia, 1992b). Studies identified at least four enzymes to have  $\alpha$ -secretase cleavage properties that belong to the family of “**a disintegrin and metallo proteinases**”: ADAM9, ADAM10, ADAM17 and ADAM19 (Allinson et al, 2003). All ADAM-proteins are type I transmembrane proteins and require zinc as a co-factor for their activity (Sisodia, 1992a). The predominant form in neuronal cells was recently discovered to be ADAM10 (Kuhn et al, 2010).  $\alpha$ -Secretase activity can be regulated by protein kinase C (PKC). Phorbol esters stimulate PKC activity and increase the  $\alpha$ -secretory cleavage of APP resulting in both, elevated secretion of sAPP $\alpha$  (Buxbaum et al, 1990) and decreased generation of A $\beta$  (Hung et al, 1993). However, ADAM proteins not only cleave APP, but also several other proteins like Notch receptors, tumor necrosis factor  $\alpha$  (TNF $\alpha$ ), cadherins and IL-6 (Seals & Courtneidge, 2003). This highlights the physiologic relevance of ADAM-proteases also documented by the *in utero* lethality of ADAM10 or ADAM17 knockout mice (Hartmann et al, 2002; Peschon et al, 1998).

### *$\beta$ -Secretase*

$\beta$ -secretase or BACE1 ( $\beta$ -site APP cleaving enzyme) (Sinha et al, 1999; Vassar et al, 1999; Yan et al, 1999) initiates the generation A $\beta$  and is the rate limiting enzyme in the amyloidogenic pathway. Cleavage of APP by BACE1 leads to secretion of sAPP $\beta$  and the generation of  $\beta$ CTF containing the A $\beta$  domain (*Fig. 2*). BACE1 is a type I transmembrane aspartyl protease, consisting of a cytosolic c-terminus, a transmembrane domain and a luminal/extracellular domain (Hussain et al, 1999; Vassar et al, 1999). The latter contains the proteolytically active site and shows similarities to other members of the pepsin family (Hong et al, 2004). Two distinct DTGS and DSGT motifs form the catalytic center

of BACE-1. Mutations of either motif lead to complete loss of enzymatic activity (Hussain et al, 1999; Vassar et al, 1999). Two distinct cleavage sites for BACE1, Asp1 and Glu11 have been identified in APP. In human, the predominant BACE1 cleavage takes place at Glu11 of the A $\beta$  domain and precludes the generation of A $\beta$  (Liu et al, 2002). A recent study claimed, that Glu11 cleavage by BACE1 is favored, but shifting its activity towards Asp1, may be the pathologically more relevant process (Deng et al, 2013). An enzyme with 55% homology to BACE1 was identified and termed BACE2. However, BACE2 cleaves APP within the A $\beta$  domain between Phe19 and Phe20 and thus, likely does not contribute to amyloid generation (Farzan et al, 2000; Fluhner et al, 2002).

BACE1 is ubiquitously expressed, but with the highest expression in pancreatic and neuronal cells (Ehehalt et al, 2002). The high expression rate of BACE1 and APP in neuronal cells, explains why neurons mainly contribute to the generation of A $\beta$ . BACE1 as well as BACE2, contain a pro-peptide at their n-terminal domains, which undergoes furin mediated cleavage in the Golgi compartment. Block of the forward transport with brefeldin A or monensin reduces the propeptide cleavage (Bennett et al, 2000). *N*-glycosylation at Asp residues in the ectodomain takes place in the ER, while the restructuring and trimming of the glycol-moieties occurs in Golgi compartments, from where BACE1 is routed to the plasma membrane (Capell et al, 2000). Trafficking of BACE1 is regulated by its phosphorylation at Ser468. While phosphorylation facilitates retrograde transport of BACE1 to juxta nuclear Golgi compartments, non-phosphorylated BACE1 accumulates in peripheral early endosome antigen 1 (EEA1) positive vesicles (Walter et al, 2001). Phosphorylation of BACE1 regulates the interaction with adapter proteins of the Golgi associated,  $\gamma$ -adaptin ear containing, ARF binding protein (GGA) family that mediate sorting between endosomal/lysosomal compartments and the *trans*-Golgi Network (TGN) (Tesco et al, 2007; von Arnim et al, 2006; Wahle et al, 2005; Wahle et al, 2006). Most BACE1 protein can be found in these particular compartments. Especially its pH optimum of 4.5 – 5 indicates a pronounced activity of the enzyme in endosomal and lysosomal compartments (Vassar & Citron, 2000). BACE1 was also shown to undergo degradation in acidic organelles (Koh et al, 2005).

Generation of BACE1 knockout mice helped to identify the physiologic role of BACE1. Initial findings indicated no deficits in viability or fertility (Cai et al, 2001; Luo et al, 2003; Roberds et al,

2001). However, later studies with BACE1 KO mice showed subtle effects on behavior with impaired memory function or spontaneous hyperactivity (Dominguez et al, 2005; Harrison et al, 2003). Moreover, severely reduced myelination of neurons was present as well, probably caused by a precluded cleavage of neuregulin-1 (NRG1), a mediator for Schwann-cell myelination (Willem et al, 2006). Further substrates of BACE1 are voltage-dependent sodium channels (Kim et al, 2007), the type II  $\alpha$ -2,6-sialyltransferase (Kitazume et al, 2003), the platelet selectin glycoprotein ligand-1, (Lichtenthaler et al, 2003), LRP1 (von Arnim et al, 2005), APLP1/2 (Li & Sudhof, 2004) and the interleukin receptor II (Kuhn et al, 2007).

#### *$\gamma$ -secretase*

Intramembranous cleavage of both APP CTF variants,  $\alpha$ CTFs and  $\beta$ CTFs, is mediated by the  $\gamma$ -secretase. Cleavage of  $\alpha$ CTFs by the  $\gamma$ -secretase, results in the generation of the APP intracellular domain (AICD) and the secretion of the small peptide p3 (*Fig. 2*) (Haass et al, 1993). However,  $\gamma$ -secretase dependent cleavage of the  $\beta$ CTFs induces the generation of the AICD and 37 – 49 amino acid long A $\beta$  peptide variants (*Fig. 2*). The predominant variant is A $\beta$ 40 and to a lesser extent A $\beta$ 42 (Citron et al, 1996; Wiltfang et al, 2002). A $\beta$ 42 is more hydrophobic and has increased propensity to aggregate as compared to A $\beta$ 40. The additional  $\gamma$ -secretase product AICD on the other hand is released into the cytosol and may have a role in nuclear signaling (Cao & Sudhof, 2001; von Rotz et al, 2004). A series of other proteins like ErbB4 (Lee et al, 2002), Notch (Kimberly et al, 2003), CD43 (Andersson et al, 2005), ephrin B1 (Tomita et al, 2006), LRP1 (Lleo et al, 2005) and TREM2 (Wunderlich et al, 2013) also undergo cleavage by  $\gamma$ -secretase. In general,  $\gamma$ -secretase has little substrate specificity. Because  $\gamma$ -secretase requires short ectodomains and single transmembrane CTFs of the respective protein substrates, the cleavage of the different  $\gamma$ -secretase substrates is mainly regulated by ectodomain shedding of type I membrane proteins (Hemming et al, 2008)

$\gamma$ -Secretase is a multimeric multi-transmembrane enzyme-complex composed of presenilin 1 or presenilin 2 (PS1/PS2), nicastrin (NCT), anterior pharynx defective 1 (Aph1) and the presenilin enhancer 2 (PEN2) (Francis et al, 2002; Yu et al, 2000). A minimal stoichiometric ratio of 1:1:1:1 of

the components is necessary for its activity. The essential  $\gamma$ -secretase component NCT is required for substrate selection and transport of the  $\gamma$ -secretase complex in the secretory pathway (Dries et al, 2009; Shah et al, 2005; Yu et al, 2000). PEN2 facilitates the endo proteolytic cleavage of the presenilins and confers their stability (Hasegawa et al, 2004; Hu & Fortini, 2003; Prokop et al, 2004). The role of Aph1 is still elusive, but it is suspected to act as a scaffolding protein in the complex (LaVoie et al, 2003). Interestingly, the molecular weight of the whole  $\gamma$ -secretase complex is higher than the additive and predicted size of the single components, suggesting an involvement of more associated proteins or protein complexes. Some additional proteins like TMP21 (Chen et al, 2006), CD147 (Zhou et al, 2005) or the  $\gamma$ -secretase activating protein GSAP (He et al, 2010a) were recently identified. However, it could be demonstrated that these proteins are not essential for the  $\gamma$ -secretase activity (Winkler et al, 2009). The proteolytic activity of the  $\gamma$ -secretase is carried out by PS1 or PS2. The major presenilin involved in the APP cleavage is PS1, although PS2 has the ability to cleave APP as well (De Strooper et al, 1998; Wolfe et al, 1999). PS1 and PS2 have 9 transmembrane domains. The 50 kDa full-length forms of these proteins undergo autocatalytic cleavage to form 30 kDa N-terminal fragment (NTF) and a 20 kDa CTF (Thinakaran et al, 1996; Walter et al, 1997b). Both CTF and NTF form a heterodimer with one Asp residue in each fragment (*Fig. 3A*). These neighboring Asp residues in the sixth and seventh transmembrane domains form the catalytic center of the  $\gamma$ -secretase complex (Wolfe et al, 1999). Knock out of PS1 in mice, causes embryonic lethality, due to impaired processing of Notch (Herreman et al, 1999; Shen et al, 1997). The knock-out of PS2 does not lead to overt phenotypes. However, the double KO of PS1 and PS2 causes a more severe phenotype and earlier embryonic lethality as compared to the PS1 single KO, indicating a physiological relevance of PS2 (De Strooper et al, 1998).



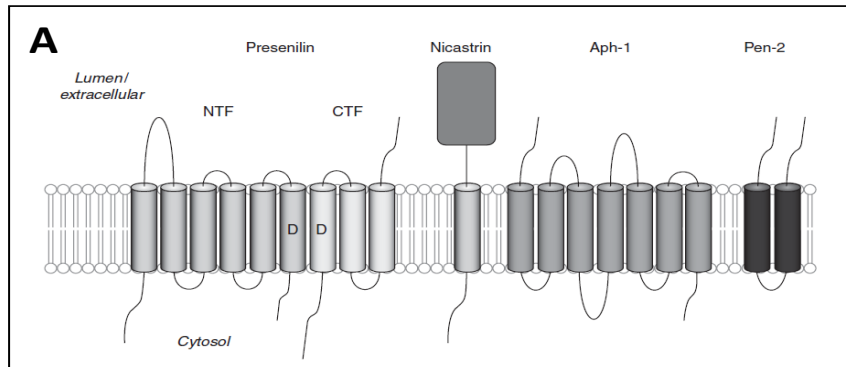


**Fig. 3:**  $\gamma$ -secretase complex and  $A\beta$  producing sequential cleavage lines. (A) The  $\gamma$ -secretase complex with subunits and membrane topology. Full length presenilin is autocatalytically cleaved into a CTF and NTF. Aspartyl residues are indicated by D. Further  $\gamma$ -secretase complex subunits nicastrin, Aph-1 and Pen-2 have supporting properties and are necessary for catalytic activity of the presenilin (De Strooper et al, 2012).

#### *Subcellular trafficking of APP and its metabolizing enzymes.*

As mentioned before, maturation of APP involves *N*- and *O*-glycosylation, as well as phosphorylation, during its transport from the ER to the Golgi compartments and forth the plasma membrane in the secretory pathway. Mature full length APP is either rapidly processed in the secretory pathways or at the plasma membrane by the  $\alpha$ -secretases or internalized into endocytic vesicles. Following the endocytosis, APP is either transported back to the plasma membrane, or delivered into endosomal or lysosomal compartments for degradation (Fig. 4). The initial internalization from the plasma membrane was shown to be dependent on a YENPTY motif at the c-terminus (Lai et al, 1995; Marquez-Sterling et al, 1997). Mutations in this motif selectively inhibited the internalization and prevented the binding of adaptor proteins like Fe65 (Borg et al, 1996; Perez et al, 1999). Fe65 binding also facilitates BACE1 and  $\gamma$ -secretase mediated processing of APP. The phosphorylation at Thr688 residue of APP introduces a conformational change and precludes interaction with Fe65 (Ando et al, 2001; Chang et al, 2006).

In neurons, APP undergoes polarized trafficking. Various proteins and lipids are involved in this regulation. After leaving the ER, APP is first transported to Golgi compartments. Interestingly, in a model for polarized cells (Madin-Darby canine kidney cells: MDCK), a substantial pool of APP can undergo cleavage already in these compartments as it was shown (Haass et al, 1995). However, non-

processed APP is then transported in post-Golgi cargo vesicles to the axonal and dendritic endings (Kins et al, 2006).

As already mentioned, APP undergoes predominant  $\alpha$ -secretase cleavage at the plasma membrane. Palmitoylation of APP leads to enrichment in lipid rafts, where immediate interaction with BACE1 takes place (Bhattacharyya et al, 2013). Palmitoylation also targets BACE1 to lipid rafts and therefore facilitates  $\beta$ -cleavage of APP in these membrane microdomains (Cordy et al, 2003; Riddell et al, 2001).

After re-internalization of BACE1 from the plasma membrane, the protein is transported to endosomal or lysosomal compartments (Pastorino et al, 2002). These acidic compartments provide a pH favorable for BACE1 activity. Interestingly, lower levels of fully assembled and active  $\gamma$ -secretase complex can be found in acidic vesicles as well (Dries & Yu, 2008; Kaether et al, 2006). The membrane lipid composition and the pH of these vesicles may be physiologically relevant for initial  $\gamma$ -secretase cleavage site (Fukumori et al, 2006). APP and its CTFs have been shown to undergo lysosomal degradation by acidic hydrolases (Haass et al, 1992a; Tamboli et al, 2011b; van Echten-Deckert & Walter, 2012a). Upon inhibition of lysosomal degradation, levels of APP  $\beta$ CTFs increase significantly thereby providing more substrates for the  $\gamma$ -secretase which results in increased generation of A $\beta$  (Tamboli et al, 2011b).

In general, endosomal and lysosomal vesicles seem to play a critical role in the metabolism of APP and likely for the pathogenesis of AD as well.

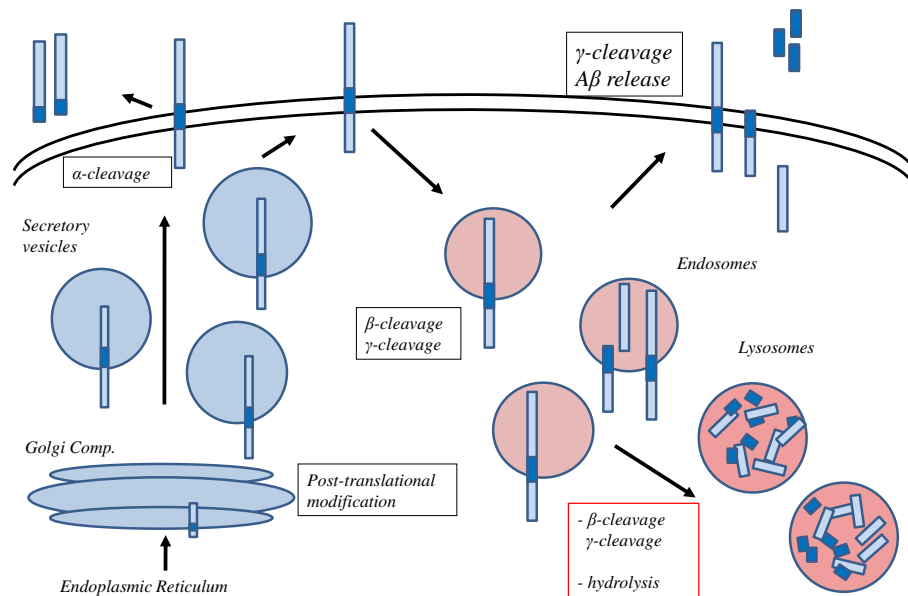


**Fig. 4: Intracellular trafficking of APP and subcellular sites for processing.** APP is synthesized in the ER and then transported to the Golgi compartment for posttranslational modification and subsequently routed to the PM for predominant  $\alpha$ -secretase cleavage. Non-processed APP is internalized into endosomes for  $\beta$ - and  $\gamma$ -secretase cleavage. Cleavage products are either transported back to the PM for further processing or internalized into lysosomal compartments. Lysosomal activity is detrimental for the BACE1 cleavage, but also for the final degradation of APP.

### 1.1.3 Physiological relevance of APP

The multiplicity of the different APP metabolizing processes and its ubiquitous expression indicates an important role in the physiology. However, the exact role of APP still remains elusive. Two additional APP homologues (amyloid like proteins: APLP-1 and APLP-2) have been identified and are expressed in several tissues of mammals, including the brain (Goldgaber et al, 1987; Zheng & Koo, 2006). Knock out of APP alone has only slight effects on learning and behavior (Senechal et al, 2008). However, double knockout combinations of APP or APLP1 with APLP2, causes *in utero* or postnatal lethality, indicating important physiological functions (Zheng et al, 1996).

APP has several functional domains like the KPI (Kunitz protease domain) or cation binding domains. Soluble APP, but also APLP2, containing the KPI domain has severe influence on the blood coagulation, since KPI containing APP variants are highly expressed in platelets where they influence blood clotting serine proteases (Van Nostrand et al, 1991; Xu et al, 2009). Binding and association studies furthermore revealed a cysteine rich domain in APP which interacts with metal ions like  $Fe^{2+}$ ,  $Cu^{2+}$ ,  $Zn^{2+}$  or  $Pb^{2+}$  and affects its processing. APP is furthermore suggested to act as a receptor for a

ligand (Rossjohn et al, 1999) or to bind to components of the extracellular matrix (Small et al, 1992). Additional domains for the interaction with heparin and several proteins have also been described and extensively reviewed (Dawkins & Small, 2014; Mattson, 1997).

Binding of adaptor proteins such as X11, ARH or Fe65 to the NPTY motif at the C-terminus of APP, play a critical role in its transport and processing (Mameza et al, 2007; McLoughlin & Miller, 2008; Rogelj et al, 2006). Especially Fe65 seems to have an AICD stabilizing activity and is involved in several transcriptional or gene regulatory processes (Fiore et al, 1995; Kimberly et al, 2001; Yang et al, 2006). However, the role of AICD on gene regulation seems to be controversial, since further studies failed to proof these results (Hass & Yankner, 2005; Hebert et al, 2006) to play a general important role in Fe65 was furthermore shown to interact with the lipoprotein receptor LRP1 and regulates the metabolism of ApoE and cholesterol (Liu et al, 2007) .

APP also seems to be tightly linked to the regulation of lipid metabolism (Grimm et al, 2007; Grosgen et al, 2010), as it was shown to bind cholesterol in its transmembrane domain and promotes the amyloidogenesis (Barrett et al, 2012). The  $\gamma$ -secretase cleavage products AICD and  $A\beta$  were also shown to regulate the lipid homeostasis. In cell culture experiments,  $A\beta$  inhibited the HMG-CoA reductase and therefore lowered the generation of cholesterol (Grimm et al, 2005). AICD on the other hand was shown to negatively regulate the LDL receptor related protein 1 (LRP1) expression in cells lacking PS1 activity and leading to a more efficient uptake of ApoE-cholesterol complexes (Liu et al, 2007).

Overall, the exact role of APP and APLPs in the physiology stays elusive. However, both APP and APLPs exert multiple, but partially redundant physiological functions.

### *1.2 Sphingolipids*

Sphingolipids are common components of cellular membranes, and together with phosphoglycerides and cholesterol determine their biophysical and biological characteristics. The class of sphingolipids is characterized by a  $C_{18}$  long-chain base (sphingoid base), an aliphatic amine with two or three hydroxyl groups and often a distinctive trans-double bond (2-amino-1,3-dihydroxy-alkanes). The most abundant

sphingoid base in tissues is sphingosine (Sph), followed by ceramide (Cer) and sphingosine-1-phosphate (S1P) (Merrill, 2011). Sphingoid bases are the precursor for all sphingolipids and are generated either *de novo* (Cer) or in recycling pathways (Sph, S1P). Ceramide can be formed in the recycling pathway as well, when sphingosine is linked to a fatty acid (Fig. 5). Sphingolipids are classified by their different head groups into glycosphingolipids (GSL) and sphingomyelin (SM) (Merrill, 2011). Glycosylation of ceramide initiates the formation of the GSLs. GSLs can be divided into two classes. Addition of uncharged carbohydrates to ceramide forms neutral GSLs (cerebrosides), whereas acidic GSLs are formed upon sulfation (sulfatides) or addition of N-acetylneuraminic acid to ceramide (gangliosides). Modification of ceramide by addition of phosphorylcholine at its C1 position forms sphingomyelin (SM). Both GSLs and SM are anchored with their ceramide-backbone into membranes, while their head groups predominantly face towards extracellular fluids and the lumen of vesicular compartments. Both GSLs and SM tend to accumulate in lipid microdomains or “lipid rafts” which are highly detergent resistant (Merrill, 2011).

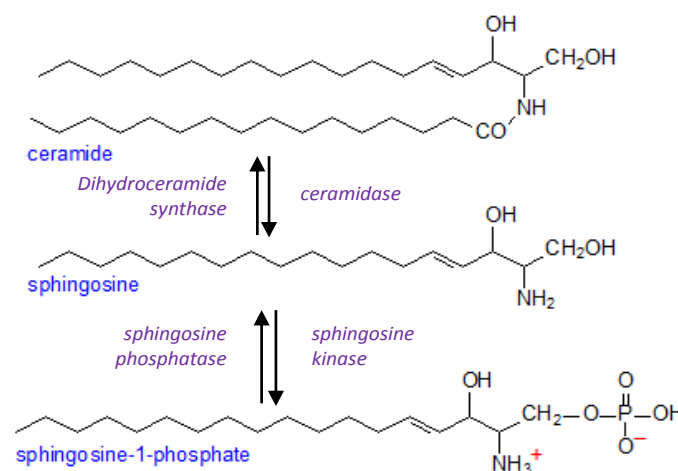


**Fig. 5: Inter-conversion of the sphingoid bases ceramide, sphingosine and sphingosine-1-phosphate.** The most common sphingoid base sphingosine, is either phosphorylated by the sphingosine-kinases 1 or 2 to form S1P, or catabolized to ceramide. Ceramidases can form sphingosine by deacylation. S1P can be dephosphorylated by sphingosine-phosphatases. (Modified after <http://lipidlibrary.aocs.org/Lipids/lcb/Figure1.png>)

The sphingolipid profiles of different brain regions and neuronal subtypes are diverse and can be highly dynamic during differentiation and development (Kracun et al, 1992b; Svennerholm et al, 1989). As components of biological membranes, sphingolipids also affect fluidity and dynamics as

well as vesicular trafficking (Goni & Alonso, 2009; Zhang et al, 2009). Ceramide and S1P furthermore exert important roles in intracellular signal transduction (Hannun & Obeid, 2008). A variety of enzymes is involved in the metabolism of sphingolipids which also can play critical roles in the pathogenesis of a wide range of diseases such as cancer (Liu et al, 2013), diabetes mellitus (Galadari et al, 2013), neurological disorders/neuro-inflammation (Davies et al, 2013; Gomez-Munoz et al, 2013) and other metabolic disorders (Hla & Dannenberg, 2012).

### 1.2.1 Topology and metabolism of sphingolipids.

All cells are able to generate sphingolipids via *de novo* synthesis starting with the condensation of serine and palmitoyl-CoA or stearoyl-CoA in the ER (Sonnino & Chigorno, 2000; van Echten-Deckert & Herget, 2006). The enzyme serine-palmitoyl-transferase catalyzes the rate-limiting step for the *de novo* synthesis and initiates the formation of 3-ketosphinganine, which subsequently metabolized to sphinganine and dihydro-ceramide and ceramide. In further steps of the *de novo* biosynthesis pathway, Cer is transported to the *cis*-Golgi compartments via vesicular trafficking or by the ceramide transfer protein (CERT) in a non-vesicular manner (Hanada et al, 2007), and then glycosylated to glucosylceramide (GluCer) at the cytoplasmic side/face of the *cis*-Golgi. Further metabolic processing of GluCer to higher GSLs takes place in the luminal Golgi. In addition, non-glycosylated Cer can be modified with phosphorylcholine by the sphingomyelin synthase to form SM. Both GluCer and SM are transported to the plasma membrane via secretory vesicles or lipid transfer proteins. A detailed description of the *de novo* synthesis is given in the legend of *Fig. 6*.

In the recycling or degradation pathway, SM and GSLs are directly catabolized to Cer at the plasma membrane or internalized into endosomal compartments. Ceramide is further catabolized to Sph, which can be phosphorylated by the sphingosine kinases (SphK1 or SphK2). S1P can undergo either dephosphorylation by S1P-phosphatases (SPP1, SPP2) or the less specific lipid phosphatases. Alternatively, S1P can be cleaved by the S1P-lyase (see 1.2.2; *Fig. 6*).

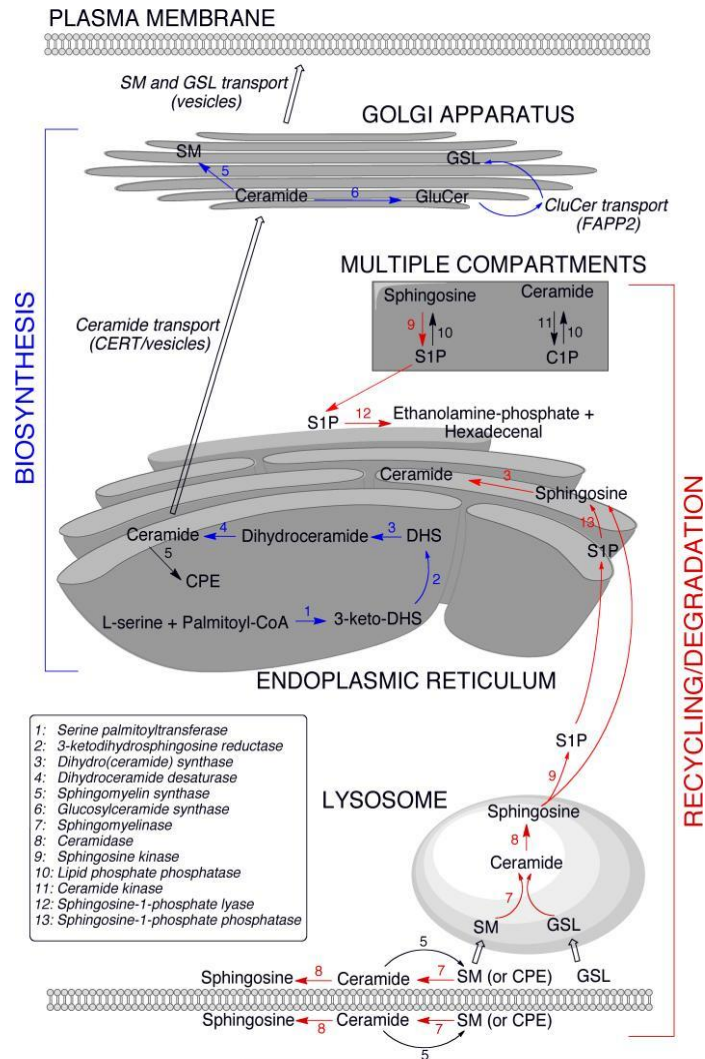


**Fig. 6: Topological biosynthesis of sphingolipids in the *de novo* and the recycling pathways.** The *de novo* synthesis (blue arrows) of sphingolipids is initiated in the ER by the condensation of serine and palmitoyl CoA through the serine palmitoyl transferase. The generated 3-sphinganine (3-ketodihydrospingosine) is further metabolized to dihydroceramide (DHS) by the dihydro(ceramide) synthase. Next DHS is desaturated to ceramide by the dihydroceramide desaturase, which is transported by CERT/vesicles to the cytoplasmic site of the Golgi membrane. Ceramide is then either metabolized to glucosylceramide (GluCer) and further to the glycosphingolipids (GSLs), or to sphingomyelin (SM) at the luminal site of the Golgi compartments. SM and GSLs are then transported to the plasma membrane. Cleavage of SM at the plasma membrane to ceramide or internalization of GSLs into endosomal/lysosomal compartments initiates the recycling pathway (red arrows). The sphingomyelinase at the PM or in endosomal/lysosomal compartments generates Cer, which can be further cleaved to sphingosine by the ceramidases. GSLs are degraded by a subset of various specific catabolic enzymes in the endosomal/lysosomal compartments. Sphingosine is subsequently phosphorylated by the sphingosine-kinases 1 or 2, either at the PM (SphK1) for direct secretion or in the ER (SphK2). S1P can translocate into the nucleus or can be irreversibly cleaved to phosphoethanolamine and hexadecenal by the S1P-lyase. Dephosphorylation of S1P by S1P-phosphatases initiates recycling of S1P to sphingosine and ceramide. (Fyrst & Saba, 2010).

### 1.2.2 S1P and metabolizing enzymes.

For a long time sphingolipids were suspected to be only passive components of biological membranes. However, it has been shown that certain GSLs, ceramide, sphingosine and S1P can undergo rapid conversion and regulate different intracellular signaling pathways.

S1P is a highly bioactive metabolite of the sphingolipid metabolism and exerts a wide range of intracellular activities. At first, Gosh and colleagues showed that S1P could induce  $\text{Ca}^{2+}$  release from the ER (Ghosh et al, 1990; Ghosh et al, 1994). It was furthermore demonstrated that S1P acts as a second messenger to promote cell proliferation (Olivera & Spiegel, 1993). Interestingly, S1P counteracts the pro-apoptotic function of ceramide by preventing intranucleosomal DNA fragmentation (Cuvillier et al, 1996). An additional effect of S1P in the nucleus was shown by Hait and colleagues. After entering the nucleus, S1P is able to regulate the transcription of genes by histone acetylation (Hait et al, 2009). S1P furthermore acts as a co-factor for the TNF receptor-associated factor 2 by binding to its RING domain and stimulating its E3 ligase activity (Alvarez et al, 2010). Of great interest for this work, S1P was recently related to the APP cleaving enzyme BACE1. Takasugi and colleagues demonstrated a positive modulatory effect of S1P on the BACE1 activity (Takasugi et al, 2011). For a detailed description of S1P in the pathogenesis of AD see 1.2.3.

In addition to the second messenger function, S1P serves as ligand for five distinct cell surface G-protein coupled receptors (S1PR1 – S1PR5). In most tissues, the basal concentrations of S1P are low. Erythrocytes however show high concentrations since they lack S1P degrading enzymes (SPPs or S1P-lyase). It is assumed, that this S1P concentration gradient is of great relevance and attracts various immune cells like lymphocytes, since the activation of S1PRs can cause egress of several types of immune cells (Chi, 2011; Schwab et al, 2005). The particular effect of the S1PRs on immune cell recruitment is briefly described in the following paragraph.

Activation of S1PR5 in natural killer T-cells is important for their recruitment and egress from lymphoid organs (Jenne et al, 2009). S1PR4 is involved in neutrophil trafficking since its deletion was shown to decrease neutrophilia and inflammation in S1P-lyase deficient mice (Allende et al, 2011). In particular, activation of the S1P - S1PR1 axis is of great interest. Phosphorylation of the sphingosine analogue FTY720 by SphK2, and binding to S1PR1 causes an internalization and degradation of the



S1PR1 in B- and T-lymphocytes. This receptor degradation causes retention of lymphocytes in lymph nodes and thus a suppression of the immune response (Schwab & Cyster, 2007).

### *Sphingosine-Kinases*

Phosphorylation of sphingosine by the sphingosine-kinases (SphK1 and SphK2) generates S1P (Kohama et al, 1998; Liu et al, 2000). Several splice variants for both kinases with a high degree of polypeptide sequence homology were identified so far (Pitson, 2011). The distinct tissue distribution and subcellular localization of SphK1 and SphK2 suggest distinct physiological roles of both enzymes (Cuvillier et al, 2010). It was demonstrated that phosphorylation of Sph by SphK1 promotes cell survival and proliferation (Hannun & Obeid, 2008; Pyne & Pyne, 2010). S1P generated by the SphK2 on the other hand appears to suppress cell growth suppression and enhance apoptosis (Maceyka et al, 2005; Okada et al, 2005). Nevertheless, experiments with specific SphK2 inhibitors also caused enhanced apoptosis, suggesting overlapping effects of SphK1 and SphK2 generated S1P (Pitman & Pitson, 2010).

Phosphorylation of SphK1 at Ser225 by ERK1/2 strongly stimulates its activity (Pitson et al, 2003). It causes a translocation of SphK1 from the cytosol to the plasma membrane, probably to phosphorylate sphingosine at the plasma membrane thereby facilitating the secretion of S1P (Pitson et al, 2003). Interaction of SphK1 with phosphatidylserine at the inner leaflet of the plasma membrane is suspected to assist in this re-localization of this protein (Stahelin et al, 2005). Rapid secretion of SphK1 generated S1P and is mediated by the different sphingolipid transporters ABCC1, ABCC2 (ATP binding cassette, sub family C) or Spn2 (spinster homolog 2) (Kawahara et al, 2009; Takabe et al, 2010).

SphK2 shares a high sequence similarity with SphK1, but lacks the Ser225 phosphorylation site. Nevertheless, it shows also contains probable phosphorylation sites for ERK1/2 at Ser351 or Thr578 (Hait et al, 2007). SphK2 is mainly located in the nucleus and the cytoplasm. However, upon activation of PKC or cell starvation, SphK2 levels at the ER increase and lead to enhanced generation of S1P (Ding et al, 2007; Maceyka et al, 2005). SphK2 generated S1P can then translocate into the nucleus and regulate gene transcription by inhibition of histone deacetylation (Hait et al, 2009).

Furthermore, the localization of SphK2 at the ER supports a role in apoptosis, since S1P generated by SphK2 is catabolized to ceramide and facilitates the ceramide-mediated pro-apoptotic signaling (Igarashi et al, 2003; Maceyka et al, 2005). This is supported by the higher resistance of cells isolated from SphK2<sup>-/-</sup> compared to SphK1<sup>-/-</sup> mice against staurosporine induced apoptosis (Hofmann et al, 2008). Interestingly, whereas SphK1 or SphK2 single knockout mice are viable and fertile, double knockout mice die *in utero* (Mizugishi et al, 2005), indicating some functional redundancy of both enzymes.

### *S1P-lyase*

The cleavage of S1P is mediated by the ER localized S1P-lyase. This hydrolysis is irreversible and presents the only point for sphingolipid intermediates to leave the sphingolipid degradation pathway. Accordingly, the inhibition of S1P-lyase causes strong accumulation of intracellular S1P (Hagen-Euteneuer et al, 2012; Ikeda et al, 2005). The mammalian S1P-lyase gene encodes a 63.5 kDa type-I transmembrane protein of 568 amino acids, with the catalytic domain facing the cytosol (Ikeda et al, 2004; Van Veldhoven & Mannaerts, 1991). Two cysteine residues at position 218 and 317 form the catalytic center. The latter is highly conserved throughout different species. Interestingly, deletion of the transmembrane domain does not impair the catalytic activity *in vitro* (Van Veldhoven, 2000). Two additional lysine residues at position 353 and 359 form a binding site for its coenzyme pyridoxal 5'-phosphate and are also highly conserved throughout all S1P orthologues (Serra & Saba, 2010; Van Veldhoven & Mannaerts, 1991; van Veldhoven & Mannaerts, 1993), and mutagenesis of Lys 353 resulted in total loss of S1P-lyase activity (Reiss et al, 2004)..

S1P-lyase cleaves S1P between the C2 and C3 carbon bond generating hexadecenal (palmitaldehyde) and phosphoethanolamine (van Echten-Deckert & Herget, 2006). In addition to S1P, S1P lyase can also degrade *D-erythro* isomers of sphingoid bases like dihydrosphingosine-1P and phytosphingosine-1P (Pyne & Pyne, 2000).

High expression levels of S1P-lyase are found in tissues high cell proliferation like the small intestine, the liver, the spleen or the olfactory mucosa (Borowsky et al, 2012; Genter et al, 2003). Tissues with low cell turnover like the brain, the heart or the skeletal muscles show lower expression of the S1P-

lyase. This pattern is consistent with the ability of S1P to suppress apoptosis and promote cell survival (Serra & Saba, 2010). The interplay of the enzymes involved in S1P metabolism, S1P-lyase and SphKs allows a fine-tuned control of intracellular S1P concentrations that are crucial for the cell survival.

### *1.2.3 Pathological Effects of altered Sphingolipid metabolism.*

Altered sphingolipid metabolism is associated with a number of different diseases, mostly affecting lipid degrading enzymes in lysosomal compartments. Most sphingolipids enter endosomal or lysosomal compartments via endocytosis and are then degraded by acidic hydrolases (Kolter & Sandhoff, 2010). Impaired degradation of these sphingolipids causes their pathogenic storage, known as sphingolipidoses. As a secondary effect of this accumulation, clearance of additional lipids and also proteins can also be affected (Aridor & Hannan, 2000; Walkley & Vanier, 2009). A high number of sphingolipidoses were described so far, like Gaucher's disease as the most frequent one, Niemann Pick A or B (NPA, NPB), Sandhoff disease, Tay Sachs disease and many others.

In Gaucher's disease, GluCer is the primarily stored lipid and causes malfunction of the liver, skeletal disorders, anemia or low blood platelets. However, storage of secondary lipids like ceramide or GM3, can also contribute to the diseases phenotype, which is not necessarily associated with the primary substance. Ceramide and GM3 storage have been shown cause an insulin resistance in patients affected by Gaucher's disease (Fuller, 2010). Further additional physiological effects are impaired inflammatory response (Hollak et al, 1997) or impaired  $Ca^{2+}$  homeostasis (Korkotian et al, 1999). Niemann Pick C (NPC) shows a primary accumulation of cholesterol due to mutations in the endosomal/lysosomal cholesterol transporter NPC1 or NPC2 (Carstea et al, 1997). However, the secondary effect emerging from this cholesterol storage manifests in additional accumulation of sphingomyelin and sphingosine (Lloyd-Evans et al, 2008). Due to the storage of sphingomyelin, similar as in NPA or NPB, NPC can also be classified as a sphingolipidosis.

Complex gangliosides can be predominantly found in neuronal membranes. Thus, it is not surprising that sphingolipidoses are also often associated with neurological symptoms (Walkley, 2003).

The composition of the gangliosides in neuronal membranes changes during the aging process, underlining the importance in neuronal activity (Svennerholm et al, 1989; Svennerholm et al, 1994). Interestingly, altered sphingolipid metabolism was also shown to be associated with a number of neurodegenerative disorders, like Parkinson's disease (Swan & Saunders-Pullman, 2013), Prion disease (Schengrund, 2010) and Huntington's disease (Desplats et al, 2007). Moreover, these late-onset neurodegenerative diseases show similar neuropathological and cyto pathological characteristics like classical sphingolipidoses (Piccinini et al, 2010).

#### 1.2.4 Sphingolipids in Alzheimer's disease.

The subcellular trafficking of APP and its metabolizing enzymes is very similar to that of sphingolipids. As described before (*see 1.1.2*), APP is posttranslationally modified in Golgi compartments and transported in secretory vesicles to the PM. Endocytosis delivers unprocessed APP to endosomes containing BACE1 and  $\gamma$ -secretase. After processing, the endosomes can recycle and fuse with the PM resulting in the secretion of A $\beta$ . Alternatively, endosomes can fuse with lysosomes to allow efficient degradation of their content (*Fig. 7*). The *de novo* synthesis of sphingolipids (GSLs and SM) also occurs in the secretory pathway from the ER via Golgi compartments to the PM. SM can be directly degraded at the PM and its metabolites are converted to Cer, Sph or SIP. Further catabolic processing of SM as well as of GSLs is mediated by acidic hydrolases in endosomal and lysosomal compartments (*Fig. 7*). Thus, disturbances in the sphingolipid metabolism might affect the intracellular trafficking and processing of APP. Lowering the levels of SM or GSLs reduced the transport of APP in the secretory pathway and therefore its availability for secretases (Sawamura et al, 2004; Tamboli et al, 2005). Ceramide on the other hand can stabilize BACE1 and thereby increase the secretion of A $\beta$  (Li et al, 2010; Puglielli et al, 2003). In addition, APP can also be stabilized by sphingolipids by impairment of APP processing (Tamboli et al, 2005; Tamboli et al, 2011c; Zha et al, 2004). Modulation of membrane thickness and its composition was shown to affect  $\gamma$ -secretase activity (Osenkowski et al, 2008; Winkler et al, 2012). On the other hand, APP metabolism could also be affected independent of secretases as demonstrated in several models of LSDs. Primary fibroblasts

from patients with NP - A, - B, Tay-Sachs or Sandhoff disease (Tamboli et al, 2011b; Tamboli et al, 2005) and *in vivo* studies of LSD model mice (Boland et al, 2010; Burns et al, 2003; Keilani et al, 2012) demonstrated accumulation of APP-FL and APP-CTFs. The majority of studies focused on the role of complex sphingolipids like SM and GSLs or the sphingoid bases Cer and Sph.

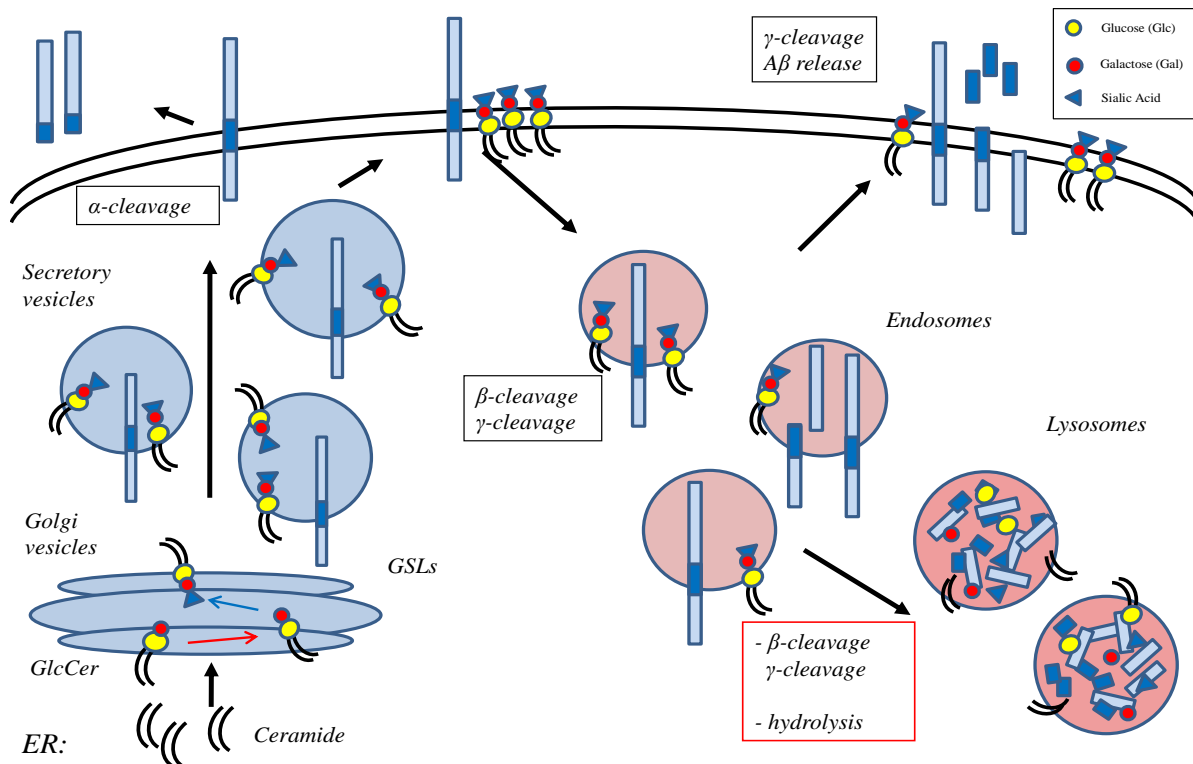


**Fig. 7: Similarities between trafficking and localization of APP and GSLs.** Cer is generated in the ER and further metabolized to GSLs in the Golgi compartments. Both GSLs and APP are transported in secretory vesicles to the PM and tend to accumulate in lipid rafts. GSLs can be internalized into endosomal/lysosomal compartments, similar to non-processed APP. The cleavage of APP and the degradation of GSLs take place in the endosomal/lysosomal compartments. Both CTFs or sphingolipids can either be transported back to the PM or undergo hydrolysis. Colocalization of highly concentrated GSLs can hamper the processing and the degradation of APP.

Only little information on the role of S1P in the metabolism of APP is currently available. One study analyzed the relationship of A $\beta$  and hyper-phosphorylated tau (PHF1) with the sphingoid bases Sph and S1P in brain samples from AD patients (He et al, 2010b). The study could not demonstrate any relationship of Sph with PHF1, but showed a negative correlation of the S1P content with A $\beta$  or PHF1 levels (He et al, 2010b). In line with this, a recent study linked the S1P signaling and the activity of SphK1 and SphK2 directly to the pathogenesis of AD. The study indicated that levels of S1P decline with disease progression and were lowest in brain regions most heavily affected by the AD pathology

(Couttas et al, 2014). The authors attributed these findings to the absence of the cytoprotective role of S1P, probably by reduced SphK1 and SphK2 activities. Consistently, mRNA expression analysis of AD brains showed a marked increase of S1P-lyase levels when compared to healthy brains (Katsel et al, 2007). Similar results were found by Ceccom and colleagues. While the expression of S1P-lyase was elevated, the expression of SphK1 and S1PR1 was significantly decreased in frontal and entorhinal cortices of AD patients (Ceccom et al, 2014). An interesting study furthermore emphasizes the role of S1P in the pathogenesis of AD. A novel liposomal vaccine, composed of A $\beta$ 42 and S1P showed positive effects on the plaque load when administered to APP/PS1 mice (Carrera et al, 2012). Vaccination with the A $\beta$ 42-S1P liposomes significantly reduced the plaque burden and the immunological response in hippocampal areas induced by amyloidosis.

The role of SphK1 seems to be crucial in the pathological processing of APP. Three independent studies analyzed the relationship of SphK1 and the APP metabolism. In the first study, application of a truncated A $\beta$  peptide (A $\beta$ <sub>25-35</sub>) reduced the expression of SphK1 significantly and showed a severe neurotoxic effect. Notably, this effect was ameliorated when SphK1 was overexpressed (Yang et al, 2014). In the second study, Zhang and colleagues demonstrated an increased plaque formation and a decrease in learning and behavior after knock-down of SphK1. They injected adenoviruses expressing siRNA into the hippocampus of APP/PS1 mice. Four weeks after transduction, the learning and memory abilities in these mice were severely aggravated (Zhang et al, 2013). The third study by on the other hand was contradictory. Jesko and colleagues showed that inhibition of SphK1 as well as SphK2 reduced the secretion of A $\beta$  in SH-SY5Y neuroblastoma cells (Jesko et al, 2014).

SphK2 on the other hand, is also of great interest in neurodegeneration. S1P generated by SphK2 was shown to induce apoptosis in primary neurons of S1P-lyase deficient mice, also providing a possible link between S1P and cell death occurring in AD (Hagen et al, 2009). In accordance, Takasugi and colleagues showed an increased level of SphK2 in AD brains and an impact of S1P on the processing of APP (Takasugi et al, 2011). S1P generated by SphK2 stimulates BACE1 activity and causes an increased secretion of A $\beta$ . The same authors showed that long term treatment with the S1PR1 agonist FTY720 decreased the levels of A $\beta$ 40, while levels of A $\beta$ 42 increased. It was assumed, that this effect is independent of known downstream signaling pathways of S1PRs (Takasugi et al, 2013).

FTY720 and Memantine®, the only clinically approved NMDA receptor antagonist against AD, were also tested in a rat model of AD. Constant application of FTY720 and Memantine ® to rats of an AD model showed a similar restoration of the behavioral outcomes. Gene profiling analysis furthermore revealed an up regulation in the expression pattern of mitogen activated protein kinases (MAPKs) and inflammatory markers (Hemmati et al, 2013). This finding suggests a beneficial effect of FTY720 by stimulating neurorestoration and cell survival in AD.

Taken together, the role of S1P in APP processing and pathogenesis of AD is gaining more and more interest. Different studies revealed a loss of the S1P cytoprotective effect in brains of AD patients. The role of the SphKs seems to be of great relevance. However, the studies are still sketchy and do not provide any clear mechanism on the AD pathology. The role of S1P-lyase on the other hand remains mainly elusive and has to be further explored.

### *1.3 Rationale*

There are clear parallels between AD and sphingolipidoses. The role of sphingolipids on the pathological processing of APP has been extensively described in numerous studies (Li & Sudhof, 2004; Puglielli et al, 2003; Sawamura et al, 2004; Tamboli et al, 2011a; Tamboli et al, 2011b; Tamboli et al, 2005). While these studies focus on sphingolipid intermediates like Cer, SM or GSL, Sph was shown to accumulate in lysosomal compartments of NPC cells (Lloyd-Evans et al, 2008). Interestingly, all of these LSDs show severe effects on the APP metabolism, either due to altered secretase activities or due to hampered lysosomal turnover.

Recent studies highlighted the role of S1P metabolizing enzymes like SphK1 or SphK2 on the pathogenesis of AD. However, the impact of S1P on the cellular APP metabolism remains largely elusive.

The main goal of this study was to understand the role of S1P in the metabolism of APP. Therefore, a genetically modified model with a deficiency of the S1P-lyase and significantly elevated concentrations of S1P was used. It was analyzed whether elevated level of S1P might affect the activity of the APP processing secretases and whether the highly sensitive S1PRs play a role. In addition, the possible role of S1P storage on lysosomal compartments and other organelles was analyzed.



## 2. Material and Methods

All chemicals used in the following experiments were purchased in purity grade “per analysi” from Sigma-Aldrich (Steinheim, Germany), LifeTechnologies (Frankfurt, Germany) Roche (Basel, Switzerland), Roth (Karlsruhe, Germany), Applichem (Darmstadt, Germany), Tocris/R&D Systems (Wiesbaden-Nordenstadt, Germany), Cayman Chemicals (Ann Arbor, USA) or SantaCruz Biotechnology (SantaCruz, USA). Cell culture media and buffers were purchased from LifeTechnologies (Frankfurt, Germany). Exceptions are stated in the respective experiment descriptions. For a list of used equipment and materials see

*Table 1.*

*Table 1: Equipment and Material*

<b>Cell culture equipment</b>	<b>Company</b>
<b>-80°C Freezer</b>	Thermo Scientific
<b>37°C CO<sub>2</sub> incubator</b>	Binder
<b>Cell culture clean bench</b>	Thermo Scientific
<b>Centrifuge (5804)</b>	Eppendorf
<b>Water bath</b>	Medigen
<b>SDS-PAGE and Blotting equipment</b>	
<b>SDS-PAGE and Blotting equipment</b>	<b>Company</b>
<b>SDS-PAGE chamber</b>	Höfer
<b>Western blotting chamber</b>	Höfer
<b>Cooling system (E100)</b>	Lauda
<b>Chemiluminescence Imager (ChemiDoc XRS) with Analysis Software Quantity One</b>	Bio-Rad
<b>LiCor Infrared Imager (Odyssey CLx) with Analysis Software Image Studio 3.1</b>	LiCor
<b>PCR Equipment</b>	
<b>PCR Equipment</b>	<b>Company</b>
<b>Cycler</b>	Eppendorf
<b>DNA-electrophoresis chamber</b>	Amersham

Cell culture clean bench	Thermo Scientific
Trans-UV illuminator (GVM 20)	Syngene
Implen Nano-Spectrophotometer P-class	Implen

General laboratory equipment	Company
Microcentrifuge (5415R)	Eppendorf
Centrifuge (5804R)	Eppendorf
Centrifuge (5804)	Eppendorf
Autoclave	H+P
Heating Block	Stuard Scientific
Thermomixer (compact)	Eppendorf
Magnetic stirrer	Velp Scientifica
pH Meter (MP 225)	Mettler Toledo
Photometer (Genesis)	Thermo Scientific
Sonifier (Sonopuls, UW 2070)	Bandelin
Overhead rotor	Scientific Industries
Vortex (MS 2 Minishaker)	IKA
Analytical Balance (Labstyle 204)	Mettler Toledo
Microtiterplate Reader (Muliskan RC)	Thermo Scientific
Ultracentrifuge Optima XPN	Beckmann Coulter
Fluorescence Microscope (AxioVert 200)	Zeiss
with ApoTome and AxioVision Analysis Software	

## 2.1 Cell biological techniques

### 2.1.1 Cell culture

#### Cell culture medium (DMEM +/-)

Dulbecco's Modified Eagle's Medium (DMEM) Glutamax™ containing 4.5 g/l D-glucose supplemented with 10 % heat inactivated fetal calf serum (FCS) and 1 % PenStrep solution (50 U/ml Penicillin, 50 Vg/ml Streptomycin)

#### Cell culture medium (EBSS)

Earle's Balanced Salt Solution (EBSS) 1 % PenStrep solution (50 U/ml Penicillin, 50 Vg/ml Streptomycin)

#### Phosphate Buffered Saline (PBS)

140 mM NaCl, 10 mM Na<sub>2</sub>HPO<sub>4</sub>, 1.75 mM KH<sub>2</sub>PO<sub>4</sub>, dH<sub>2</sub>O, pH 7.4

#### Trypsin-EDTA Solution

0.05 % (w/v) trypsin (Invitrogen), 0.53 mM EDTA, dH<sub>2</sub>O

#### Cryo medium

90 % FCS supplemented with 10 % dimethylsulfoxide (DMSO)

Cells (see *Table 2*) were cultured in DMEM containing 10 % FCS and 1 % Penicillin/Streptomycin at 37°C and 5 % CO<sub>2</sub> atmosphere. Before splitting, medium was discarded and the cells were washed once with PBS. Cells were then detached from the cell culture plate by incubation with 1 ml Trypsin-EDTA at 37°C for 5 minutes, transferred into a 15 ml reaction tube along with culturing medium and centrifuged at 500 x g for 3 min. Cells were then resuspended in fresh 5 ml of culture medium and splitted in a ratio 1:20 - 1:2 according to initial cell amount onto new 10 cm culturing dish. Exact cell numbers were determined by using a Neubauer counting chamber. For cryo stocks, cells were grown until 90 – 100 % confluency and detached as described above by trypsinization. After centrifugation, cells were resuspended in 1-2 ml of cryo medium and stored in the -80°C freezer or liquid nitrogen.

*Table 2: Cell lines*

<i>Cell lines</i>	<i>species/cell type</i>
<b>MEF-WT</b>	Mouse embryonic fibroblasts (MEFs)
<b>MEF-S1PL-KO</b>	MEFs, lacking functional SIP-lyase
<b>MEF-WT- APP695<sub>swe</sub></b>	MEFs, stably expressing human APP695 <sub>swe</sub> variant
<b>MEF-S1PL-KO- APP695<sub>swe</sub></b>	MEFs and stably expressing human APP695 <sub>swe</sub> variant
<b>HEK293-WT</b>	Human embryonic kidney cell (HEKs)
<b>HEK293-APP695<sub>WT</sub></b>	HEKs, stably expressing human APP695 <sub>WT</sub>
<b>HEK293-APP695<sub>swe</sub></b>	HEKs, stably expressing human APP695 <sub>swe</sub>
<b>N9</b>	Murine microglial cells

### 2.1.2 Pharmacological treatment

For pharmacological treatments, conditioned media were removed and fresh medium containing the indicated compounds was added for the indicated periods. For lipid treatments or induction of starvation, cells were washed three times with PBS to remove the remaining serum. The pharmacological modulators, chemicals and supplements, and the applied concentrations are listed in *Table 3*.

Table 3: List of pharmacological compounds.

Compound	Function	Concentrations
<b>BAPTA-AM</b>	Ca <sup>2+</sup> chelator	0,1 - 1 $\mu$ M
<b>BIM I</b>	PKC inhibitor	1 $\mu$ M
<b>Rapamycin</b>	mTOR inhibitor	10 $\mu$ M
<b>Sphingosine</b>	cellular sphingolipid and S1P precursor	10 $\mu$ M
<b>S1P</b>	activates S1PRs	10 $\mu$ M
<b>JTE-013</b>	S1PR2 antagonist	150 nM
<b>W146</b>	S1PR1 antagonist	150 nM
<b>Chx</b>	translational elongation inhibitor	20 $\mu$ g/ml
<b>GPN</b>	lysosomal membrane disrupting peptide	200 $\mu$ M
<b>2ABP</b>	IP <sub>3</sub> channel inhibitor	5 - 25 $\mu$ M
<b>SKiII</b>	Sphingosine-Kinase inhibitor	5 $\mu$ M
<b>Thapsigargin</b>	SERCA inhibitor	500 nM

### 2.1.3 Immunocytochemistry.

#### Phosphate Buffered Saline (PBS)

140 mM NaCl, 10 mM Na<sub>2</sub>HPO<sub>4</sub>, 1,75 mM KH<sub>2</sub>PO<sub>4</sub>, dH<sub>2</sub>O, pH 7.4

#### Fixation (Paraformaldehyde) Solution

4 % (w/v) Paraformaldehyde in PBS

#### Permeabilization Solution

0,25% (v/v) Triton X-100 in PBS

#### Blocking Solution

10 % (w/v) BSA, 0.25 % (v/v) Triton X-100 in PBS

#### Washing Buffer

0,125 % (v/v) Triton X-100 in PBS

#### Antibody Solution

5 % (w/v) BSA, 0,125 % (v/v) Triton X-100 in PBS + Antibody (see *Table 6* and *Table 7*)

#### LD540

Kind gift from Prof. Dr. Christoph Thiele (LIMES Institute, Bonn)

For immunocytochemistry, cells were seeded and cultured on glass cover slips. Conditioned media was discarded and cells were washed briefly with pre-warmed PBS (37°C). All following steps were performed at room temperature. Cells were first fixed with 4 % paraformaldehyde for 10 min, before washing three times for 5 min with PBS and permeabilization with 0,25 % triton for 3 min. Next, cells were incubated with BSA buffer for 1 h to block unspecific binding epitopes. Cells were then incubated for 1 h with the respective primary antibody solutions (see *Table 6* for antibody dilutions), followed by repetitive washing (three times for 5 min). Incubation with the secondary antibodies was

performed for 1 h as indicate in *Table 7*. Unbound antibodies and low affinity bound antibodies were removed by additional washing steps (three times for 5 min). Nuclei were stained by incubation of the cells for 2 min with PBS containing DAPI, followed by a final washing step with dH<sub>2</sub>O. Cells were embedded in ImmuMount (Thermo Scientific) and stored at 4°C under light exclusion until analysis. Lipid droplets were stained using the lipophilic dye LD540 (Spandl et al, 2009) and was kindly provided by Prof. Dr. Christoph Thiele from the LIMES Institute in Bonn. Cells were incubated with 0,05 – 0,1 µg/ml LD540 diluted in and incubated for 10 min on the cells. The dye was discarded and cells were washed three times for 5 min with PBS before fixating and mounting.

#### 2.1.4 Transient transfection

**Phosphate Buffered Saline (PBS)**

140 mM NaCl, 10 mM Na<sub>2</sub>HPO<sub>4</sub>, 1.75 mM KH<sub>2</sub>PO<sub>4</sub>, dH<sub>2</sub>O, pH 7.4

**Cell culture medium**

Dulbecco's Modified Eagle's Medium (DMEM) Glutamax<sup>TM</sup> containing 4.5 g/l D-glucose and 1 % PenStrep solution (50 U/ml Penicillin, 50 Vg/ml Streptomycin)

**Lipofectamin 2000**

Life-Technologies

Transient transfection of proteins was performed using Lipofectamin2000 (Life-Technologies). Cells were grown until 80 % confluency and briefly washed 1 x with PBS and 1 x with DMEM<sup>-/-</sup>. Volume of transfection medium (DMEM<sup>-/-</sup>), amount of DNA and appropriate volume of transfection reagent were chosen and handled according to manufacturer's instructions. Cells were kept for 6 h at 37°C and 5 % CO<sub>2</sub>. Transfection medium was changed to 10 % FCS – DMEM and cells were incubated for at least 24 h before further use.

#### 2.1.5 Viral transduction

**Phosphate Buffered Saline (PBS)**

140 mM NaCl, 10 mM Na<sub>2</sub>HPO<sub>4</sub>, 1.75 mM KH<sub>2</sub>PO<sub>4</sub>, dH<sub>2</sub>O, pH 7.4

**Cell culture medium (DMEM +/+)**

Dulbecco's Modified Eagle's Medium (DMEM) Glutamax<sup>TM</sup> containing 4.5 g/l D-glucose supplemented with 10 % heat inactivated fetal calf serum (FCS) and 1 % PenStrep solution (50 U/ml Penicillin, 50 Vg/ml Streptomycin)

Life-Technologies

WT and S1P-lyase deficient cells were transduced with a lentivirus construct encoding the human APP695 isoform containing the Swedish mutation. The construct drives furthermore a separate

expression of GFP by an internal ribosomal entry site (IRES). One day prior the transduction, cells were seeded into 6 well plates and cultured in 10 % FCS-DMEM to a confluency of 50 %. Cells were then incubated with lentiviral particles at  $2 \times 10^6$  IP/100000 cells for 15 hours and washed four times with DMEM and cultured for additional 48 hours. In a final step, transduced and GFP expressing cells were separated from non-transduced cells by using FACS (fluorescence-activated cell sorting).

### 2.1.6 RNAi transfection

#### **Phosphate Buffered Saline (PBS)**

140 mM NaCl, 10 mM Na<sub>2</sub>HPO<sub>4</sub>, 1.75 mM KH<sub>2</sub>PO<sub>4</sub>, dH<sub>2</sub>O, pH 7.4

#### **Cell culture medium (DMEM ++)**

Dulbecco's Modified Eagle's Medium (DMEM) Glutamax<sup>TM</sup> containing 4.5 g/l D-glucose supplemented with 10 % heat inactivated fetal calf serum (FCS) and 1 % PenStrep solution (50 U/ml Penicillin, 50 Vg/ml Streptomycin)

Life-Technologies

#### **Hiperfect**

Qiagen

#### **siRNA-FlexiTube**

Negative-control, Sgpl1 (S1P-lyase), Qiagen

For efficient genetic knock-down, murine N9 cells transfected with siRNA using the reverse-transfection method. First 25  $\mu$ l of siRNA solution (10  $\mu$ M in dH<sub>2</sub>O) was spotted into 24 well plates. Next, 100  $\mu$ l of 1:20 diluted transfection reagent Hiperfect (Qiagen) was added onto the siRNA solution and incubated for 15 min. N9 cells were trypsinized and counted using a Neubauer counting chamber. A cell suspension with 150.000 cells/150  $\mu$ l 10 % FCS-DMEM was prepared and added onto the siRNA-transfection reagent spot. Cells were incubated at 37°C and 5 % CO<sub>2</sub> for 6 h, before replacing the medium. Cells were harvested and prepared for protein analysis after additional incubation for 24 h.

### 2.1.7 Calcium measurement

#### **Cell culture medium (DMEM ++)**

Dulbecco's Modified Eagle's Medium (DMEM) Glutamax<sup>TM</sup> containing 4.5 g/l D-glucose supplemented with 10 % heat inactivated fetal calf serum (FCS) and 1 % PenStrep solution (50 U/ml Penicillin, 50 Vg/ml Streptomycin)

#### **Fura-2AM**

Molecular Probes, Life-Technologies

#### **Phosphate Buffered Saline (PBS)**

140 mM NaCl, 10 mM Na<sub>2</sub>HPO<sub>4</sub>, 1.75 mM KH<sub>2</sub>PO<sub>4</sub>, dH<sub>2</sub>O, pH 7.4

#### **Artificial Cerebrospinal Fluid (ACSF)**

119mM NaCl, 26,2mM NaHCO<sub>3</sub>, 2,5mM KCl, 1mM NaH<sub>2</sub>PO<sub>4</sub>, 1,3mM MgCl<sub>2</sub>, 10mM glucose, dH<sub>2</sub>O (+ 200  $\mu$ M GPN in DMSO)

Cells were grown on cover slips until 70 % confluency and loaded with the  $\text{Ca}^{2+}$  sensitive dye Fura-2AM® (Molecular Probes) for 30 min at 37°C. For measurements, cells were placed in a bathing chamber and incubated in ACSF under a constant flow. ACSF and GPN were washed in with a peristaltic pump (1 ml /min). Binding of  $\text{Ca}^{2+}$  to Fura2-AM changes its excitation peak from 340 nm to 380 nm and emits at a wavelength of 505 nm.  $\text{Ca}^{2+}$  concentrations were determined with a Axioskop FS2A microscope (Zeiss) and the Tida program (HEKA electronics). Quantitative analysis was carried out with IGOR 6.22 (WaveMetrics).

## 2.2 Protein biochemical techniques

### 2.2.1 Protein extraction

#### **Phosphate Buffered Saline (PBS)**

140 mM NaCl, 10 mM  $\text{Na}_2\text{HPO}_4$ , 1.75 mM  $\text{KH}_2\text{PO}_4$ ,  $\text{dH}_2\text{O}$ , pH 7.4

#### **STEN-Lysis Buffer**

50 mM Tris, 150 mM NaCl, 2 mM EDTA, 1 % (v/v) NP40 (Sigma-Aldrich), 1 % (v/v) Triton X-100 (Sigma-Aldrich),  $\text{dH}_2\text{O}$ , pH 7.4

#### **25 x Protease inhibitor (PI) cocktail**

1 x Tablets in 2 ml  $\text{dH}_2\text{O}$

Cells were washed briefly with ice-cold PBS, and kept on ice to reduce metabolic activity and degradation. Cells were harvested with a rubber policeman in 300 – 400  $\mu\text{l}$  STEN-Lysis buffer containing Complete® protease inhibitor. The cell homogenates were kept on ice for 15 minutes and subsequently centrifuged at 16000 x g for 10 min. The supernatant was used for further analysis.

### 2.2.2 Extraction of membrane proteins

#### **Phosphate Buffered Saline (PBS)**

140 mM NaCl, 10 mM  $\text{Na}_2\text{HPO}_4$ , 1.75 mM  $\text{KH}_2\text{PO}_4$ ,  $\text{dH}_2\text{O}$ , pH 7.4

#### **STEN-Lysis Buffer**

50 mM Tris, 150 mM NaCl, 2 mM EDTA, 1 % (v/v) NP40 (Sigma-Aldrich), 1 % (v/v) Triton X-100 (Sigma-Aldrich),  $\text{dH}_2\text{O}$ , pH 7.4

#### **Hypotonic Buffer**

10 mM Tris, 1 mM EDTA, 1 mM EGTA,  $\text{dH}_2\text{O}$ , pH 7.6

#### **25 x Protease inhibitor (PI) cocktail**

1 x Tablets in 2 ml  $\text{dH}_2\text{O}$

Similar to 2.2, cells were kept on ice and washed briefly with PBS. Next, cells were harvested with a rubber policeman in 750  $\mu\text{l}$  of hypotonic buffer containing protease inhibitor and incubated on ice for 15 min. Cells were then disrupted by repetitive suspension through a 0,6 mm cannula. The cell

homogenate was centrifuged at 1800 x g and 4°C for 5 min. The remaining supernatant was then centrifuged at 16000 x g and 4°C for 60 min to sediment cellular membranes. The cytosolic supernatant was discarded and the membranous pellet was lysed in STEN-lysis buffer. After 10 min of lysis on ice, particulate material was pelleted by a final centrifugation step at 16000 x g and 4°C for 10 min and supernatant subjected to further analysis.

### 2.2.3 Cell fractionation

**Phosphate Buffered Saline (PBS)**

140 mM NaCl, 10 mM Na<sub>2</sub>HPO<sub>4</sub>, 1.75 mM KH<sub>2</sub>PO<sub>4</sub>, dH<sub>2</sub>O, pH 7.4

**STEN-Lysis Buffer**

50 mM Tris, 150 mM NaCl, 2 mM EDTA, 1 % (v/v) NP40 (Sigma-Aldrich), 1 % (v/v) Triton X-100 (Sigma-Aldrich), dH<sub>2</sub>O, pH 7.4

**Hypotonic D Buffer**

10 mM Tris, 10 mM NaCl, 0,1 mM EGTA, 25 mM β-Glycerophosphate, 1 mM DTT, 1xPI, dH<sub>2</sub>O, pH 7.4

**Hypotonic C Buffer**

25% Glycerol, 20 mM HEPES pH 7,9, 0,4 M NaCl, 1 mM EDTA pH 8,0, 1 mM EGTA, 25 mM β-Glycerophosphate, 1 mM DTT, 1xPI, dH<sub>2</sub>O, pH 7.4

**25 x Protease inhibitor (PI) cocktail**

1 x Tablets in 2 ml dH<sub>2</sub>O

**Optiprep diluent**

0,25 mM Sucrose, 6 mM EDTA, 60 mM HEPES-NaOH, dH<sub>2</sub>O, pH 7,4

To separate the cell homogenates into cytosolic, membranous and nuclear fractions, cells were briefly washed with PBS and harvested in 300 µl hypotonic-D buffer containing protease inhibitor and 1 mM DTT (*see* 2.2.2). Cells were first incubated on ice and disrupted by resuspension through a 0.6 mm cannula and 1 ml syringe, and then centrifuged at 1800 x g and 4°C for 5 min. The nuclei containing pellet was stored at -20°C until further handling. The supernatant was subsequently centrifuged at 16000 x g to separate membrane and cytosolic fractions. The cytosolic supernatant was also stored at -20°C, whereas the membrane pellet was lysed in STEN-lysis for 15 min on ice. Insoluble particles were separated by centrifugation at 16000 x g and 4°C for 10 min, and stored at -20°C. The nuclei containing pellet was resuspended in 75 – 100 µl of buffer C and incubated for 20 min on ice. After a final centrifugation step at 16000 x g and 4°C for 10 min, pellet was discarded and supernatant containing the nuclear fraction was stored at -20°C for further processing.

For a more subtle fractionation, subcellular compartments were separated by density centrifugation. Confluent cell cultures were briefly washed with PBS and membranes isolated as described in 2.2.2.



After discarding the nucleus and cytosolic fractions, pelleted membranes were resuspended in 500  $\mu$ l hypotonic buffer containing protease inhibitor and stirred overnight on a magnetic stirrer at 4°C. Samples were then loaded on a discontinuous gradient prepared with OptiPrep™ (Sigma Aldrich) according to *Table 4*. Separation was performed at 100000 x g at 4°C for 8 h with no break

*Table 4: Dilution scheme for the Optiprep (iodixanol) gradient.*

% layer	Optiprep (ml)	Diluent (ml)	Total Volume (ml)
50%	10	0	10
30%	6	4	10
20%	4	6	10
17,50%	3,5	6,5	10
15%	3	7	10
12,50%	2,5	7,5	10
7,50%	1,5	8,5	10
5%	1	9	10
2,50%	0,5	9,5	10

#### 2.2.4 Protein extraction from mouse brain

**Phosphate Buffered Saline (PBS)**

140 mM NaCl, 10 mM Na<sub>2</sub>HPO<sub>4</sub>, 1.75 mM KH<sub>2</sub>PO<sub>4</sub>, dH<sub>2</sub>O, pH 7.4

**STEN-Lysis Buffer**

50 mM Tris, 150 mM NaCl, 2 mM EDTA, 1 % (v/v) NP40 (Sigma-Aldrich), 1 % (v/v) Triton X-100 (Sigma-Aldrich), dH<sub>2</sub>O, pH 7.4

**Sucrose Buffer**

0,32 M Sucrose 1xPI, dH<sub>2</sub>O

**SDS Buffer**

2% SDS (w/v) dH<sub>2</sub>O

**25 x Protease inhibitor (PI) cocktail**

1 x Tablets in 2 ml dH<sub>2</sub>O

Depending on the experimental setup, mouse brains were either directly lysed in STEN-lysis buffer (whole brain lysate) or fractionized. The brains were first weighed and then homogenized in STEN-lysis buffer for whole brain lysis and homogenized using plastic hand homogenizer. Next, the homogenates were sonicated by applying 20 pulses at 70 % intensity, followed by 20 seconds of incubation on ice (5 repeats). After sonification, homogenates were kept for 30 min on ice and then

centrifuged at 16000 x g at 4° for 45 min. Pellets were discarded and the supernatants stored at -80°C for further analysis.

For fractionation, first soluble protein were extracted from weight brain in 0.32 M sucrose buffer containing protease-/phosphatase-inhibitor in a ratio of 1:5 (mg:µl) using a plastic hand homogenizer. Next, homogenates were sonicated and centrifuged as described above. While the soluble proteins containing supernatants were stored at -80°, the pellets were further used to extract water insoluble proteins. The pellets were first homogenized in 0.5 – 1 ml of 2 % SDS buffer containing protease-/phosphatase-inhibitor and then sonificated as before. After 30 min of incubation on ice the homogenates were then centrifuged for 45 min at 16000 x g at 4°C and the supernatants were stored at -80°C for further analysis.

### 2.2.5 Immunoprecipitation

**Phosphate Buffered Saline (PBS)**

140 mM NaCl, 10 mM Na<sub>2</sub>HPO<sub>4</sub>, 1.75 mM KH<sub>2</sub>PO<sub>4</sub>, dH<sub>2</sub>O, pH 7.4

**STEN-Lysis Buffer**

50 mM Tris, 150 mM NaCl, 2 mM EDTA, 1 % (v/v) NP40 (Sigma-Aldrich), 1 % (v/v) Triton X-100 (Sigma-Aldrich), dH<sub>2</sub>O, pH 7.4

**STEN Washing Buffer**

50 mM Tris, 150 mM NaCl, 2 mM EDTA, 0.2 % (v/v) NP40 (Sigma-Aldrich), pH 7.6

**STEN-NaCl**

50 mM Tris, 500 mM NaCl, 2 mM EDTA, 0.2 % (v/v) NP40 (Sigma-Aldrich), dH<sub>2</sub>O, pH 7.6

**25 x Protease inhibitor (PI) cocktail**

1 x Tablets in 2 ml dH<sub>2</sub>O

**Protein G sepharose** (Invitrogen)

Particular proteins can be precipitated with specific antibodies coupled to protein A sepharose beads from cell lysates. To prevent unspecific protein-bead interaction, first 30 µl of the beads were first pre-incubated with cell lysates (*see* 2.2.1) at 4°C on a rotatory shaker for 1 h. Beads were centrifuged after pre-clearing at 9300 x g and 4°C for 10 min and the supernatant was transferred to fresh 30 µl beads including antibody (*see* Table 6). The sepharose-antibody-sample solution was incubated overnight at 4°C on a rotatory shaker. Protein A is coupled to the sepharose beads and binds rabbit IgG, which in turn is capable of binding the protein of interest. After sedimentation of the beads at 9300 x g and 4°C for 10 min, the supernatants were discarded and the beads washed successively once with STEN-NaCl buffer and three times STEN-washing buffer on a rotatory shaker. After each washing step, beads were

collected by centrifugation. After a final centrifugation, beads were first dried, then supplemented with 20  $\mu$ l of 2 x loading buffer and boiled for 10 min at 95°C.

### 2.2.6 Protein estimation

**BCA protein assay kit (Thermo Scientific)**  
 140 mM NaCl, 10 mM Na<sub>2</sub>HPO<sub>4</sub>, 1.75 mM KH<sub>2</sub>PO<sub>4</sub>, dH<sub>2</sub>O, pH 7.4  
**5 x Loading/Sample Buffer**  
 50 % (v/v) Glycerin, 7.5 % (w/v) SDS, 0.1 M DTT, 0.025 mg/ml bromphenol blue  
**4 x LDS/Sample Buffer**  
 Life-Technologies

Samples were analyzed for their protein concentration using the bicinchoninic acid assay (Thermo Scientific) in 96 well plates. This colorimetric assay is based on the reduction of Cu<sup>2+</sup> to Cu<sup>1+</sup> in the presence of peptide bonds, which is proportional to the protein amount. For determination of the protein concentration, samples were diluted 1:10 – 1:20 and mixed with the reaction reagent according to the manufactures protocol. After 30 min of incubation at 37°C, the samples were analyzed at 562 nm in a plate reader (Thermo Scientific). Protein concentrations were estimated using a standard curve obtained with BSA. All protein samples were adjusted to the same protein concentration (1 – 2,5  $\mu$ g/ $\mu$ l) adding 5 x loading buffer (final concentration 1 x) and H<sub>2</sub>O. Samples used for NuPage® were prepared with a commercially available 4 x LDS buffer and supplemented with 10 mM DTT. For detection of presenilins, the H<sub>2</sub>O in the loading buffer was substituted by 8 M urea. Samples were boiled at 100°C for SDS-PAGE, 80°C for NuPage® and 70°C for presenilins.

### 2.2.7 Sodium dodecyl sulfate polyacrylamide gel electrophoresis (SDS-PAGE)

**Acrylamide/Bisacrylamide solution**  
 30% (v/v) Acrylamide/Bisacrylamide (ratio 37,5:1)  
**Separation Buffer**  
 1.5 M Tris, 0.4 % (w/v) SDS, dH<sub>2</sub>O, pH 8.8  
**Stacking Buffer**  
 500 mM Tris, 0.4 % (w/v) SDS, dH<sub>2</sub>O, pH 6.8  
**Ammonium persulfate**  
 10 % (w/v) Ammonium persulfate, dH<sub>2</sub>O  
**Tetramethylethylenediamine (TEMED)**  
 Carl Roth  
**Running Buffer SDS (2x)**  
 25 mM Tris, 200 mM Glycine, 0.1 % (w/v) SDS, dH<sub>2</sub>O  
**Running Buffer LDS**  
 Life-Technologies

## Material and Methods

SDS-PAGE was carried out to separate proteins according to their molecular weight. First, a separation gel was poured in between a pair of glass plates and polymerized. Next, a stacking gel with a lower pH was poured on top of the separation gel. The concentration of the buffers and acrylamide/bis-acrylamide and their resolution capacity is displayed in the *Table 5*. Proteins separate in the SDS containing buffer due to a negative charge towards the cathode of an electric field with a constant current of 140 – 150V and 400mA.

In some applications, proteins were separated on NuPage® (LifeTechnologies) gels. This system uses a bis-tris buffer, which allows a lower pH during the run and therefore reduces the smile-shape running of the samples. The used gels had a continuous acrylamide/bis-acrylamide gradient from 4 – 12%, which allowed the detection of proteins with very different molecular masses on the same gel. The samples were separated under similar current conditions of 140 – 150 V and 400mA.

*Table 5: Composition of the SDS gels for protein separation.*

Buffer	Separation			Stacking
Percentage	7%	10%	12%	5%
AA/BA	4,7 ml	6,7 ml	8 ml	1,3 ml
Tris/SDS Buffer	5 ml (pH 8,8)	5 ml (pH 8,8)	5 ml (pH 8,8)	2,5 ml (pH 6,8)
H <sub>2</sub> O	10,3 ml	8,3 ml	7 ml	6,2 ml
APS	50 µl	50 µl	50 µl	25 µl
TEMED	50 µl	50 µl	50 µl	25 µl
MW range	120 – 80 kDa	80 – 40 kDa	40 – 10 kDa	-

## 2.2.8 Western immunoblotting

**Blotting Buffer**5 mM Tris, 200mM Glycine, 10% (v/v) methanol, dH<sub>2</sub>O**Ponceau Solution**3 % (w/v) Ponceau S, 3 % (w/v) trichloroacetic acid, dH<sub>2</sub>O**Phosphate Buffered Saline +/- Tween**

PBS, 0.05 % (v/v) Tween20, pH 7.4

**Skim Milk Blocking Buffer**

PBS/T, 4 % (w/v) skimmed milk powder (Roth)

**LiCor Blocking Solution**

LiCor

**Antibody Solution**PBS-T, specific antibody (for dilution see *Table 6* for primary and *Table 7* for secondary antibodies)**Enhanced chemiluminescence (1:1)**Solution 1 0.1 M Tris pH 8.5, 0.4 mM cumaric acid, 0.25 mM luminol, dH<sub>2</sub>OSolution 2 0.1 M Tris pH 8.5, 0.018 % H<sub>2</sub>O<sub>2</sub>, dH<sub>2</sub>O

Proteins separated in by gel electrophoresis where subsequently transferred onto a nitrocellulose membrane by Westernblotting. The nitrocellulose membrane was put on the gel both packed between filter papers soaked and surrounded by transfer buffer. The transfer was carried out for period of 2 h at 400 mA and 180V. After transfer, the membranes were briefly checked for protein transfer efficiency by staining with ponceaus S, a reversible and unspecific diazo dye, and then blocked in 5% skim milk in PBS-T for 45 min. Primary antibody incubation was carried out either at 4°C overnight or at room temperature for 2 h on a rotator. The membranes were then subsequently washed with PBS-T three times for 10 min, before incubating with the secondary HRP-conjugated antibodies for 60 min at room temperature. The primary and secondary antibodies and respective concentrations are listed in *Table 6* and *Table 7*. Before detection, membranes were washed repetitively five times for 5 min with PBS-T and bathed in a 2-competent enhanced chemiluminescence (ECL) solution. The conjugated HRP leads to an enzymatic reaction within in the ECL solution emitting photons. These photons then were detected and quantified using the BioRad ChemiDoc™ imager and the Quantity One 1D-analysis software. For the LiCor method, membranes were washed three times for 10 min with PBS-T after primary antibody incubation. Secondary IR-fluorescence conjugated antibodies were then incubated with the membranes for 60 min at room temperature and washed repetitively five times for 5 min with PBS-T and additionally 5 min with PBS. Due to the different emission wavelength of the IR-conjugates, this technique allows simultaneous detection of two proteins. All secondary antibodies and

## Material and Methods

used concentrations are listed in *Table 7*. Detection and quantification of signals was carried out using the LiCor Odyssey CLx™ imager and the embedded Odyssey CLx™ imaging software.

*Table 6: List of the primary antibodies used for western immunoblotting, immunocytochemistry and immunoprecipitation.*

Antibody	Target	WB (dilution)	ICC (dilution)	IP (dilution)	Species	Company
<b>C1/6.1</b>	APP - c-terminus	1:1000	1:400	-	mouse	Covance
<b>m3.2</b>	APP - A $\beta$ domain	1:1000	1:400	-	mouse	Covance
<b>6E10</b>	APP - A $\beta$ domain (human specific)	1:1000	-	-	mouse	Covance
<b>Sgpl1</b>	S1P-lyase	1:1000	-	-	rabbit	Abcam
<b><math>\alpha</math>GFP</b>	GFP	1:5000	-	-	mouse	Roche
<b><math>\beta</math>-Actin</b>	Actin	1:4000	-	-	mouse	Sigma-Aldrich
<b>192sw</b>	sAPP $\beta$ (Swedish variant specific)	1:1000	-	-	Rabbit	(Knops et al, 1995)
<b>140</b>	APP - c-terminus	1:1000	-	3 $\mu$ g	Rabbit	Lab AG Walter
<b>31.09</b>	PS1-c loop	-	-	3 $\mu$ g		Lab AG Walter
<b>Abl93</b>	Lamp2	1:2000	1:500	-	rat	DSHB
<b><math>\alpha</math>cathepsin D</b>	cathepsin D	1:1000	1:250	-	rabbit	Lab AG Hönig
<b><math>\alpha</math>Gm2a</b>	Gm2a	1:1000	-	-	rabbit	Lab AG Sandhoff
<b>LC3</b>	LC3	1:1000	-	-	rabbit	MBL
<b>H-70</b>	Calnexin	1:1000	1:250	-	rabbit	SantaCruz
<b>Bip/GRP78</b>	Bip/GRP78	-	1:250	-		BD Bioscience
<b>TGN46</b>	TGN46	-	1:250	-		Sigma-Aldrich
<b>Giantin</b>	Giantin	-	1:250	-		Signa-Aldrich
<b>EEA1</b>	EEA1	-	1:250	-	mouse	BD Bioscience
<b>PKC</b>	PKC	1:1000	-	-	rabbit	Abcam

Table 7: List of secondary antibodies used for western immunoblotting and immunocytochemistry.

Antibody	Target	WB (dilution)	ICC (dilution)	Company
<b><math>\alpha</math>-mouse-HRP</b>	mouse IgG	1:25000	-	Sigma-Aldrich
<b><math>\alpha</math>-rabbit-HRP</b>	rabbit IgG	1:25000	-	Sigma-Aldrich
<b><math>\alpha</math>-rat-HRP</b>	rat IgG	1:5000	-	
<b><math>\alpha</math>-mouse-IRDye800CW</b>	mouse IgG	1:15000	-	LiCor
<b><math>\alpha</math>-rabbit-IRDye800CW</b>	rabbit IgG	1:15000	-	LiCor
<b><math>\alpha</math>-rat-IRDye800CW</b>	rat IgG	1:15000	-	LiCor
<b><math>\alpha</math>-mouse-IRDye680CW</b>	mouse IgG	1:15000	-	LiCor
<b><math>\alpha</math>-rabbit-IRDye680CW</b>	rabbit IgG	1:15000	-	LiCor
<b><math>\alpha</math>-rat-IRDye680CW</b>	rat IgG	1:15000	-	LiCor
<b>ms-Alexa 488</b>	mouse IgG	-	1:1000	LifeTechnologies
<b>ms-Alexa 546</b>	mouse IgG	-	1:1000	LifeTechnologies
<b>ms-Alexa 647</b>	mouse IgG	-	1:500	LifeTechnologies
<b>rb-Alexa 488</b>	rabbit IgG	-	1:1000	LifeTechnologies
<b>rb-Alexa 546</b>	rabbit IgG	-	1:1000	LifeTechnologies
<b>rb-Alexa 647</b>	rabbit IgG	-	1:500	LifeTechnologies
<b>rat-Alexa 488</b>	rat IgG	-	1:1000	LifeTechnologies

### 2.2.9 Measurements of A $\beta$

For detection of A $\beta$ , 500  $\mu$ l of fresh media was added to cells overnight. Conditioned media was cleared by centrifugation and then analyzed by electrochemiluminescence technology (MesoScale Discovery) for A $\beta$ 40 and A $\beta$ 42 according to the manufacturer's protocol.

### 2.3 Molecular biological techniques

#### 2.3.1 mRNA extraction and Reverse-Transcription polymerase chain reaction (rt-PCR).

**Micro RNeasy mRNA Isolation Kit**

Qiagen

**DNA Digestion.**

 6 µg RNA, 2 µl DNaseI, 4 µl DNase Buffer, add 20 µl dH<sub>2</sub>O

**SuperScript III Reaction Mix**

 10 µl DNA free mRNA, 1 ml Random Hexamers, 1 µl dNTPs, 2 µl 10xRT Buffer, 4 µl MgCl<sub>2</sub>, 2 µl DTT, 1 µl RNaseOUT, 1 µl SuperScript III

**TBE Buffer**

 9 mM Tris-Borat, 2 mM EDTA, dH<sub>2</sub>O, pH 8,0

**6 x Orange Loading Dye**

 60 % Glycerin, 0,15 % Orange G, 60 mM EDTA, 10 mM Tris, dH<sub>2</sub>O, pH 7,6

**Agarose-Gel**

1 – 2 % (w/v) Agarose in TBE Buffer + 1:10000 GelRed (Biotium)

Messenger RNA from WT and S1P-lyase deficient cells was isolated using the RNeasy micro kit (Qiagen) according to the manufacturer's protocol. Prior to the reverse transcription-PCR (rt-PCR), the isolated mRNA was incubated with DNaseI and to digest remaining DNA. Reverse transcription was then performed using the SuperScriptIII kit (Qiagen) according to manufacturer's protocol. Next transcripts were amplified in a PCR using the primers listed in *Table 8*. The PCR program for the amplification was set to following temperatures and times.

- |                         |      |        |
|-------------------------|------|--------|
| 1. Initial Denaturation | 94°C | 3 min  |
| 2. Denaturation         | 94°C | 30 sec |
| 3. Annealing            | 59°C | 30 sec |
| 4. Elongation           | 72°C | 30 sec |
| 5. Final Elongation     | 72°C | 5 min  |

Steps 2 – 4 were repeated for 30 cycles and the final PCR products were prepared with 6 x orange loading dye and analyzed in a 1 - 2 % continuous agarose gel with GelRed.

#### 2.3.2 Quantitative real time PCR (q-PCR)

**dH<sub>2</sub>O**

RNase free

**SYBR green PCR Master Mix**

Applied Biosystems

Quantitative analysis of mRNA expression was performed by *q-PCR*. First mRNA of WT and S1P-lyase cells were isolated as described in 2.3.1 and mixed with SYBR green (Applied Biosystems, Life-



Technologies), RNase free dH<sub>2</sub>O and primers for analysis. The program for amplification was set to following temperatures and times.

1. Initial Denaturation      95°C    10 min
2. Denaturation              95° C   15 sec
3. Annealing & Elongation    60° C   1 min
4. Dissociation               95° C   15 sec

Steps 2 – 3 were repeated for 40 cycles and the respective PCR products were analyzed in the Applied Biosystems 7300 Real-Time PCR System.

*Table 8: List of primers used for rt-PCR and q-PCR.*

target gene	primer sequence	method
<b>S1pr1</b>	For: ctctccgcagctcagtctct	<i>rt-PCR</i>
	Rev: taatgccatggctcttctcc	
<b>S1pr2</b>	For: actggctatcgtggctctgt	<i>rt-PCR</i>
	Rev: cagccagcagatgatgaaaa	
<b>S1pr3</b>	For: gggagggcagtatgttcgta	<i>rt-PCR</i>
	Rev: agcacatcccaatcagaagg	
<b>S1pr4</b>	For: ggctactggcagctatcctg	<i>rt-PCR</i>
	Rev: aagagcacatagcccttgga	
<b>S1pr5</b>	For: aacttgctgtgctcttggt	<i>rt-PCR</i>
	Rev: ccggacagtaggatgttggt	
<b>Gm2a</b>	not available (Qiagen: QT00071967)	<i>q-PCR</i>
<b>HexA</b>	not available (Qiagen: QT00100247)	<i>q-PCR</i>
<b>HexB</b>	not available (Qiagen: QT00113946)	<i>q-PCR</i>

#### 2.4 Secretase activity measurements

Secretase measurements were in living cells (2.4.1) and in purified membranes (2.4.2) were performed in collaboration with Prof. Dr. Tobias Hartmann and Dr. Marcus Grimm (Department of Experimental Neurology, Saarland University).

**Phosphate Buffered Saline (PBS)**

140 mM NaCl, 10 mM Na<sub>2</sub>HPO<sub>4</sub>, 1.75 mM KH<sub>2</sub>PO<sub>4</sub>, dH<sub>2</sub>O, pH 7.4

**Life Cell Imaging Solution**

40 mM NaCl, 5 mM KCl, 8 mM CaCl<sub>2</sub>, 1 mM MgCl<sub>2</sub>, 20 mM HEPES, dH<sub>2</sub>O, pH 7.4

(30 μM β- γ-secretase fluorogenic substrate)

(12 μM γ-secretase fluorogenic substrate)

**Secretase Activity Sucrose Buffer**

10mM Tris/HCl, 1 mM EDTA, 200mM sucrose, dH<sub>2</sub>O, pH 7,5

**Hypotonic Buffer**

10 mM Tris, 1 mM EDTA, 1 mM EGTA, dH<sub>2</sub>O, pH 7.6

**25 x Protease inhibitor (PI) cocktail**

1 x Tablets in 2 ml dH<sub>2</sub>O

**Citrate Buffer**

150 mM Sodium citrate, dH<sub>2</sub>O, pH 6,4 (citric acid adjusted)

#### 2.4.1 β- and γ-secretase assay in living cells

Detection of secretase activity in living cells was performed as described previously with slight modifications (Grimm et al, 2013). Shortly after incubation, cells were washed two times with pre-warmed life cell imaging solution (Hepes buffer, pH 7,4). Next, buffer was removed and 50 μl life cell imaging solution containing 30 μM β- and 12 μM γ-secretase fluorogenic substrate (Calbiochem, Darmstadt, Germany) was added. Fluorescence was measured continuously at an excitation wavelength of  $355 \pm 10$  nm and emission wavelength of  $440 \pm 10$  nm for gamma-secretase or  $345 \pm 5$  nm/ $500 \pm 2,5$  nm for beta-secretase at 37° C under light exclusion using a Safire Infinity Fluorometer (Tecan, Crailsheim, Germany).

#### 2.4.2 β- and γ-secretase assay in purified membranes

Measurements were performed as described previously (Burg et al, 2013). In brief, after incubation cells were washed three times with ice-cold PBS, harvested in sucrose buffer and homogenized using a PotterS (Braun, Melsungen, Germany) at maximum speed (25 strokes). Protein amount was determined according to Smith et al. (Smith et al, 1985). PNFs were ultracentrifuged at 135500 x g for 75min at 4°C. Purified membranes were reconstituted in sucrose buffer using a Minilys (Bertin Technologies, Montigny-le-Bretonneux, France) with Precelly glass beads (Pcqlab, Erlangen, Germany) at medium speed for 10 s. Protein amount was adjusted to 125 μg for β-secretase activity and 250 μg for γ-secretase activity. Fluorogenic β-secretase substrate (20 μM) and γ-secretase substrate (10 μM) was added (Calbiochem, Darmstadt, Germany). Fluorescence was measured

continuously at an excitation wavelength of  $355 \pm 10$  nm and an emission wavelength of  $440 \pm 10$  nm for  $\gamma$ -secretase or  $345 \pm 5$  nm/ $500 \pm 2,5$  nm for  $\beta$ -secretase at  $37^\circ$  C under light exclusion using a Safire Infinity Fluorometer (Tecan, Crailsheim, Germany).

#### 2.4.3 *In vitro* $\gamma$ -secretase assay

**Phosphate Buffered Saline (PBS)**

140 mM NaCl, 10 mM  $\text{Na}_2\text{HPO}_4$ , 1.75 mM  $\text{KH}_2\text{PO}_4$ ,  $\text{dH}_2\text{O}$ , pH 7.4

**Hypotonic Buffer**

10 mM Tris, 1 mM EDTA, 1 mM EGTA,  $\text{dH}_2\text{O}$ , pH 7.6

**25 x Protease inhibitor (PI) cocktail**

1 x Tablets in 2 ml  $\text{dH}_2\text{O}$

**Citrate Buffer**

150 mM Sodium citrate,  $\text{dH}_2\text{O}$ , pH 6,4 (citric acid adjusted)

The *in vitro*  $\gamma$ -secretase for APP cleavage was previously described by Sastre and colleagues (Sastre et al, 2001). First, isolated cell membranes (*see* 2.2.2) were resuspended in citrate buffer containing protease inhibitor. Membrane-citrate buffer solutions were divided into aliquots of same volume and incubated under different conditions indicated in the respective experiments. Next, samples were centrifuged at  $16000 \times g$  for 60 min. The resulting pellets and supernatants were prepared for SDS-PAGE and western immunoblotting as indicated in 2.2.7 and 2.2.8.

#### 2.5 Lipid analysis

**Phosphate Buffered Saline (PBS)**

140 mM NaCl, 10 mM  $\text{Na}_2\text{HPO}_4$ , 1.75 mM  $\text{KH}_2\text{PO}_4$ ,  $\text{dH}_2\text{O}$ , pH 7.4

**ExMi**

Chloroform/Methanol/ $\text{H}_2\text{O}$  (2:1:0,2)

**RP-18**

Carl Roth

**Diethylaminoethylcellulose (DEAE)**

Carl Roth

**Running Buffer**

Chloroform / Methanol / 0,22 %  $\text{CaCl}_2$  (60/35/8)

##### 2.5.1 Lipid extraction and thin layer chromatography

Cells were cultured until 90 % confluency and washed three times with PBS. Cells were harvested in 1 ml PBS and mixed vigorously with 4 ml of methanol and 3 ml of ExMi for 48 h at  $37^\circ\text{C}$  for lipid extraction. The supernatant was first filtered through a cotton filter and subsequently vaporized with

N<sub>2</sub>. Next, the lipid pellet was resuspended in 1 ml 2:1 chloroform/methanol and mixed with 62,5 µl 4 M NaOH for alkaline hydrolysis at 37°C for 2 h. Suspension was then neutralized by adding 10 µl acetic acid and vaporized. For deionization, first glass-wool columns were filled with 2 ml RP-18 and rinsed with a chloroform/methanol/0,1 M KCl (6/96/94) mix. The remaining samples were reconstituted in 1 ml methanol and sonicated. After addition of 1 ml 300 mM NH<sub>4</sub>Ac, samples were added to the columns and washed two times with 200 µl of 300 mM NH<sub>4</sub>Ac and six times with 300 µl H<sub>2</sub>O. Samples were eluted from the column by washing with 8 ml 1:1 chloroform/methanol and vaporized with N<sub>2</sub>. For separation of acidic and neutral lipids, samples were first reconstituted in 1 ml chloroform/methanol/H<sub>2</sub>O (3:7:1) and subsequently filtered through a DEAE-sepharose column. Flow through of the filtrated samples represents the neutral lipids, while acidic lipids were eluted from the column separately with 1 ml chloroform/methanol mix. Both fractions were vaporized with N<sub>2</sub> and remaining lipids were reconstituted in 400 µL methanol and stored at -80°C until separation.

For thin layer chromatographic separation of the lipids, methanol solubilized samples were first vaporized with N<sub>2</sub>, then reconstituted in 25 µM ExMi and applied to silica gel plates. Samples were separated in a chloroform/methanol/0,22 % CaCl<sub>2</sub> (60/35/8) running buffer and detected after immersion in a phosphoric acid-copper sulfate solution and carbonization at 180°C.

### 2.5.2 Mass spectrometry analysis

Liquid chromatography coupled to triple-quadruple mass spectrometry (LC/MS/MS) analysis was performed in collaboration with Prof. Dr. Markus Gräler (Clinic for Anesthesiology and Intensive Care Medicine, University Hospital Jena). Cells were cultured on 60 cm<sup>2</sup> dishes, washed three times with PBS and harvested in 1 ml PBS. For lipid extraction, cell suspensions were mixed with 200 µl 6N hydrochloric acid, 1 ml of methanol and 2 ml chloroform. Lower chloroform phases were isolated and vacuum-dried at 50°C for 50 min. Lipid extracts were dissolved in 100 µl methanol/chloroform (4:1, v/v) and used for LC/MS/MS as previously described (Karaca et al, 2014). Level of S1P and sphingosine were normalized to the protein concentrations of the individual samples.

### *2.6 Statistical analysis*

All experiments were performed at least two times and the individual values for statistical analysis are indicated in the respective figure legends. Statistical analyses were carried out by a two-sided student's t-test and indicated as followed P-values:  $p < 5\%$ , \*;  $p < 1\%$ , \*\*;  $p < 0,1\%$ , \*\*\*.

### 3. Results

#### 3.1 Modulation of the intracellular S1P concentration affects the metabolism of APP.

##### 3.1.1 Accumulation of S1P in S1P-lyase deficient cells.

Lysosomal lipid storage could affect the metabolism of APP. Accumulation of the ganglioside GM2 in Sandhoff disease or cholesterol and sphingosine in Niemann-Pick C (NPC1) have been shown to modulate the generation of A $\beta$  and the proteolytic turnover of APP in endosomal/lysosomal compartments (Jin et al, 2004; Keilani et al, 2012; Malnar et al, 2012; Tamboli et al, 2011b; Tamboli et al, 2005). There is also evidence for altered processing of APP in other LSDs like Tay-Sachs disease or Niemann-Pick A (Keilani et al, 2012; Tamboli et al, 2011b). However, little is known about the impact of S1P on the metabolism of APP. To investigate the role of S1P, first mouse embryonic fibroblast of WT and S1P-lyase deficient mice were used. As expected, Western immunoblotting proved the lack of S1P-lyase in the S1PL-KO cells (*Fig. 8A*). LC/MS/MS analysis revealed a significant elevation of intracellular S1P concentrations in S1P-lyase KO cells as compared to WT cells (*Fig. 8B*). However, the concentrations of S1P in the conditioned media of WT and S1PL-KO cells were similar, indicating a predominant effect of S1PL deficiency on the intracellular S1P pool (*Fig. 8C*).

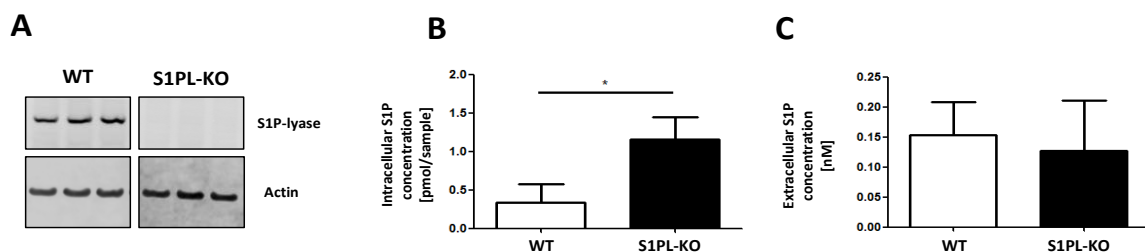


**Fig. 8: Effect of S1P-lyase knock-out on S1P concentration.** (A) Detection of S1P-lyase in isolated membranes of WT and S1P-lyase KO cells by Western immunoblotting. (B, C) Mass spectrometry analysis of intracellular and extracellular S1P concentrations in WT and MEF-S1PL-KO. Cells were washed and lipids extracted according to protocol (*see 2.5.2*) and subjected to LC/MS/MS (B). Levels of S1P were measured in conditioned media of cells (C) (n=3).

### 3.1.2 Genetic deletion of S1P-lyase results in increased levels of APP-FL and APP-CTFs.

After demonstration of functional effects of the S1P-lyase KO on the intracellular S1P concentration, the expression of APP-FL and APP-CTFs was investigated. First, membranes of WT and S1P-lyase deficient MEFs were isolated and analyzed by Western immunoblotting. Cells lacking S1P-lyase showed a significant accumulation of APP-FL and its derivatives from proteolytic processing, including  $\alpha$ CTFs,  $\beta$ CTFs and  $\beta$ CTFs\* (Fig. 9A, B). APP- $\beta$ CTF\* is an additional cleavage product of APP generated by alternative processing at position Glu11 within the A $\beta$  domain of APP (Fluhrer et al, 2002; Haass et al, 1992b; Liu et al, 2002). Consistent with a previously described conversion of  $\beta$ CTFs and  $\beta$ CTFs\* into  $\alpha$ CTFs by the  $\alpha$ -secretase (Fluhrer et al, 2002), highest accumulation was observed for  $\alpha$ CTFs. In addition to cells of WT and S1PL-KO, brain homogenates of respective mice were analyzed. Interestingly, level of APP-FL and APP-CTFs in brain lysates of WT and S1PL-KO mice showed only little if any differences (Fig. 9C). However, this experiment was performed with single individuals of 2 weeks old mice and has to be repeated with a higher number of individuals of different age. To rule out potential clonal variations between WT and S1PL-KO cells, a knock down by RNAi was performed in an independent cell line. Targeting S1P-lyase mRNA significantly decreased the expression of the relevant protein. Interestingly, levels of APP-FL were increased upon RNAi-mediated knock-down of S1P lyase (Fig. 9D, E, F). APP-CTFs could not be detected in this experiment due to a general low expression of APP in this cell type. Thus, these data point to an influence of S1P-lyase deficiency on APP levels, which might be due to increased levels of intracellular of S1P.

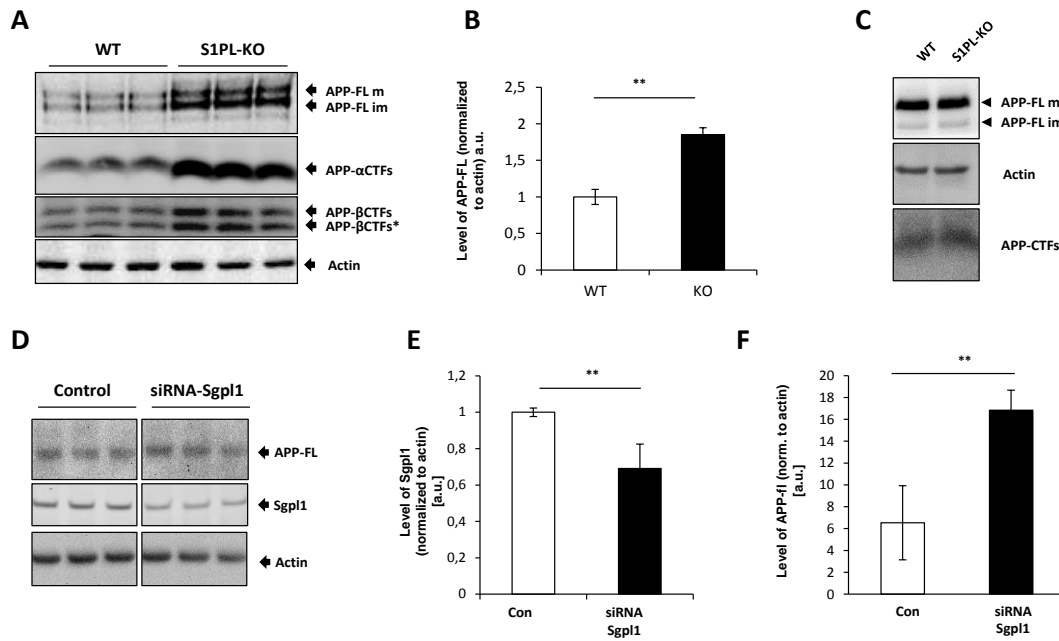


**Fig. 9: Genetic deletion of the S1P-lyase gene results in accumulation of APP-FL and APP-CTFs.** (A) Detection of APP-FL, APP- $\alpha$ CTFs, APP- $\beta$ CTFs and APP- $\beta$ CTFs\* in WT and S1P-lyase KO cells by western immunoblotting. (B) Quantification and statistical analysis of APP-FL in WT and S1P-lyase KO cells (n=9). (C) Analysis of brain lysate of 2 week old WT and S1PL-KO mice by western immunoblotting. A slight increase in APP-FL and APP-CTFs of S1PL-KO mice are present. (D) siRNA transfection of murine N9 cells to knock down the S1P-lyase expression. Targeting S1P-lyase mRNA decreases S1P-lyase protein level and increases APP-FL and APP-CTFs. (E) Quantification of the S1P-lyase expression efficiency of (D) for cells treated with target and control siRNA (n=3). (F) Quantification of the APP-FL levels after siRNA transfection in N9 cells of (D) (n=3).

### 3.1.3 Pharmacological inhibition of sphingosine kinase decreases APP-FL and APP-CTFs.

To test whether the accumulation of APP-FL and APP-CTFs involves elevated S1P concentration, phosphorylation of sphingosine to S1P was inhibited by the specific sphingosine-kinase inhibitor SKiII. The effect of SKiII on APP was tested in WT and S1P-lyase KO cells, as well as in HEK293 cells expressing different human APP variants. First, the levels of intracellular S1P and sphingosine were determined using LC/MS/MS to proof inhibition of sphingosine phosphorylation. While concentrations of S1P were too low for quantitative analysis (data not shown), the S1P precursor sphingosine was significantly elevated in both WT and S1PL-KO cells upon application of SKiII (Fig. 10A). This data suggests an efficient inhibition of the sphingosine-kinases. Moreover, a 3 – 4 fold increased concentration of sphingosine was also observed in S1PL-KO cells (Fig. 10A). To show an effect of SKiII on S1P, cells were pretreated with sphingosine. Application of sphingosine enhances the sphingosine-kinase dependent phosphorylation of sphingosine to S1P. After 2 h of pre-incubation



with sphingosine, the sphingosine-kinase activity was inhibited by using 5  $\mu\text{M}$  of SKiII. The following mass spectrometry detection showed a significant reduction of S1P in both WT and S1P-lyase deficient cells (*Fig. 10B*). Notably, the concentration of S1P in WT cells fell below the minimum detection level (*Fig. 10B*). As shown by Takasugi and colleagues, S1P has a positive stimulatory effect on BACE1 mediated processing of APP (Takasugi et al, 2011). However, reduction of intracellular S1P by applying SKiII on WT and S1P-lyase deficient cells decreased the levels of APP-FL and  $\alpha\text{CTFs}$ . In addition, sAPP $\alpha$  levels in the conditioned medium were also reduced, indicating that the observed reduction of APP is not caused by its enhanced secretion (*Fig. 10C*). A further independent experiment with HEK293 and HEK-APP695 cells proved an influence of lowering S1P concentrations by SKiII on the levels of endogenous APP-FL and APP-CTFs (*Fig. 10D*). Notably, levels of overexpressed APP695-FL were not significantly affected by treatment with SKiII (*Fig. 10D*).

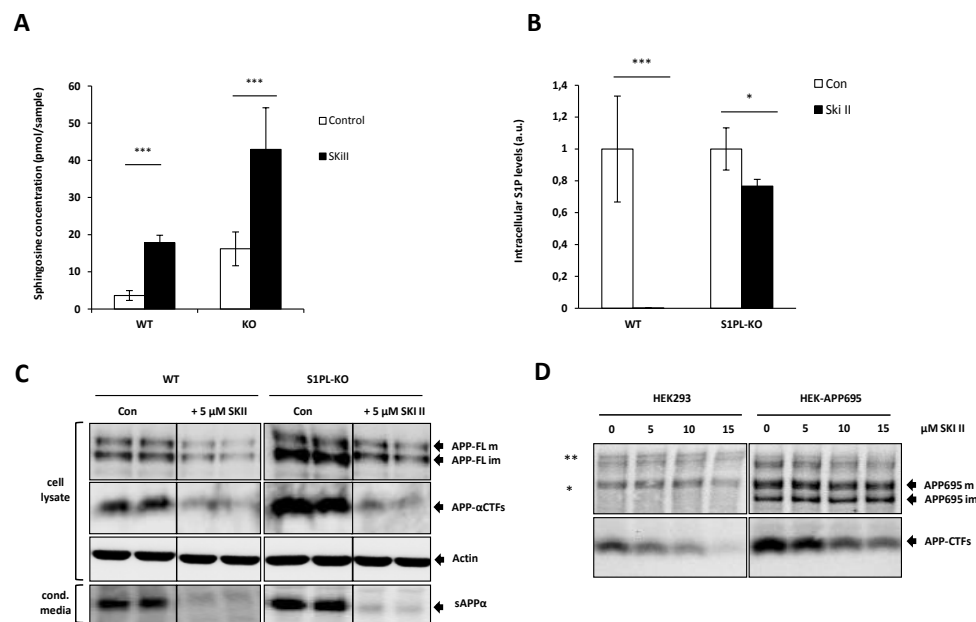


**Fig. 10: Pharmacological inhibition of sphingosine-kinases.** (A) Concentrations of sphingosine in WT and S1PL-KO cells determined by LC/MS/MS. Sphingosine was measured under basal condition and upon treatment with 5  $\mu\text{M}$  SKiII for 24 h. (n=3) (B) LC/MS/MS analysis of WT and S1P-lyase KO cells pretreated with 10  $\mu\text{M}$  sphingosine for 2 h, prior to the treatment with 5  $\mu\text{M}$  with SKiII (24 h) (n=3). (C) Western immunoblotting of purified membranes from WT and S1P-lyase KO cells treated with 5  $\mu\text{M}$  SKiII. (D) Western immunoblotting analysis of HEK293 cells expressing endogenous APP and overexpressing APP695. \* and \*\* indicate endogenous immature and mature APP isoforms, respectively.

### 3.1.4 Overexpression of S1P-lyase increases APP-FL and APP-CTFs.

Having shown that genetic deletion of the S1P-lyase causes a significant elevation of the intracellular S1P levels, as well as an accumulation of APP-FL and APP-CTFs, the next step was to reconstitute the gene by transfection. Both, WT and S1P-lyase deficient cells were transfected with a functional S1P-lyase-GFP fusion construct. In addition, an enzymatically inactive K353L mutant of the S1P-lyase-GFP cDNA was used as a control. Point mutation at position K353L inhibits binding of the co-factor pyridoxal-5'-phosphate and therefore the catalytic activity of S1P-lyase (Reiss et al, 2004). Both, WT and S1P-lyase deficient cells were transfected using different conditions of the transfection reagent and the cDNAs. After 30 h of transfection, membranes of WT and S1P-lyase KO cells were isolated and subjected to Western immunoblotting. The signal for S1PL-GFP increased consistently with an increase in the ratio of lipofectamine to DNA. Surprisingly, expression of both variants led to increased levels of APP-FL and APP-CTFs (*Fig. 11*). This increase of APP-FL and APP-CTFs is contradictory to the previously observed S1P-lyase effects. Overexpression of the construct might have induced stress and therefore caused an elevation of APP-FL. However, interpretation of this data is difficult, since intracellular concentrations of S1P were not measured. Nevertheless, similar effects of the catalytically active and inactive S1P-lyase constructs suggest an S1P independent effect of the transfection.

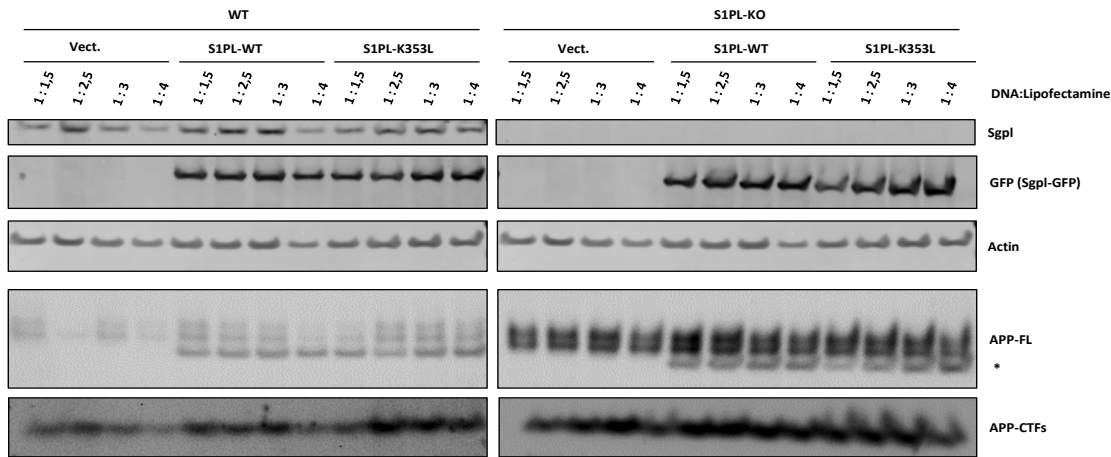


**Fig. 11: Reconstitution of S1P-lyase variants elevates the levels of APP-FL and APP-CTF.** Both WT and S1P-lyase deficient cells were transfected with an enzymatically active (WT) and inactive form (353L) of the S1P-lyase cDNA fused to a green fluorescent protein, as well as an empty pcDNA3.0 vector. Cells were transfected with different ratios of the transfection reagent (lipofectamine) and the S1P-lyase constructs. Expression of the S1PL-GFP is elevated with increasing lipofectamine to DNA ratio. APP-FL and APP-CTFs in WT and S1P-lyase deficient cells show a slight increasing trend upon transfection. Notably, the effects were independent of the enzymatically active or inactive S1P-lyase form. Bands marked with \* show residual signal from S1PL-GFP detection.

### 3.2 Modulation of the S1P-receptor activity has no effect on APP.

Although concentrations of S1P in conditioned media of WT and S1P-lyase deficient cells were not significantly different (Fig. 8C), the potential impact of S1P receptor mediated signaling on the APP metabolism was analyzed. First, the expression of the five G-protein coupled S1P receptors was analyzed. mRNA from WT and S1P-lyase deficient cells was isolated and analyzed as described in the section 2.3.1. rt-PCR revealed an expression of the S1PR1 and the S1PR2 in both WT and S1P-lyase deficient cells (Fig. 12A). While expression levels of S1PR1 was relatively low in both WT and S1P-lyase KO cells, signals for S1PR2 were stronger as compared to that of S1PR1 (Fig. 12A). To assess the potential functional involvement of S1PRs, cells were treated with their natural ligand S1P or specific receptor antagonists W146 and JTE-013. However, cell treatment with S1P for 6 h did not change levels of APP-FL or APP-CTF (Fig. 12B). Long-term treatment with 10  $\mu$ M S1P (24 – 48 h) also showed no effects on APP-FL and APP-CTFs (data not shown). Subsequently, both WT and S1P-lyase deficient cells were exposed to the antagonists JTE-013 and W146 that potently inhibit S1PR1 and S1PR2, respectively (Arikawa et al, 2003; Gonzalez-Cabrera et al, 2008; Osada et al, 2002; Sanna et al, 2006). While JTE-013 had no impact on APP-FL or the CTFs, W146 caused a slight decrease of

APP-FL in S1P-lyase KO cells (Fig. 12C). However, this effect was highly variable in different experiments and did not reach statistical significance (data not shown). Thus, the expression of S1PR1 and S1PR2 was shown for WT and S1P-lyase deficient cells, but a functional involvement of the receptors in APP metabolism remains unclear.

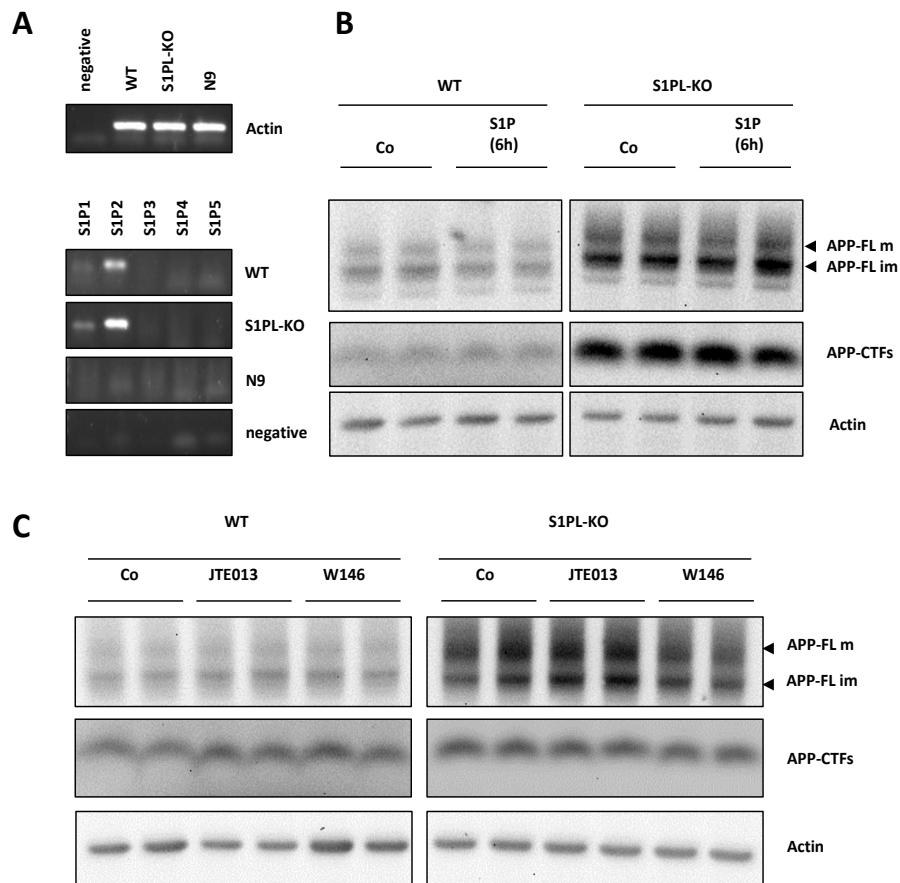


**Fig. 12: Inhibition of S1PR1 and S1PR2 using potent antagonists.** (A) Reverse transcriptase-PCR of S1PR1 – 5 in MEF-WT, MEF-S1PL-KO and N9 cells. WT and S1PL-KO cells show expression of S1PR1 and S1PR2. No expression detected in N9 cells or NTC (negative). (B, C) Western immunoblotting of isolated membranes from WT and S1P-lyase KO cells after activation of the S1P receptors with 10 $\mu$ M S1P for 6 h (B) and pharmacological inhibition of the S1PR1 (W146, 150 nM) and S1PR2 (JTE-013, 150 nM) for 24 h.

### 3.3 S1P-lyase deficiency affects the proteolytic processing of APP.

#### 3.3.1 Lack of S1P-lyase modulates the generation of A $\beta$ in APP695<sub>swe</sub> overexpressing cells.

To investigate whether S1P-lyase deficiency affects the generation of A $\beta$ , both WT and S1P-lyase deficient cells were stably transduced with a lentivirus construct encoding the human APP695 isoform containing the Swedish mutation. The construct also drives the separate expression of GFP by an internal ribosomal entry site (IRES). Western immunoblotting showed comparable expression levels of the construct in WT and S1P-lyase deficient cells as indicated by similar levels of GFP (*Fig. 13A*). Importantly, further analysis revealed a strong difference in the levels of APP695 between WT and S1P-lyase deficient cells. Cells lacking the S1P-lyase have strongly elevated levels of APP695 (*Fig. 13A*). Lack of APP695 signals in non-transduced cells demonstrated the specificity of the 6E10 antibody for the human APP isoform without cross-reaction for the endogenous mouse APP (*Fig. 13A*). Thus, these data confirm the effect of S1P lyase deficiency on APP metabolism even upon overexpression (see *Fig. 9A, D, F*). Conditioned medium of both, WT and S1P-lyase deficient cells was collected for 24 h and concentrations of different A $\beta$  variants determined using the highly sensitive MesoScale system. When levels of A $\beta$ 40 were normalized to GFP expression, S1P-lyase deficient cells showed a higher secretion compared to WT cells (*Fig. 13B*). Detection of A $\beta$ 42 levels however, revealed no significant differences between WT and S1P-lyase KO cells (*Fig. 13C*). Interestingly, secretion of both A $\beta$ 40 and A $\beta$ 42 was significantly decreased in S1P-lyase deficient cells, when levels of A $\beta$  were normalized to cellular levels of APP695-FL (*Fig. 13D, E*). This alteration in the product-precursor relationship of A $\beta$  and APP, points to an altered proteolytic processing of APP by secretases in the absence of S1P-lyase. Thus, further analysis of both A $\beta$  generating secretases, BACE1 and the  $\gamma$ -secretase is of great interest.

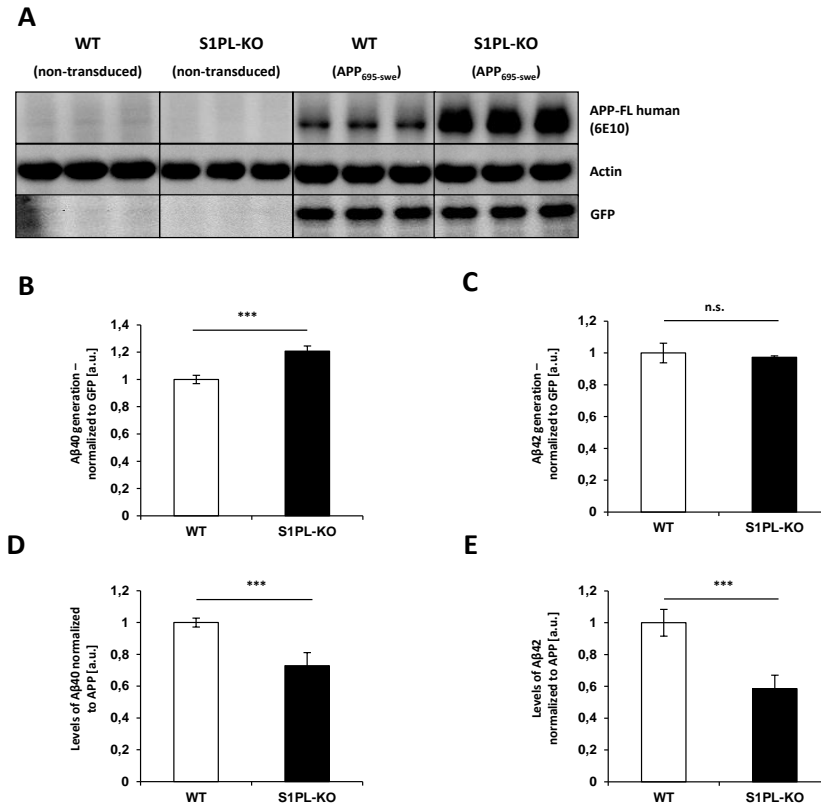


**Fig. 13: Decreased secretion of A $\beta$  in S1P-lyase KO cells.** (A) Western immunoblotting of isolated membrane from WT and S1PL-KO cells stably transduced with human APP<sub>695<sub>sw</sub></sub>-IRES-GFP. APP-FL was detected using a human specific antibody (6E10). The GFP levels show the expression rate of the construct. (B, C) MesoScale measurement of A $\beta$ 40 and A $\beta$ 42 levels in WT and S1P-KO cells normalized to GFP. (D, E) Levels of A $\beta$ 40 and A $\beta$ 42 normalized to the intracellular levels of human APP-FL (n=3).

### 3.3.2 Elevation of the S1P concentration decreases the activity of $\gamma$ - and $\beta$ -secretase.

#### 3.3.2.1 Direct modulation of the $\beta$ -secretase BACE1 through S1P.

A recently published study showed a stimulatory effect of S1P on the activity of BACE1 in neuronal N2a cells (Takasugi et al, 2011). To test whether secretase activities are altered in S1P-lyase deficient cells, a highly specific fluorogenic BACE1 activity assay was performed (Burg et al, 2013). BACE1 activity was measured either in living cells or in purified cellular membranes. The basal activity of BACE1 in S1P-lyase deficient cells was lowered by approximately 80% in comparison to WT cells (Fig. 14A). Notably, addition of 10  $\mu$ M S1P to living WT cells reduced BACE1 activity by 20 % (Fig. 14B). However, the same concentrations of S1P showed no significant effects on BACE1 activity in living S1PL-KO cells (Fig. 14C). The activity of BACE1 in isolated cell membranes of S1P-lyase

deficient cells is also significantly lower when compared to that of WT cells. This effect is less pronounced as in living cells, but still significant (*Fig. 14D*). Exogenous application of S1P to purified membranes of WT cells resulted in a significant reduction in the enzymatic activity by 15 % (*Fig. 14E*). BACE1 activity in purified membranes of S1P-lyase however, was not significantly changed by exogenous S1P (*Fig. 14F*). Taken together, the enzymatic assays demonstrate a role of S1P-lyase and S1P on the  $\beta$ -secretase BACE1.

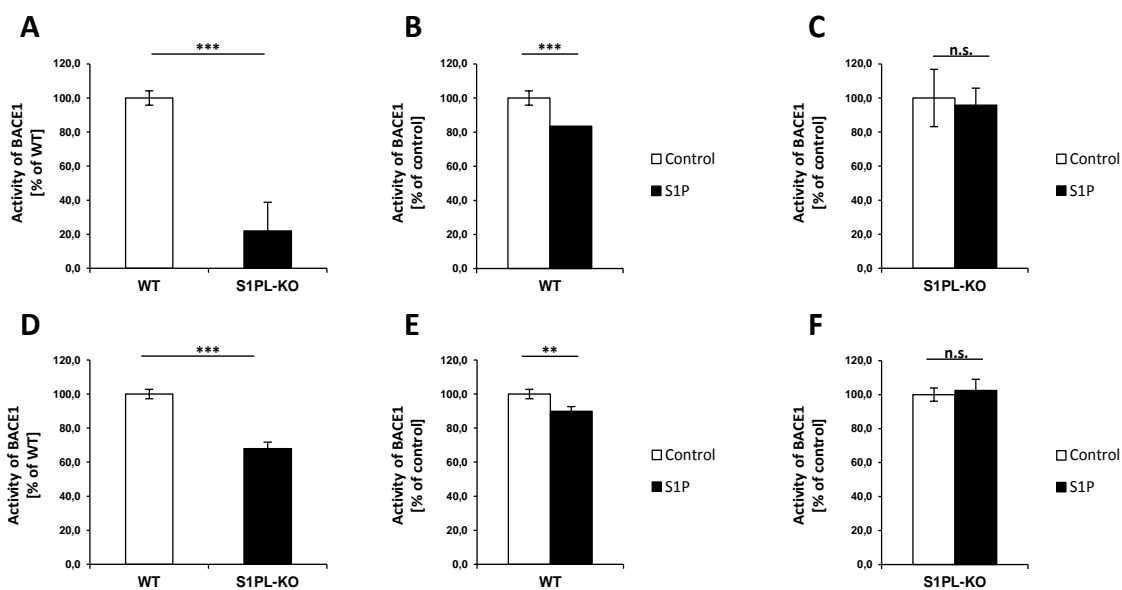


**Fig. 14: S1P reduces BACE1 activity.** Fluorogenic activity assay for BACE1 measured in WT and S1P-lyase deficient cells. Assays were performed in living WT and S1P-lyase deficient cells under control condition and after application of 10  $\mu$ M S1P (A – C). Additional BACE1 activity determination was performed in purified membranes of WT and S1P-lyase deficient cells (D – E). Measurements were performed under control conditions and after application of 10  $\mu$ M S1P (n=5).

To further test altered BACE1 activity in WT and S1P-lyase deficient cells, the level of the BACE1 cleavage product sAPP $\beta$  in conditioned media was analyzed. Since basal levels of sAPP $\beta$  from endogenous APP are very low (not shown), previously described APP695<sub>swe</sub> overexpressing cells were used (*see 3.3.1*). The familial AD causative KM to NL mutation in the APP residues 595-596 favors the processing of APP by BACE1 (Citron et al, 1992). As shown in *Fig. 15A* and *B*, the ratio of sAPP $\beta$  to sAPP $\alpha$  is increased in S1P-lyase deficient cells. Furthermore, when lowering the levels of S1P by treatment with SKiII, a strong increase in the secretion of sAPP $\beta$  and a simultaneous reduction in

sAPP $\alpha$  were observed in both WT and S1P-lyase deficient cells (*Fig. 15A, C, D*). These results further support a role of S1P in the regulation of BACE1 activity.

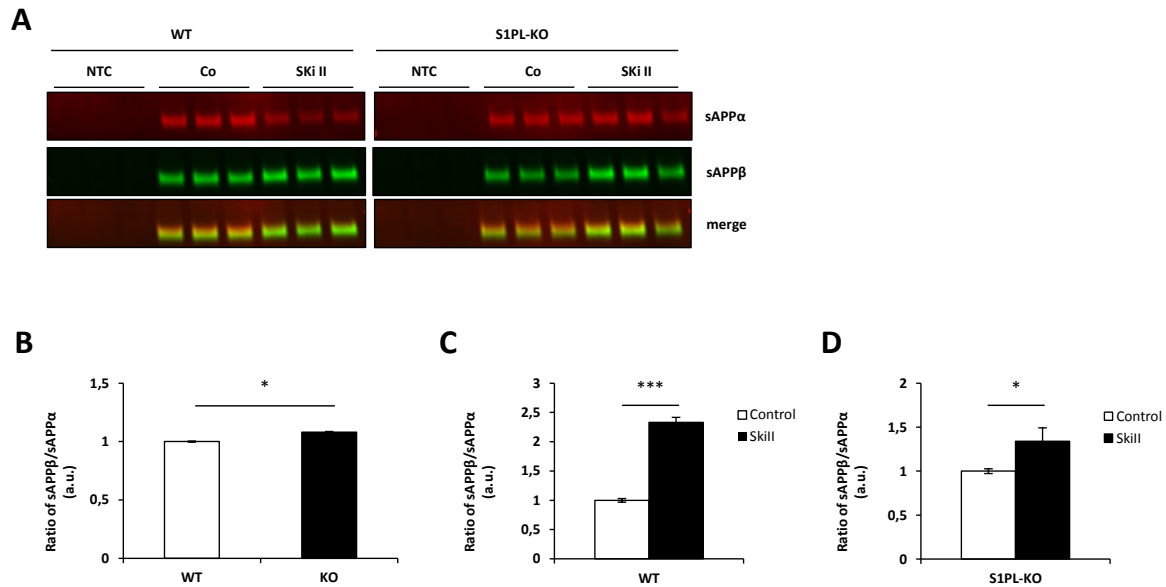
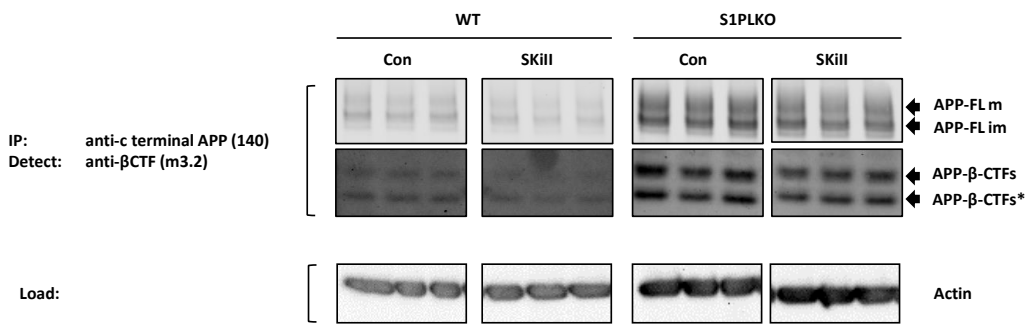


**Fig. 15: Determination of the sAPP $\beta$ /sAPP $\alpha$  ratio using APP695<sub>swe</sub>-overexpressing cells.** (A) Western immunoblotting of sAPP $\alpha$  (6E10) and sAPP $\beta$  (192sw). Conditioned media of WT and S1P-lyase deficient cells overexpressing APP695<sub>swe</sub> was loaded onto a 7 % SDS gel. (B - D) Quantification of the sAPP $\beta$  and the sAPP $\alpha$  levels, as well as determination of the ratio in WT and S1P-lyase KO cells. Ratios were determined under control conditions (B) and after treatment with 5 $\mu$ M SKiII for 24 h (C, D) (n=3).

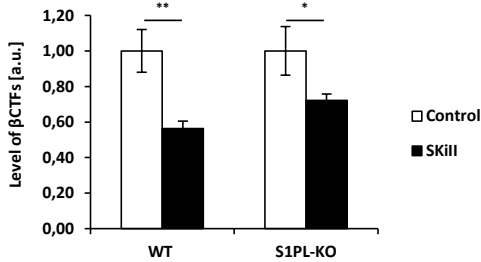
Next, the c-terminal cleavage products of BACE1, APP- $\beta$ CTFs and  $\beta$ CTFs\* were analyzed. CTFs were immunoprecipitated from cell lysates and then detected by Western immunoblotting. Both,  $\beta$ CTFs as well as  $\beta$ CTFs\* were significantly decreased upon treatment of WT or S1P-lyase deficient cells with 5  $\mu$ M SKiII (*Fig. 16A - C*). As observed before (*Fig. 10*), SKiII treatment also decreased APP-FL.



A



B



C

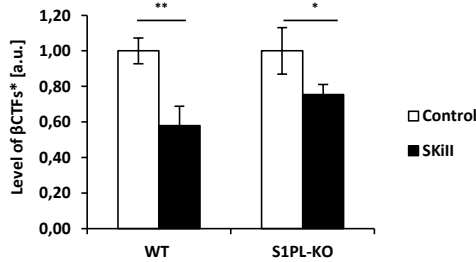


**Fig. 16: Immunoprecipitation of APP-FL and APP-CTFs.** APP-FL and CTFs were pulled down from full cell lysates with a c-terminal specific antibody (140). Levels of βCTFs and βCTF\* were detected using the m3.2 antibody. Actin level shows equal protein level prior the IP. (B, C) Quantification analysis of βCTF and βCTF\* levels in WT and S1P-lyase deficient cells. Level in both cell lines were quantified under control condition and upon treatment with 5 μM SKiII for 24 h (n=3).

Overall, the data shown in Fig. 14 - Fig. 16 demonstrate an impact of S1P metabolism on BACE1 activity. However, data in Fig. 15 and Fig. 16 showed contrary results for βCTFs and sAPPβ levels. While application of SKiII to WT and S1P-lyase deficient cells increased the level of sAPPβ (Fig. 15), level βCTF and βCTF\* were significantly decreased (Fig. 16). This difference could indicate an additional effect of S1P on the γ-secretase activity.

### 3.3.2.2 S1P impairs γ-secretase activity.

While an effect of S1P on the BACE1 activity was previously shown (Takasugi et al, 2011), a role of S1P in the modulation of γ-secretase is unknown so far. Thus, the basal γ-secretase activity was first measured in living WT and S1P-lyase deficient cells. Measurements revealed a reduced γ-secretase activity by 20 % in S1P-lyase deficient cells as compared to WT cells (Fig. 17A). Interestingly, application of exogenous S1P to WT cells also decreased γ-secretase activity thereby mimicking the effect of S1P-lyase deletion (Fig. 17B). S1P-lyase deficient cells also showed a decrease of the γ-

secretase activity by 20 % upon treatment with 10  $\mu$ M S1P (*Fig. 17C*). However, when  $\gamma$ -secretase activity was measured in purified membranes of WT and S1P-lyase deficient cells, no differences were detected (*Fig. 17D*). Along with this result, exogenous application of S1P to purified membranes of WT and S1P-lyase deficient cells showed no influence on the  $\gamma$ -secretase activity (*Fig. 17E, F*). Overall, the activity of the  $\gamma$ -secretase is selectively decreased by S1P in living cells, but not in purified membranes.

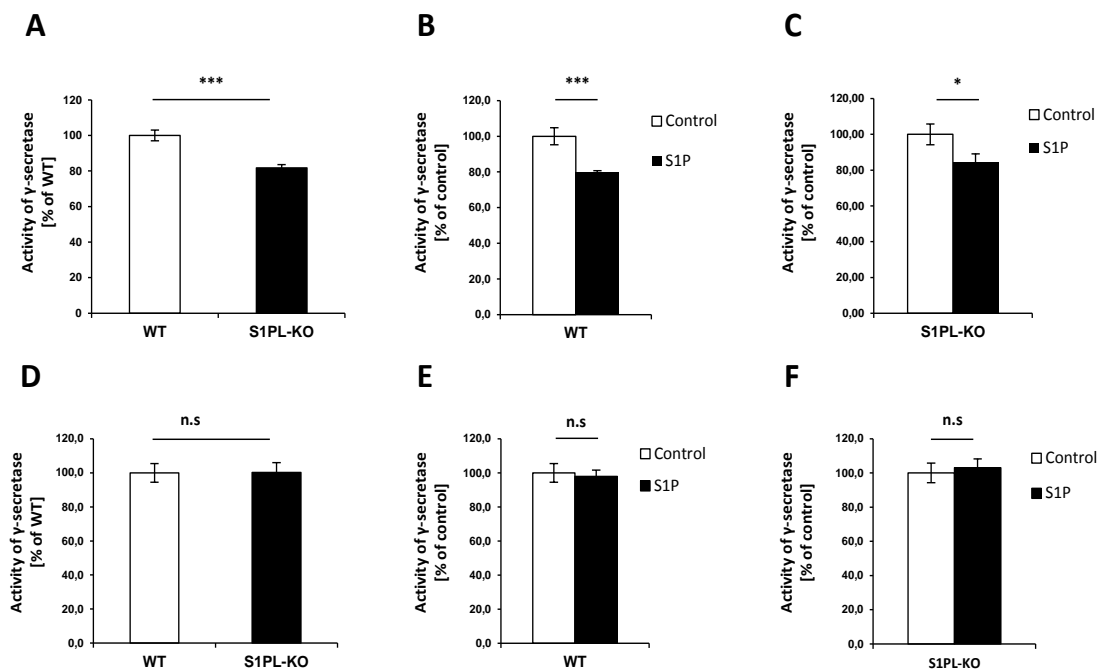


**Fig. 17: Presence of high S1P concentrations selectively affects the  $\gamma$ -secretase activity in living cells.** Fluorogenic activity assay of the  $\gamma$ -secretase in living cells and purified membranes of WT and S1P-lyase deficient cells. Living cells were measured under control conditions (A) and after treatment with 5  $\mu$ M of SKiII (B, C). Determination of the  $\gamma$ -secretase activity was additionally performed in purified membranes of WT and S1P-lyase deficient cells (D – E). Measurements were performed under control conditions (D) and after application of 5  $\mu$ M SKiII (E, F). (Analysis was performed with n=5)

In addition to the fluorogenic activity assay,  $\gamma$ -secretase dependent cleavage of APP-CTFs was analyzed in purified membranes as described previously (Sastre et al, 2001). Western immunoblotting revealed a lower turnover of APP-CTFs to the AICD during the first hour of incubation as compared to three hours of incubation (*Fig. 18A*). Determination of the AICD to CTF ratio revealed a significantly reduced generation of the AICD by approximately 70 % in S1P-lyase deficient cells as compared to WT cells (*Fig. 18B*). The ratio of AICD to CTFs after 3 h was not quantified. However, the levels of AICD after 3h at 37°C are higher, than the levels of APP-CTFs at 4°C. This result was

present in WT as well as in S1P-lyase deficient cells (*Fig. 18A*) and suggests an ongoing cleavage of the APP-FL variant by either  $\alpha$ - or  $\beta$ -secretase to produce APP-CTFs.

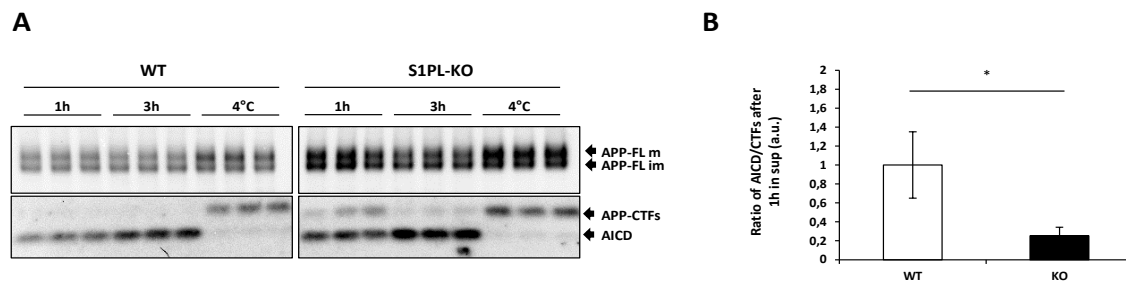


**Fig. 18:** *In vitro*  $\gamma$ -secretase assay revealed a reduced generation of AICD in S1P-lyase deficient cells. (A) *In vitro*  $\gamma$ -secretase assay of WT and S1PL-KO cells. Purified membranes were reconstituted in citric buffer and incubated for 1 and 3 h at 37°C or 3 h at 4°C. (B) Quantification of AICD to CTFs ratio after incubation for 1 h at 37°C ( $n=3$ ).

The presenilins (PS1 or PS2) represent the catalytic center of the  $\gamma$ -secretase complex (Wolfe et al, 1999). The PS protein is endo proteolytically cleaved between the sixth and seventh transmembrane (TM) domain, generating stable NTFs and CTFs. To assess expression of PS1 in WT and S1P-lyase deficient cells, PS1-CTFs were detected after immunoprecipitation by Western immunoblotting. Two bands representing phosphorylated and non-phosphorylated PS1-CTF variants were detected (Walter et al, 1996). However, levels of both PS1-CTF variants were very similar in WT and S1P-lyase deficient cells (*Fig. 19*). Interestingly, treatment with SKiII reduced PS1-CTFs in both WT and S1P-deficient cells (*Fig. 19A, C, D*), without changing the ratio of p-PS1-CTFs to non-phosphorylated PS1-CTFs (*Fig. 19A, F, G*).

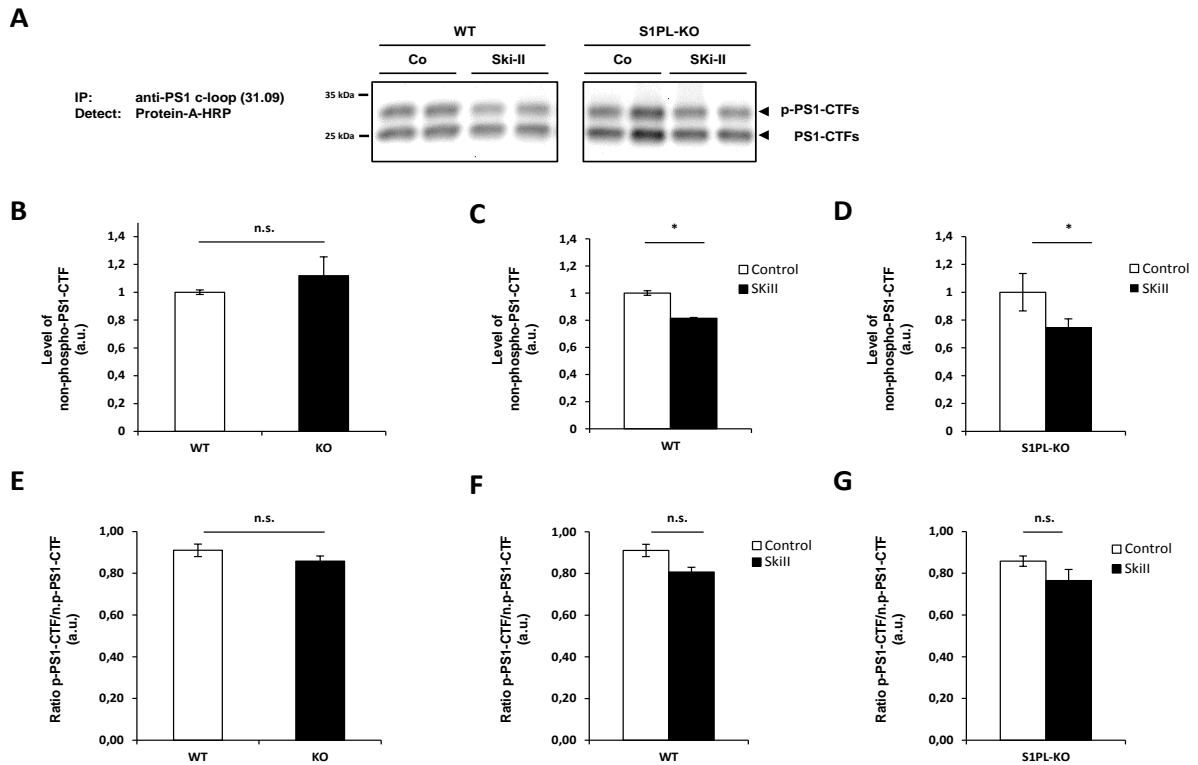


**Fig. 19: Sphingosine kinase inhibition reduces PS1-CTFs.** (A) PS1-CTF immunoprecipitation of WT and S1P-lyase deficient cells under control conditions and upon 5  $\mu$ M SKiII for 24 h. PS1-CTFs were immunoprecipitated with 3109 antibody and detected by western immunoblotting using protein-A-HRP. (B - D) Quantification of non-phosphorylated PS1-CTFs in WT and S1P-lyase KO cells under control conditions (B) or after treatment with 5  $\mu$ M SKiII. (C, D) (n=3). (E) Quantification PS1-CTF phosphorylation in WT and S1P-lyase KO cells. (n=3) (F, G) Determination of the ratio in p-PS1-CTFs to non-phosphorylated PS1-CTFs. Ratio was determined for control condition and after treatment with 5  $\mu$ M SKiII in WT and S1P-lyase KO cells (n=3).

Taken together, deficiency in the S1P-lyase reduces the activity of the  $\gamma$ -secretase. Exogenous application of S1P to WT cells partially mimics this effect (Fig. 17). Furthermore, SphK1/2 activity seems to be crucial for PS1-CTFs and therefore for the  $\gamma$ -secretase activity (Fig. 19). However, to this point it is unclear whether reduction of PS1-CTFs is a result of reduced endo proteolytic cleavage or generally lowered PS1-FL level. Changes in PS1 expression or metabolic turnover of PS1-FL could affect PS1-CTFs as well. Nevertheless, reduction of PS1-CTFs upon SKiII, would suggest a lowered catalytic activity of the  $\gamma$ -secretase.

### 3.4 S1P-lyase deficiency impairs lysosomal function

#### 3.4.1 Accumulation of APP-CTFs in lysosomal compartments.

The proteolytic turnover of APP-FL and APP-CTF also takes place in lysosomal compartments by acidic proteases, including cathepsin D (Agholme et al, 2012; Haass et al, 1992a). LSDs for example, show impaired proteolytic turnover of several proteins, including APP-FL and APP-CTFs (Tamboli et al, 2011b; Tamboli et al, 2011c). Thus, the localization of APP in lysosomal compartments was analyzed by co-staining of cells with antibodies against the APP C-terminus and the lysosomal membrane protein 2 (lamp2). The number and the size of lamp2 positive structures in S1P-lyase deficient cells were increased, and appear to be more juxtannuclear in S1P-lyase deficient cells as compared to WT cells (*Fig. 20A*). S1P-lyase deficient cells also show a higher intensity of C-terminally labeled APP that partially co-localizes with lamp2 positive structures (*Fig. 20A, white arrows*). In contrast, the number of vesicles with co-localizing lamp2 and APP is lower in WT cells. To further test accumulation of APP-CTFs in lysosomal compartments, a sub-cellular fractionation was performed. *Fig. 20B* demonstrates that APP-CTFs of WT cells accumulate in fractions of higher density, whereas in S1P-lyase deficient cells APP-CTFs accumulate strongly in earlier fractions positive for cathepsin D (*Fig. 20B*). These results indicate a selective accumulation of APP-CTFs from S1PL-KO cells in lysosomal compartments and are in line with observations for lysosomal lipid storage diseases (Jin et al, 2004; Keilani et al, 2012; Tamboli et al, 2011b; Tamboli et al, 2005; Tamboli et al, 2011c).

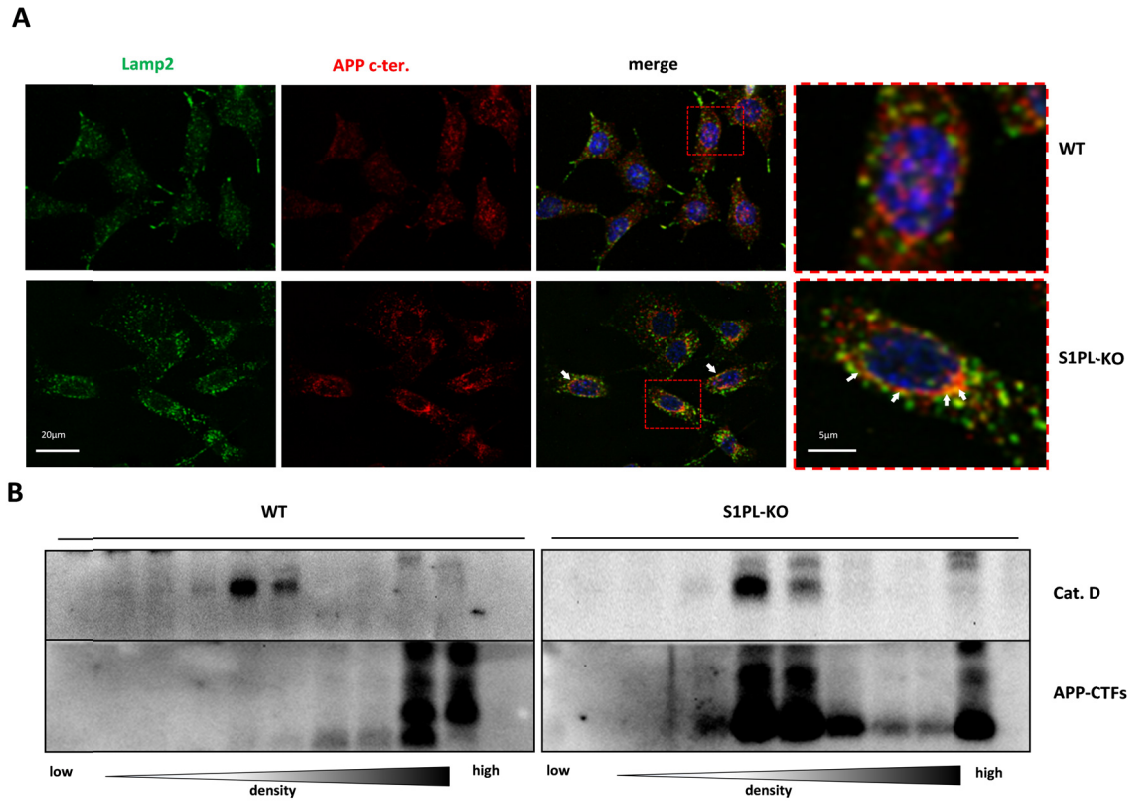


**Fig. 20: Accumulation of APP-CTFs in lysosomal compartments.** (A) Co-immunostaining of lamp2 and APP-C -terminus in WT and S1PL-KO cells. The red frame in the merged image indicates the enlarged area (outer right images). The white arrows indicate structures with co-localization of lamp2 and APP-CTFs. (scale bars: for normal=20 µm, for enlarged=5 µm). (B) Western immunoblotting of APP-CTFs and Cathepsin D upon sub-cellular fractionation of WT and S1P-lyase deficient cells. S1P-lyase deficient cells show a selective accumulation of APP-CTFs in cathepsin D positive fractions.

### 3.4.2 Increased stability of APP in S1P-lyase deficient cells.

Besides the proteolytic turnover of APP-CTFs in acidic organelles, mature APP-FL is also targeted to endosomal/lysosomal compartments, where it can undergo degradation (Haass et al, 1992a). To study the stability of APP-FL in WT and S1P-lyase deficient cells, the ratio of APP-FL<sub>m</sub> to APP-FL<sub>im</sub> was determined. Quantification revealed a significantly elevated ratio of mature to immature APP-FL in S1P-lyase deficient cells (Fig. 21A, B), suggesting a stabilization of mature APP-FL. To specifically assess the stability of APP-FL, both WT and S1P-lyase deficient cells were treated with cycloheximid (Chx), a potent inhibitor of protein biosynthesis. Interestingly, treatment with Chx shows that both WT and S1P-lyase deficient cells have a similar maturation rate during the first 15 minutes after treatment (Fig. 21C, D). However, longer chase periods revealed a differential effect of Chx. The ratio of mature-to-immature APP-FL is lower in WT cells as in S1P-lyase deficient cells (Fig. 21C, D). The

data suggest a similar maturation of APP in both cell types, but indicates an increased stability of APP-FL<sub>m</sub> in S1P-lyase deficient cells. This finding is in line with the previously described effect on the secretases in cells lacking S1P-lyase activity (Fig. 14). Moreover, reduced lysosomal turnover of APP-FL 30 – 60 min after its expression could explain its increased stability.

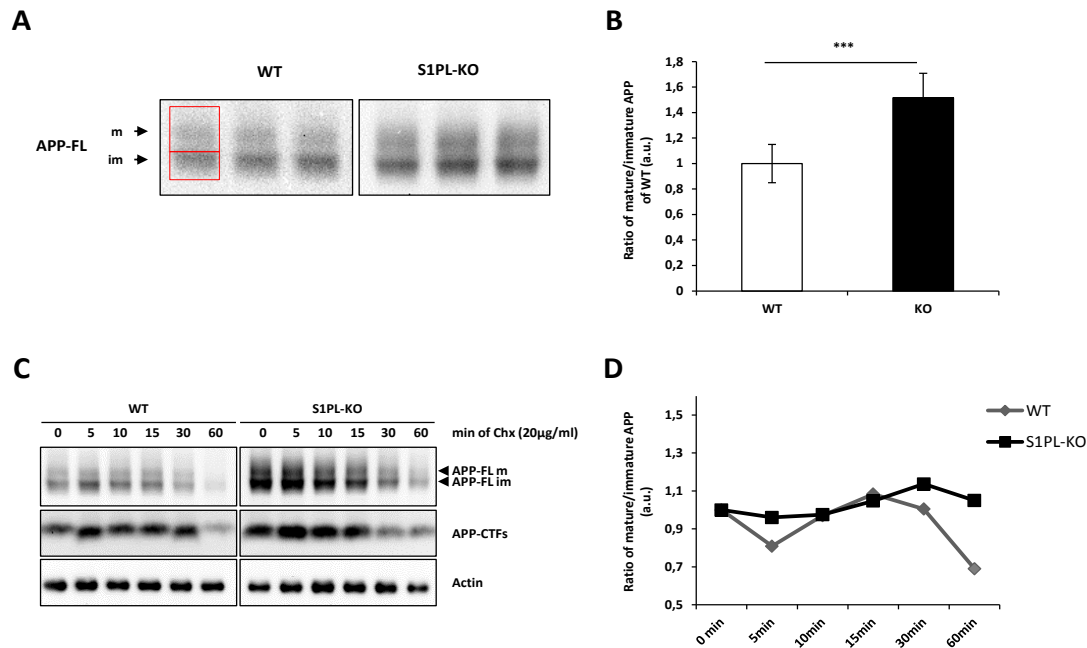


**Fig. 21: APP-FL is more stable in S1P-lyase deficient cells than in WT cells.** (A) Representative western immunoblotting of APP-FL in WT and S1PL-KO cells. Red frames show areas for quantification of mature and immature APP-FL. (B) Quantification and determination of the ratio of mature to immature APP-FL. (n=9). (C) Western immunoblotting of WT and S1P-lyase deficient cells. Protein synthesis was inhibited by treatment with 20 µg/ml cycloheximid. (D) Quantification and determination of the APP-FL mature to immature ratio.

### 3.4.3 Deletion of the S1P-lyase impairs the maturation of cathepsin D.

Cathepsin D is a well described marker for lysosomal compartments. Upon trans-location from Golgi-compartments to lysosomes, the acidic milieu allows autocatalytic cleavage of pro- and intermediate forms of cathepsin D to the catalytically active form (Gieselmann et al, 1983). Thus, changes in the ratio of the active to the precursor forms could indicate altered lysosomal activity. To analyze whether S1P-lyase deletion affects the processing of cathepsin D, membranes of WT and S1P-lyase deficient cells were isolated and subjected to western immunoblotting. Quantification revealed a significantly reduced ratio of active cathepsin D to the pro-/intermediate forms in S1P-lyase deficient cells as

compared to that in WT cells (*Fig. 22A, B*). To further analyze maturation of cathepsin D in an independent approach, S1P-lyase expression was down-regulated by RNAi. The RNAi mediated suppression of S1P-lyase also reduced the active form and increased the intermediate form of cathepsin D in comparison to cells transfected with scrambled siRNA (*Fig. 22C, D*).

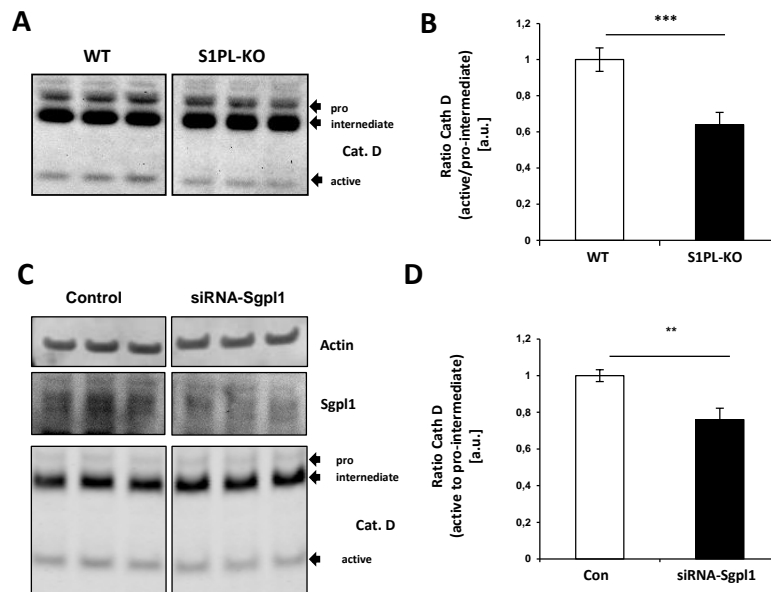


**Fig. 22: S1P-lyase affects the maturation of cathepsin D.** (A, B) Western immunoblotting and quantification of the cathepsin D forms in purified membranes of WT and S1PL-KO cells (A). The ratio of the active forms to the pro- and intermediate forms of cathepsin D in S1P-lyase deficient cells is higher than in WT cells (B). (n=3). (C) Western immunoblotting of cathepsin D in siRNA transfected murine N9 cells. The S1P-lyase knock down was carried out for 30 h prior the sample preparation. (D) Quantification and determination of cathepsin D active to pro-/intermediate forms. Transfected cells show a significantly lowered ratio of the cathepsin D active form to the pro-/intermediate forms than non-transfected cells (n=3).

Having shown a deficit in the processing of the lysosomal hydrolase cathepsin D, the next step was to check whether S1P-lyase deletion might also affect other lysosomal proteins. Western immunoblotting of purified membranes showed a significant increase of lamp2 in S1P-lyase deficient cells when compared to WT cells (*Fig. 23A, B*). This result was consistent with increased lamp2 positive structures in immunocytochemical detection (*Fig. 20A*) and indicates a reduced turnover of lamp2 in lysosomes. In addition, the lysosomal GM2 activator protein (Gm2a), which is involved in the degradation of glycosphingolipids (Sandhoff & Kolter, 1998), was also increased in S1P-lyase deficient cells (*Fig. 23C, D*).



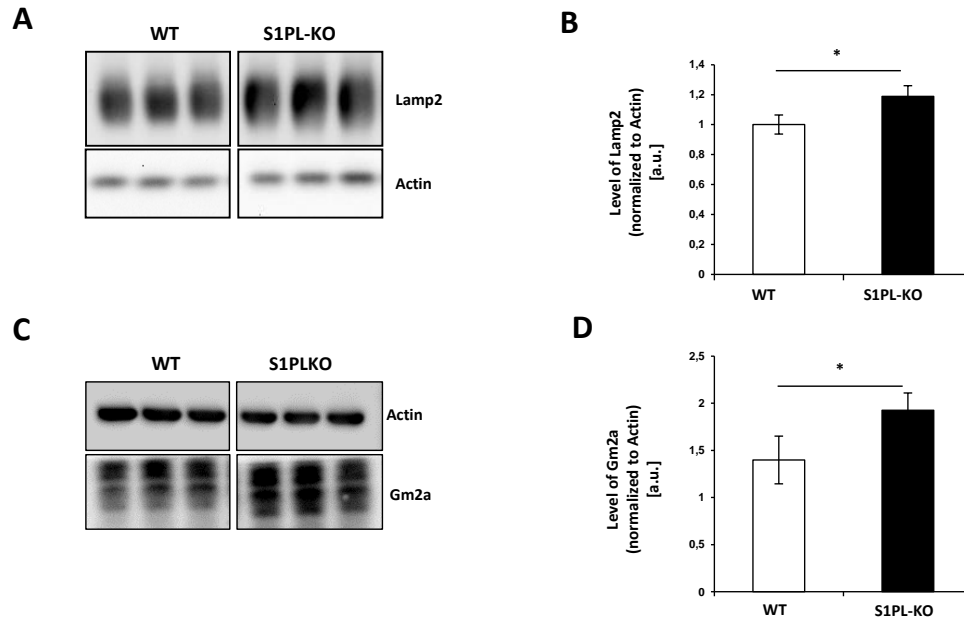


**Fig. 23: Accumulation of Lamp2 and Gm2a in S1P-lyase deficient cells.** Westernblot analysis (A, C) and quantification (B, D) of lamp2 (A,B) and Gm2a (C,D) in purified membranes of WT and S1PL-KO cells. S1P-lyase deficient cells show significantly elevated levels for the lysosomal membrane protein lamp2 (B) and the ganglioside degradation activator proteins Gm2a (D) (n=3).

### 3.4.4 Impaired autophagic turnover in S1P-lyase deficient cells.

To assess the role of S1P lyase deficiency on global protein turnover, a pulse-chase experiment by metabolic labeling was carried out. WT and S1P-lyase deficient cells were labeled with <sup>35</sup>S-methionine for 15 minutes, followed by chase periods for 0,5 – 16 h. Radiolabeled proteins were separated by SDS-PAGE and detected by autoradiography. As indicated in Fig. 24A and B, WT cells showed a pronounced decrease in labeled proteins from 0 to 4 h. In contrast, S1P-lyase deficient cells showed little if any protein turn-over until 4 h of chasing time. When comparing the level of radiolabeled proteins between 4 and 16 h, WT cells show a reduction from 60 % to 40 %, whereas in S1P-lyase deficient cells the a reduction from 100 % to 80 % is present (Fig. 24B). While this indicates a similar turnover rate for long-lived proteins in both WT and S1P-lyase deficient cells, the latter shows only little effect on the turnover of short-lived proteins as compared to WT cells. This finding suggests an effect of the S1P-lyase deficiency on the proteasomal degradation machinery.

To assess an involvement of autophagy, both WT and S1P-lyase KO cells were starved in EBSS medium. Interestingly, starvation for 2 h induced a strong decrease of APP-CTFs in both cell lines. Western immunoblotting also revealed an efficient conversion of LC3-I to LC3-II in WT and S1P-lyase deficient cells when incubated in EBSS, thereby indicating similar induction of autophagy (Fig. 25A). Prolonged starvation for 6 h leads to the consumption of LC3-II in WT cells (Fig. 25A). Interestingly, consumption of LC3-II was strongly reduced in S1P-lyase deficient cells (Fig. 25A). This finding indicates an efficient induction of autophagy for both WT and S1P-lyase deficient cells, but prolonged starvation shows a less efficient consumption of LC3-II in S1P-lyase deficient cells. This could suggest a lowered autophagic activity due to lysosomal impairment. Next, both WT and S1P-lyase deficient cells were treated with the mTOR inhibiting and autophagy inducing compound rapamycin. Conversion of LC3-I to LC3-II was followed during 0 – 16 h of the treatment. Here LC3-II levels in WT cells remained largely unaffected during the first 8h of treatment. S1P-lyase deficient cells on the other hand, showed a clear increase of LC3-II during the same period (Fig. 25B). Interestingly, while LC3-II in WT cells dramatically decreased between 8 – 16 h, LC3-II levels in S1P-lyase deficient cells were still elevated as compared to 0 h (Fig. 25B). This data suggests indeed a higher stability of LC3-I and LC3-II in cells lacking the S1P-lyase.

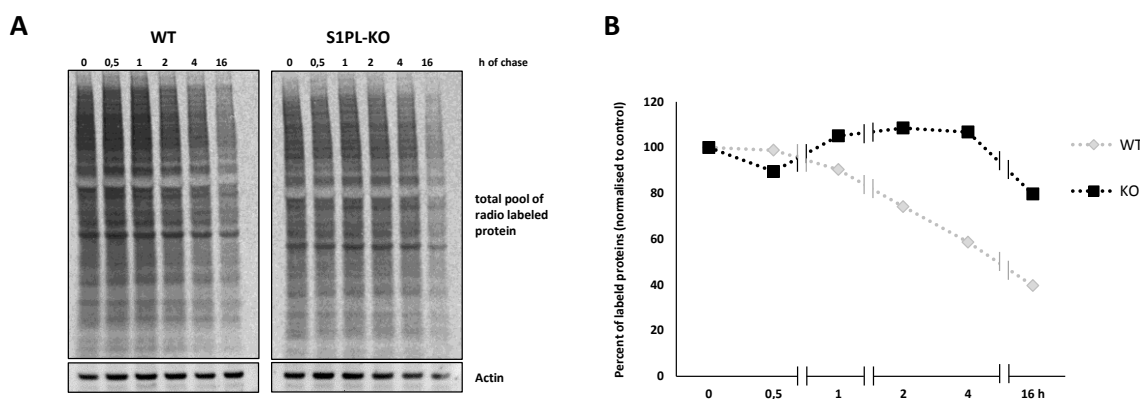


**Fig. 24: Impaired turnover of radiolabeled proteins during shorter chasing times in S1P-lyase KO cells.** (A) Pulse chase radiolabeling experiment cells were first pulsed for 15 minutes, and subsequently chased for a period of 0 – 16 h. (B) Quantification of total radio-labeled proteins (A) in WT and S1PL-KO cells.

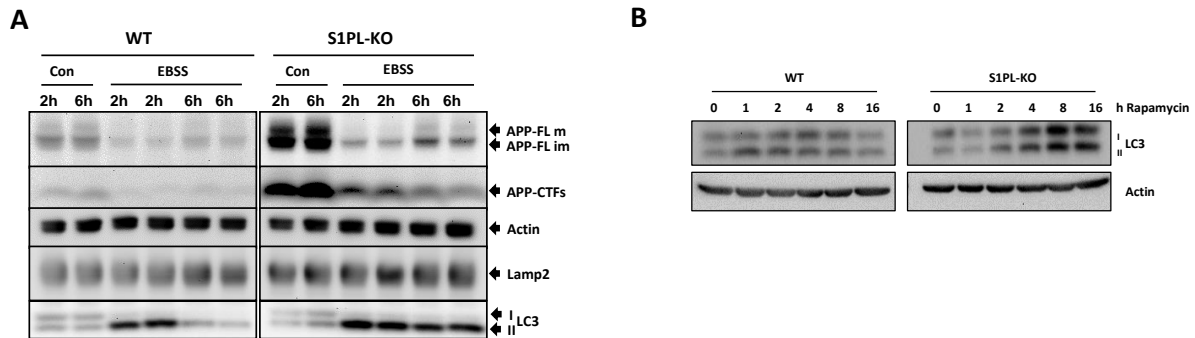


**Fig. 25: Impaired autophagic turnover in S1P-lyase deficient cells. (A)** Western immunoblotting of starvation induced autophagy in WT and S1PL-KO cells. **(B)** Western immunoblotting of WT and S1PL-KO cells. Treated with 10 μM rapamycin for the time dependent conversion of LC3 I to LC3 II. **(C)** Quantification and determination of LC3 II to LC3 I ratio from **(B)**.

Taken together, induction of autophagy seems to be unaffected in S1P-lyase deficient cells. The data rather suggest a lysosomal impairment.

### 3.5 Distribution of subcellular compartments is altered in S1PL- KO cells.

Having shown differences in the subcellular distribution and activity of lysosomes in S1P-lyase deficient cells, the next step was to analyze additional compartments which are also involved in the metabolism and transport of APP. As previously mentioned, APP-FL is transported from the ER, via the Golgi compartments to the PM, from where it is internalized into endosomal/lysosomal compartments. WT and S1P-lyase deficient cells were co-immunostained for the ER marker proteins calnexin and Bip/GRP78. The latter is an ER localized chaperone and involved in the protein folding, as well as in the forward transport of proteins in the secretory pathway (Dudek et al, 2009; Hendershot et al, 1994). Immunocytochemistry revealed a more intensive staining of calnexin in the S1P-lyase deficient cells (Fig. 26). While the staining intensity of Bip/GRP78 was similar, the distribution was slightly different WT cells show a pronounced Bip/GRP78 localization at the nuclear envelope, whereas in S1P-lyase deficient the protein showed a rather reticular distribution (Fig. 26).

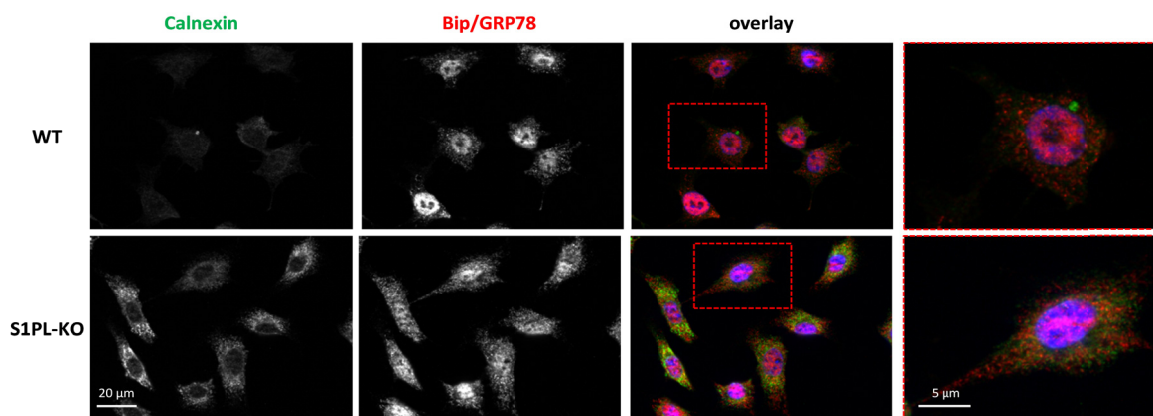


**Fig. 26: Co-staining of endoplasmic reticulum reveals increased reactivity for calnexin in S1P-lyase deficient cells.** WT and S1P-lyase deficient cells were co-immuno stained against the ER marker calnexin and Bip/GRP78. Cells were prepared as indicated (see 2.1.3). The red frame in the merged image indicates the enlarged area (outer right images). S1P-lyase deficient cells show a more intense staining of calnexin and a reticular distribution of Bip/GRP78. (scale bars: normal = 20  $\mu\text{m}$ , enlarged = 5  $\mu\text{m}$ ).

To study the distribution and morphology of early and late Golgi compartments, cells were co-immunostained with antibodies against giantin and TGN47. While WT cells show a smaller and less intensive staining for giantin, S1P-lyase deficient cells show severely increased giantin-positive structures (Fig. 27). This result demonstrates an accumulation of giantin in the early-golgi compartments and might indicate either an impaired trafficking between ER and Golgi or an alteration in the structure of this compartment. Staining of TGN46, however, showed only weak signals in both WT and S1P-lyase deficient cells (Fig. 27), and did not allow any conclusion.

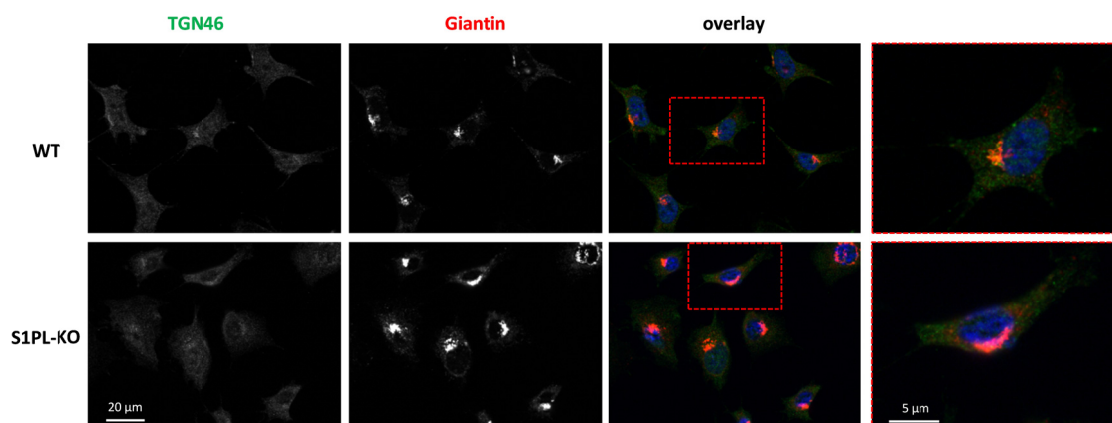


**Fig. 27: Co-immunostaining of early and late golgi marker.** WT and S1P-lyase deficient cells were co-stained for early/cis-Golgi with a giantin-specific antibody. Late/trans-Golgi compartments were visualized using a specific antibody against TGN46. Cells were prepared as indicated in section 2.1.3. The red frame in the merged image indicates the enlarged area (outer right images). S1P-lyase deficient cells show strong increase in the sized and intensity of giantin positive structures. (Scale bars: normal = 20  $\mu\text{m}$ , enlarged = 5  $\mu\text{m}$ ).

Next, cells were co-stained with antibodies against EEA1 and cathepsin D to visualize early endosomal and lysosomal compartments, respectively. EEA1 staining in WT cells showed small and round vesicular structures (*Fig. 28*). In contrast EEA1 positive structures in S1P-lyase deficient cells appeared more tubular and intense (*Fig. 28*). Cathepsin D positive structures were also more intensive and pronounced in S1P-lyase deficient cells as compared to WT cells (*Fig. 28*). This finding is in line with the elevated levels for lamp2 and supports the hypothesis of a lysosomal impairment in S1P-lyase deficient cells (*Fig. 20A*). The immunocytochemical analysis furthermore indicates an altered morphology of early endosomes in S1P KO cells.

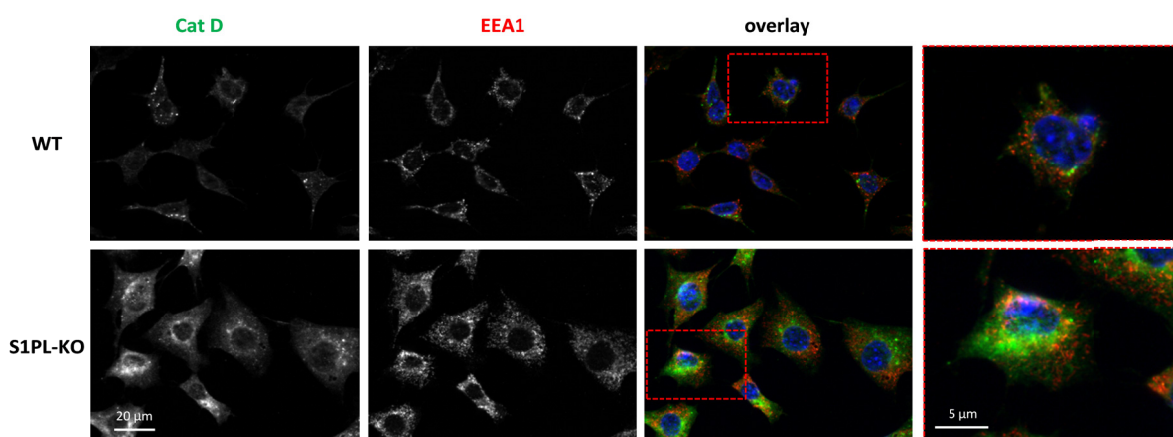


**Fig. 28: Co-immuno staining revealed strong differences in EEA1 and cathepsin D between WT and S1P-lyase deficient cells.** WT and S1P-lyase deficient cells were co-immuno stained for early endosomal marker (EEA1) and lysosomal marker (cathepsin D) as indicated in the section 2.1.3. The red frame in the merged image indicates the enlarged area (outer right images). S1PL-KO cells show elevated, tubular EEA1 staining. Cathepsin D positive structures are more intense in S1P-lyase deficient cells. (Scale bars: normal = 20  $\mu\text{m}$ , enlarged = 5  $\mu\text{m}$ ).

### 3.6 Alteration in lipid metabolism in S1P-lyase deficient cells.

As described above, S1P-lyase deficient cells not only have elevated concentrations of intracellular S1P (*Fig. 8B*), but also of sphingosine (*Fig. 10B*). Therefore it was of interest to analyze the membrane lipid composition of these cells in comparison to WT cells. TLC analysis revealed a strong accumulation of GD3 and LacCer in S1P-lyase deficient cells as compared to WT cells. Most of the other lipids like Cer, GlcCer and SM also appear slightly elevated in S1P-lyase deficient cells (*Fig. 29A*). Interestingly, GM3 levels were also accumulated severely in S1P-lyase deficient cells (*Fig. 29A*). The lysosomal storage disorders, Sandhoff's disease and Tay - Sachs disease are induced by

mutations in GM2 degrading hexosaminidases HexA and HexB respectively. Both diseases show severe effects on the APP metabolism (Tamboli et al, 2011b; Tamboli et al, 2005). To see whether S1P-lyase deficiency might affect the hexosaminidases, a gene expression analysis for HexA, HexB and their co-activator Gm2a were performed. Statistical analysis of the mRNA level of both HexA and HexB was significantly reduced in S1P-lyase deficient cells (*Fig. 29B, C*). The enzymatic activity of HexA/B depends on its co-factor Gm2a. S1P-lyase deficient cells show a clear reduction in the levels of Gm2a mRNA (*Fig. 29D*). This finding is contradictory to the previously described and significantly increased protein level of Gm2a in S1P-lyase deficient cells (*Fig. 23C*) and indicates to general alteration of the lipid homeostasis.

A high number of lipids, mainly triglycerides and cholesterol ester, but also sphingolipids are stored in lipid droplets. Thus, the size, number and intensity of lipid droplet were analyzed by fluorescence microscopy using LD540 (Spandl et al, 2009). Interestingly, S1P-lyase KO cells showed a strong increase in the size and number of lipid droplets (*Fig. 29E*), further supporting a more general impairment of cellular lipid metabolism upon inhibition of S1P degradation.

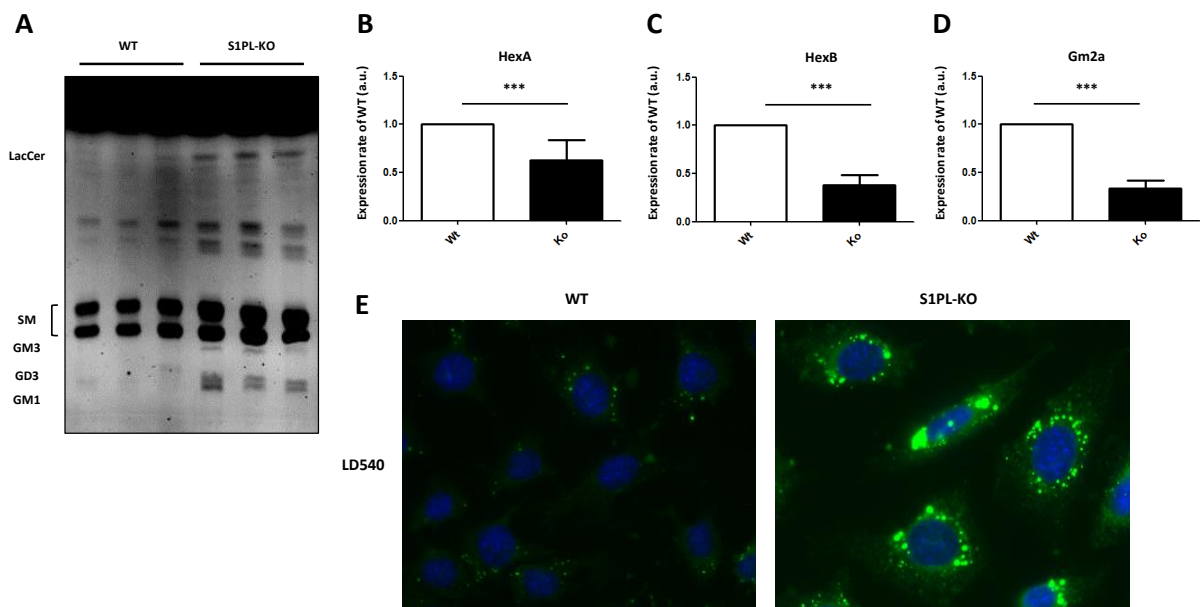


**Fig. 29:** S1P-lyase deficient cells show several alterations in lipid homeostasis in comparison to WT. (A) Thin-layer chromatography of neutral lipids for WT and S1P-lyase deficient cells. (B - D) Quantitative real-time-PCR for HexA (B), HexB (C) and Gm2a (D) mRNA in WT and S1P-lyase deficient cells. (E) Staining of lipid droplets (green) with LD540 in WT and S1P-lyase deficient cell. Merged shows same cells with additional DAPI staining for the nuclei. (Scale bar = 20µm).

### 3.7 Immediate elevation of intracellular $Ca^{2+}$ reduces APP-FL and APP-CTF levels.

S1P has been shown to affect  $Ca^{2+}$  mobilization from intracellular stores and  $Ca^{2+}$  related signaling pathways (Hinkovska-Galcheva et al, 2008; Tornquist, 2012). S1P-lyase deficient cells also show elevated storage of  $Ca^{2+}$  and an augmented release from the ER upon thapsigargin treatment (Claas et al, 2010). Thapsigargin selectively inhibits the SERCA-pump and blocks efficiently the reuptake of  $Ca^{2+}$  (Treiman et al, 1998). Thus the effect of  $Ca^{2+}$  modulation on APP metabolism in WT and S1P KO cells was tested. First, cytosolic  $Ca^{2+}$  was increased by inhibition of the SERCA-pump with thapsigargin. Thapsigargin induced an efficient reduction of APP-CTF levels in both cell lines within 1 h of treatment (*Fig. 30*). During prolonged treatment for 2 – 4 h the levels of APP-CTFs remained at low levels. However, levels of APP-CTFs in S1P-lyase deficient cells were higher than in WT cells at each time point (*Fig. 30*).

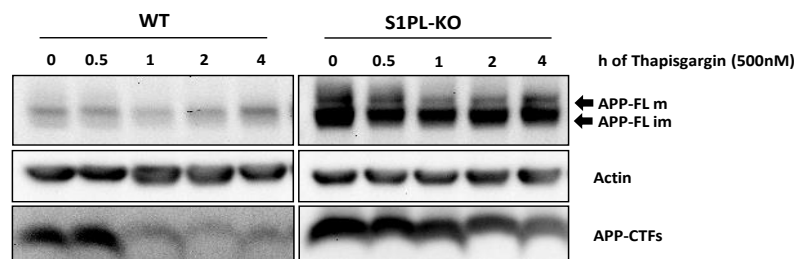


**Fig. 30: Increase of intracellular  $Ca^{2+}$  affects the metabolism of APP-FL and APP-CTFs.** Western immunoblotting of purified membranes of WT and S1P-lyase deficient cells under control condition and upon treatment with 500 nM thapsigargin for indicated time-points. Immediate effects on APP-FL and APP-CTFs after 1 h of treatment are present in both WT and S1P-lyase deficient cells.

Two previous studies reported impaired mobilization of  $Ca^{2+}$  from lysosomal stores in NPC models (Dong et al, 2010; Lloyd-Evans et al, 2008). Gly-Phe  $\beta$ -naphthylamide (GPN) is reported to induce a selective release of  $Ca^{2+}$  from lysosomal stores. When GPN was applied to cells, the ratiometric analysis showed an immediate increase of free cytosolic  $Ca^{2+}$  concentrations in both WT and S1P-lyase deficient cells (*Fig. 31A*, black arrows). Free  $Ca^{2+}$  concentrations rapidly decreased when GPN was washed out (*Fig. 31A*, blue arrows), demonstrating the rapid and selective effect of GPN. Next, the effect of lysosomal  $Ca^{2+}$  mobilization by GPN on APP metabolism was analyzed. Levels of APP-FL were increased after 2 – 16 h in WT cells. However, GPN had nearly no effect on APP-FL in S1P-

lyase deficient cells (*Fig. 31B*). Notably, APP-CTFs showed a biphasic behavior upon treatment with 200  $\mu$ M GPN in both cell lines. After a strong decrease within the first hour of treatment, the levels of APP-CTFs recover steadily from 8 – 16 h.

The combined data for thapsigargin and GPN indicate a role of  $\text{Ca}^{2+}$  in altered APP metabolism of S1P lyase KO cells. Thus, the analysis of  $\text{Ca}^{2+}$  dependent signaling pathways might give more detailed insights into the S1P-lyase dependent APP metabolism.

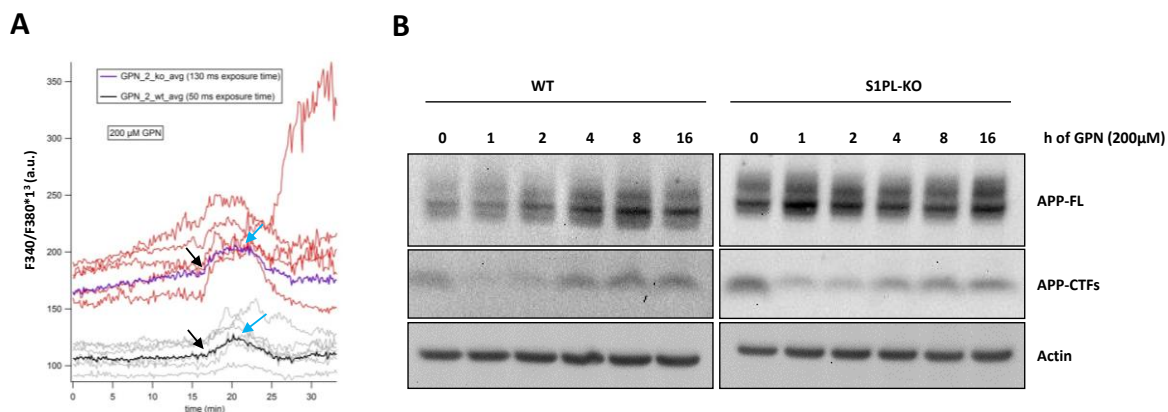


**Fig. 31: Selective release of lysosomal  $\text{Ca}^{2+}$  affects the APP metabolism.** (A) Ratio metric analysis of cytosolic  $\text{Ca}^{2+}$ . WT and S1P-lyase deficient cells loaded with 5  $\mu$ g of Fura2-AM for 30 min at 37°C and subsequently analyzed. (B) Western immunoblotting of APP-FL and APP-CTFs after time-dependent GPN treatment in WT and S1P-lyase deficient cells.

### 3.8 Alterations in protein kinase C signaling in S1P-lyase deficient cells.

#### 3.8.1 Lack of the S1P-lyase affects the localization of activated PKC.

A critical enzyme in intracellular  $\text{Ca}^{2+}$  signaling is the protein kinase C (PKC). To assess a potential alteration of PKC in S1P-lyase deficient cells, localization of PKC was studied. Classical PKC isoforms contain C2 and C1 domains which bind to  $\text{Ca}^{2+}$  and DAG, respectively, thereby leading to a translocation to the plasma membrane and enzyme activation.

At first, the distribution of PKC in cytosolic and membrane fractions of WT and S1P-lyase deficient cells were analyzed. When analyzing PKC localization under control conditions, S1P-lyase deficient cells showed a significantly higher ratio of cytosolic to membrane localized PKC than WT cells (*Fig. 32A, B*), suggesting a reduced activity of PKC. Notably, treatment with SKiII selectively increased the



localization of PKC in the cytosol of WT cells (Fig. 32A, C), but not in S1PL-lyase deficient cells (Fig. 32A, D). Rather, a trend for increased PKC association with cellular membranes was observed.

Because reducing intracellular S1P concentration in WT cells with SKiII increased PKC in the cytosol (Fig. 33), it is unlikely that increased PKC in the cytosolic fraction of S1P-lyase cells are caused by elevated S1P concentrations. This finding rather points to the involvement of sphingosine. Increased concentrations for sphingosine were observed upon SKiII treatment as well as in the S1P-lyase deficient cells when compared to WT cells (Fig. 10B).

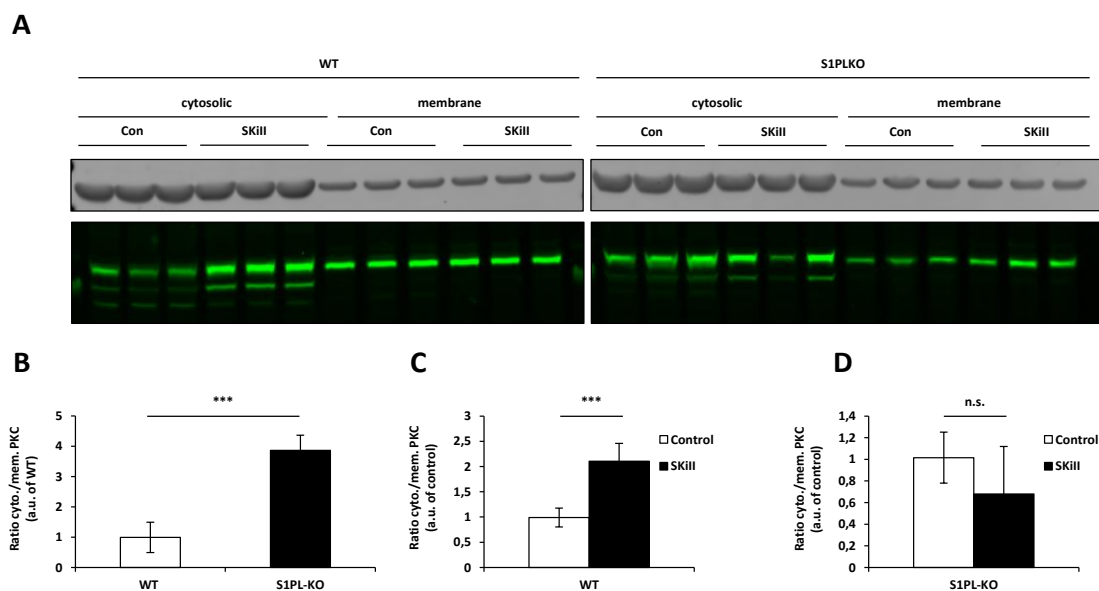


**Fig. 32: Analysis of PKC localization in WT and S1PL-KO cells.** (A) Western immunoblotting of fractionated WT and S1PL-KO cells. Cells were non-treated or subjected to 5  $\mu$ M SKiII (24 h) and checked for localization of PKC. (B) Quantification of PKC localization in WT and S1PL-KO cells (normalized to actin). (n=3) \* indicates unspecific binding of the antibody. (C, D) Ratio of cytosolic and membrane localized PKC in WT and S1PL-KO cells (normalized to actin). Cells were treated with 5  $\mu$ M SKiII for 24h (n=3).

### 3.8.2 Inhibition of PKC causes its translocation into membrane fractions and increases APP.

Since the lower association of PKC with cellular membranes observed in S1P-lyase deficient cells could indicate decreased PKC activity, it was to test whether inhibition of PKC would mimic the effects on APP-FL or APP-CTFs. Thus, cells were treated with the PKC inhibitor bisindolylmaleimide I (BIM I) and analyzed for PKC localization as well as for APP levels. In line with the previous experiment (Fig. 32A, B), WT cells showed a significantly higher association of PKC with cellular

membranes as compared to S1P lyase KO cells (Fig. 33A, B). Notably, levels of PKC in the cytosol markedly decreased upon inhibition with BIM I in both WT and S1P-lyase cells (Fig. 33C, D). Cells lacking the S1P-lyase furthermore showed a strong increase in membrane associated PKC (Fig. 33A). This finding is in line with the PKC localization in S1P-lyase deficient cells when treated with SKiII (Fig. 32A). In parallel, PKC inhibition strongly elevated levels of APP-FL and APP-CTFs in both cell lines (Fig. 33A). PKC inhibition further increased the pro- and intermediate forms of cathepsin D (Fig. 33A), suggesting reduced lysosomal turnover upon PKC inhibition in both cell types. Interestingly, PKC inhibition also led to detection of the membrane associated cathepsin D intermediate form in the cytosolic fractions of both WT and S1PL-KO cells. Thus indicating that maturation or sorting of cathepsin D into lysosomal compartments is impaired.

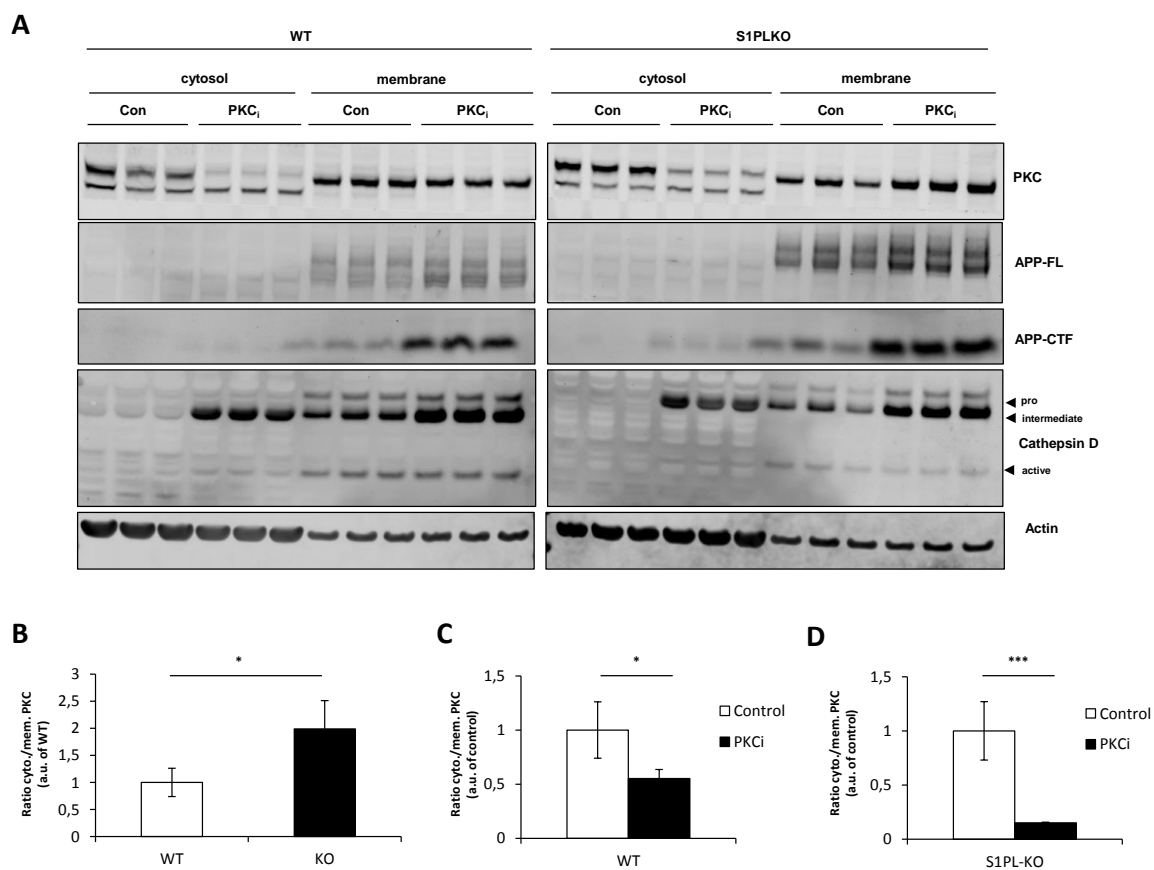


**Fig. 33: Analysis of PKC localization and APP metabolism in WT and S1P-lyase deficient cells upon PKC inhibition.** (A) Western immunoblotting of WT and S1P-lyase deficient cells. Cells were fractionized after subjecting to PKC inhibitor and vehicle. \* indicates unspecific binding of the antibody. (B) Quantification of the PKC localization in WT and S1P-lyase deficient cells (normalized to actin). (n=3) (C, D) Ratio of cytosolic to membrane localized PKC in WT and S1PL-KO cells (normalized to actin). Cells were treated with 1  $\mu$ M PKC<sub>i</sub> for 24 h (n=3).

### 3.8.3 Sphingosine causes PKC translocation and increases APP levels.

After showing a correlation of S1P-lyase deficiency, PKC and APP-metabolism, next the effect of sphingosine was further examined. WT and S1P-lyase deficient cells treated with sphingosine for 24 h revealed no significant effects on APP-FL or APP-CTFs (data not shown). In contrast, shorter treatment with sphingosine resulted in a time-dependent increase of APP-FL in both, WT and S1P-lyase deficient cells (*Fig. 34A, B*). Analysis of PKC revealed a slight increase in the ratio of cytosolic vs. membrane localized PKC upon 4 h of treatment in both WT and S1P-lyase deficient cells (*Fig. 34A, C*). Prolonged sphingosine treatment tended to increase the ratio of cytosolic vs. membrane localized PKC in WT cells, but to decrease this ration in S1P-lyase cells (*Fig. 34C*). This observation on PKC localization is in line with the previously observed data (*Fig. 32A, C* and *Fig. 33A, C*). However, further quantitative experiments would be necessary to allow a conclusion. Interestingly, treatment with sphingosine also triggered an accumulation of the cathepsin D pro/intermediate forms, indicating a lower lysosomal activity (*Fig. 34A*). This finding is also consistent with the elevated levels of the cathepsin D pro/intermediate forms upon PKC inhibition (*Fig. 33A*).

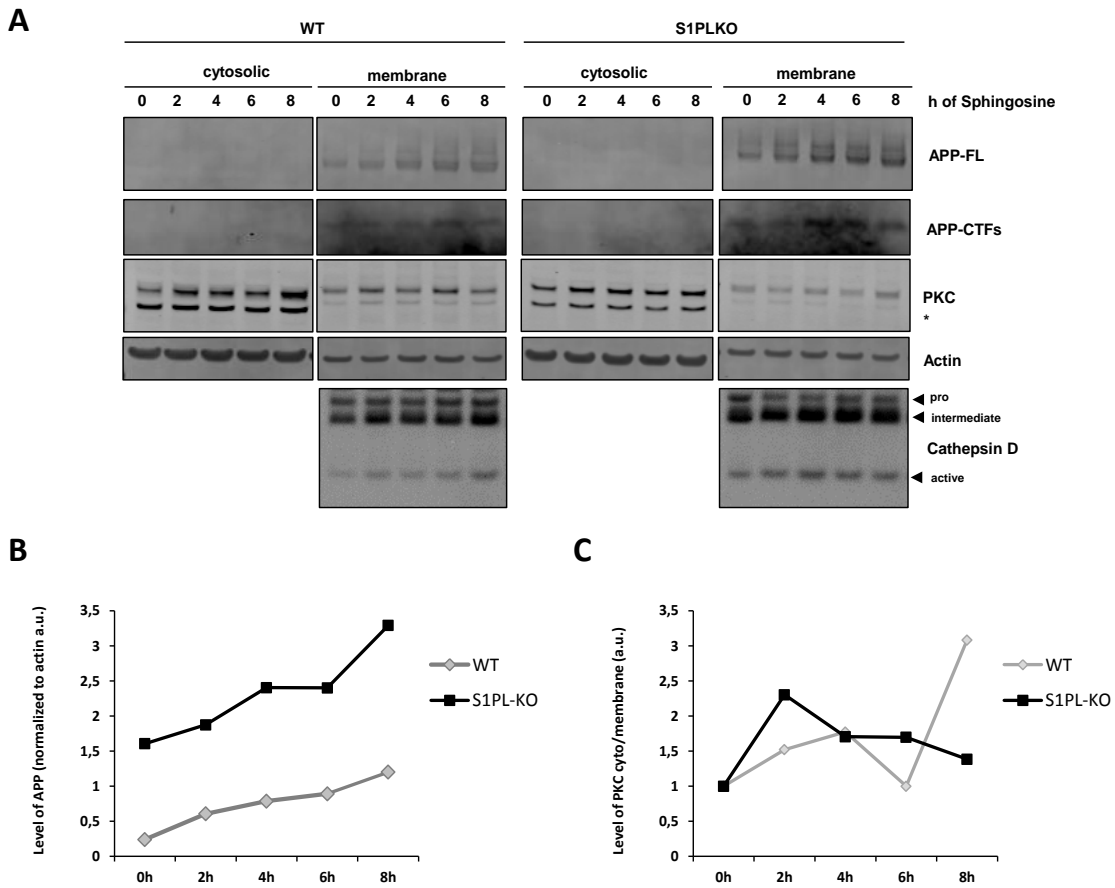


**Fig. 34: Time-dependent treatment of WT and S1P-lyase deficient cells with 10  $\mu$ M sphingosine causes APP-FL elevation.** (A) Western immunoblotting of WT and S1P-lyase deficient cells treated with 10  $\mu$ M sphingosine for 0 – 8h. (B) Quantification of APP-FL after time-dependent treatment with 10  $\mu$ M sphingosine. (n=1) (C) Quantification of PKC localization in cytosolic and membrane fractions of WT and S1P-lyase deficient cells. (n=1)

## 4. Discussion

The aim of this work was to characterize the role of the bioactive sphingolipid S1P in the metabolism of the AD associated APP. The results demonstrate an important function of the S1P cleaving enzyme S1P-lyase in proteolytic processing of APP by specific secretases and in the regulation of lysosomal activity. Cells lacking the S1P-lyase gene showed strong accumulation of APP and its C-terminal fragments due to impaired degradation of these proteins in endo-lysosomal compartments. Moreover, S1P also impaired the activity of  $\beta$ - and  $\gamma$ -secretase thereby affecting the generation of A $\beta$ . Interestingly, mobilization of Ca<sup>2+</sup> from ER or lysosomal stores partially rescued the observed effects on the accumulation of APP. Further experiments indicated an involvement of PKC in the observed effects.

Together, these findings revealed highly similar phenotypes of the S1P-lyase deficient cell model with classical LSD models like Niemann Pick A, -B, Tay-Sachs or Sandhoff Disease (Burns et al, 2003; Keilani et al, 2012; Tamboli et al, 2005).

### 4.1 *The role of S1P metabolism in the proteolytic processing of APP.*

Previous studies showed a link between the processing of APP and several lipids (Bhattacharyya et al, 2013; Grimm et al, 2013; Tamboli et al, 2005; Tamboli et al, 2008). Analytic studies revealed complex changes in the lipid composition of human AD brains and during aging in general (Kracun et al, 1992a; Svennerholm et al, 1989; van Echten-Deckert & Walter, 2012b). However, results of these post-mortem studies are controversial. Nevertheless, sphingolipids have been shown to impair the proteolytic processing as well as the intracellular trafficking of APP. Two independent studies showed that lowering the levels of SM or GSLs impairs the forward transport and availability of APP for secretase-mediated cleavage (Sawamura et al, 2004; Tamboli et al, 2005). Ceramide also affects the processing of APP by stabilizing the  $\beta$ -secretase BACE1 and increases the generation of A $\beta$  (Li et al, 2010; Puglielli et al, 2003).

A general metabolite in SL degradation is the bioactive molecule S1P. It plays a key role in the recruitment of numerous immune cells by the activation of a subset of G-protein coupled receptor (S1PR1 – 5) (Spiegel & Milstien, 2003; Spiegel & Milstien, 2011). S1P was also shown to act as second messenger and to modulate a wide range of cellular processes like the gene transcription (Hait et al, 2009), counter-acting the pro-apoptotic propensity of ceramide (Olivera & Spiegel, 1993), regulation of intracellular  $\text{Ca}^{2+}$  signaling (Ghosh et al, 1994) and the BACE1 mediated processing of APP (Takasugi et al, 2011).

Deficiency of the S1P-lyase not only results in elevated intracellular concentrations of S1P and sphingosine (*Fig. 8B, Fig. 10A*), but also in the accumulation of APP-FL and the different APP-CTF variants (*Fig. 9*). Along with this, S1P-lyase deficient cells also showed higher levels of  $\text{A}\beta$  in the conditioned medium (*Fig. 13B, C*). However, when determining the precursor-product relationship, S1P-lyase deficient cells showed lower generation of  $\text{A}\beta$  as compared to WT cells (*Fig. 13D, E*). These findings indicated a role of S1P-lyase related metabolites on the secretase dependent processing of APP. When analyzing the activity of  $\beta$ -secretase BACE1 (*Fig. 14*) and the  $\gamma$ -secretase (*Fig. 17* and *Fig. 18*), a significant reduction for both secretases was observed in S1P-lyase deficient cells. Reduction of the  $\gamma$ -secretase activity is in line with the lowered generation of  $\text{A}\beta$  (*Fig. 13*). However, the mode of action causing the decreased activity remains elusive. Several studies showed that the  $\gamma$ -secretase activity can be impaired by either the membrane thickness (Winkler et al, 2012), the lipid microenvironment (Osenkowski et al, 2008) or the lipid composition (Holmes et al, 2012). Lipid analysis either by mass spectrometry (*Fig. 10A*) or by thin-layer chromatography (*Fig. 29A*) indeed indicated complex changes in the lipid composition. These findings could support the hypothesis of lipid mediated effects on the secretase activities and could also be applied on to the S1P-lyase deficient cells as well. However, a direct interaction of S1P on the  $\gamma$ -secretase has not been described yet.

A direct effect of S1P on BACE1 on the other hand was recently described. Takasugi and colleagues demonstrated a stimulatory effect of S1P on the activity of BACE1. The resulting increase of  $\beta$ CTFs led to elevated secretion of both  $\text{A}\beta_{40}$  and  $\text{A}\beta_{42}$  in primary neurons or neuronal N2a cells (Takasugi et al, 2011). However, in the present work a significant reduction in BACE1 activity was observed in

S1P-lyase deficient cells. Moreover, direct addition of exogenous S1P to living WT cells or to purified membranes of WT cells also decreased the activity of BACE1 (*Fig. 14*). S1P-lyase deficient cells showed an 80 % reduced activity of BACE1 compared to WT cells. Additional application of exogenous S1P had no further impact on this decrease (*Fig. 14C*). However, the reason for the conflicting findings in this work and the work of Takasugi and colleagues is unclear. The usage of different cellular models (neuronal cells vs. mouse embryonic fibroblasts) and enzymatic assays might contribute to the observed differences. Neuronal cells are post-mitotic and show strong differences in their membrane composition in comparison to other cells (van Echten-Deckert & Walter, 2012b). As mentioned before, membrane thickness (Winkler et al, 2012), local lipid microenvironment (Osenkowski et al, 2008) and the lipid composition in general play a crucial role in processing of APP (Walter, 2012; Williamson & Sutherland, 2011). Proteolytic activity of BACE1 on the other hand has been shown to be stimulated by cerebroside, GSLs and sterols (Kalvodova et al, 2005). Furthermore, palmitoylation of BACE1 causes a stabilization and translocation into lipid rafts causing an elevated generation of  $\beta$ CTFs and presumably  $A\beta$  (Bhattacharyya et al, 2013).

Inhibition of the sphingosine-kinases with SKiII decreased intracellular S1P and increased the concentration of its precursor sphingosine (*Fig. 10A, B*). SKiII also decreased levels of APP-FL and APP-CTFs (*Fig. 10C, D*). Interestingly, both WT and S1P-lyase deficient cells showed a decrease in APP-FL and APP-CTFs upon inhibition of sphingosine phosphorylation, suggesting a S1P-lyase independent effect. Since S1P-lyase deficient cells show constitutively higher levels of sphingosine than WT cells. The effect upon SKiII treatment might rather come from reduced levels of S1P instead of elevated concentrations of sphingosine. However, while treatment of WT and S1P-lyase deficient cells with sphingosine increased APP-FL and APP-CTFs (*Fig. 34*), S1P had no effects (*Fig. 12*). Sphingosine is more permeable than S1P and might require dephosphorylation prior to cellular penetration (Peest et al, 2008). Sphingosine penetrates membranes more easily compared to S1P and thus, enters cells more efficiently. After penetration sphingosine can undergo phosphorylation leading to higher concentrations of intracellular S1P (*Fig. 10B*).

Analysis of sAPP $\beta$  level revealed a significantly elevated secretion in S1P-lyase deficient cells overexpressing APP695<sub>swe</sub> compared to cells with functional S1P-lyase activity (*Fig. 15*). This finding

is contradictory to the lowered activity of BACE1 observed in the fluorogenic analysis (*Fig. 14*). However, the comparison between these two experiments is difficult. The activity of BACE1 was measured using an artificial synthetic substrate in non-transduced cells (*Fig. 14*), while the levels of soluble APP were derived from cells expressing the APP695<sub>swe</sub> variant (*Fig. 15*). The Swedish variant of APP favorably undergoes BACE1 cleavage resulting in higher A $\beta$  generation (Citron et al, 1992), in both the secretory and the endocytic pathways (Perez et al, 1996). Treatment of APP695<sub>swe</sub> overexpressing cells with SKiII furthermore increased the generation of sAPP $\beta$  and reduced the generation of sAPP $\alpha$ , suggesting an elevated activity of BACE1 (*Fig. 15*). This finding, on the one hand, is in line with the lowered BACE1 activity under high concentrations of S1P (*Fig. 14*), but on the other hand, does not explain the reduced level of APP- $\beta$ CTFs (*Fig. 16*). Immunoprecipitation of APP- $\beta$ CTF variants from WT and S1P-lyase deficient cells revealed a decrease upon treatment with SKiII. This finding is in line with the study of Takasugi and colleagues, who postulated a positive modulatory effect of S1P on BACE1 activity (Takasugi et al, 2011). Although BACE1 activity in S1P-lyase deficient cells is significantly lower than in WT cells, an accumulation of APP- $\beta$ CTFs was evident. The molecular mechanism underlying this effect is unclear, but the data strongly indicate an impairment of non-secretase dependent proteolysis of APP.

Interestingly, the  $\gamma$ -secretase subunit PS1-CTFs were also shown to regulate the lysosomal activity by maintaining its Ca<sup>2+</sup> homeostasis (Neely Kayala et al, 2012). They are further associated with the lysosomal membranes and suggested to act as a lysosomal protease participating in the lysosomal turnover (Pasternak et al, 2003). Autocatalytic cleavage of PS1-FL generates the PS1-CTFs and PS1-NTFs, which form the catalytic center for the  $\gamma$ -secretase mediated cleavage of APP and other substrates (De Strooper et al, 2012; Thinakaran et al, 1996). Immunoprecipitation of PS1-CTFs was used to determine the expression level of PS1. Western immunoblotting analysis showed similar levels of PS1-CTF in WT and S1P-lyase deficient cells. However, treatment with SKiII significantly reduced the PS1-CTF levels (*Fig. 19A, C, D*), indicating either a reduced autocatalytic cleavage of the full length and therefore a low activity of the  $\gamma$ -secretase in general, or an increased degradation of PS1-CTFs. Nevertheless, since the effect of SKiII on PS1-FL was not determined in this experiment, a general reduction of PS1-FL expression cannot be ruled out at this point. Further expression analysis



would help to uncover the effect of SKiII on PS1 metabolism. The role of S1P metabolism on the processing of PS2-FL was not analyzed and needs to be addressed in further experiments.

Taken together, modulation of S1P metabolism by genetic deletion of the S1P-lyase or inhibition of sphingosine kinases affects the proteolytic processing of APP by altering the enzymatic activities and/or intracellular trafficking of secretases. However, the results also indicate the involvement of secretase-independent effects on APP metabolism.

#### *4.2 Deficiency of the S1P-lyase impairs the lysosomal turnover.*

Early studies by Haass and colleagues demonstrated the targeting of APP- $\beta$ CTFs to lysosomal compartments for degradation (Haass et al, 1992a). Moreover, an accumulation of APP-CTFs in lysosomal compartments was shown in cellular and animal models of different lipid storage diseases (Keilani et al, 2012; Tamboli et al, 2011b; Tamboli et al, 2005; Tamboli et al, 2011c). Using cell biological and biochemical methods, this study also demonstrated strong accumulation of APP-FL and APP-CTFs in lysosomal compartments and a co-localization to lysosomal marker proteins (*Fig. 20*). Interestingly, the reduced autocatalytic cleavage capacity of cathepsin D further suggested a decrease in lysosomal activity in S1P-lyase deficient cells (*Fig. 22*) (Benes et al, 2008; Gieselmann et al, 1985; Gieselmann et al, 1983). A potential cause for the decreased maturation rate of cathepsin D might be triggered by a general elevation of the lysosomal pH as it was shown by several other studies (Altan et al, 1999; Samarel et al, 1989; Toimela et al, 1995). Nevertheless, further determination of the intra-lysosomal pH in S1P-lyase deficient cells would be necessary. Interestingly, deficiency of cathepsin D was shown to resemble a neuronal ceroid lipofuscinosis (NCL) phenotype (Koike et al, 2000). NCL is a rare lipid-protein storage disorder affecting mostly endosomal compartments, emphasizing the role of cathepsin D for lysosomal turnover of proteins as well as lipids. Moreover, deficiency of the lysosomal hydrolase cathepsin E also leads to accumulation of lamp2 and an increased in the lysosomal pH (Yanagawa et al, 2007). These findings demonstrate the tight relationship of lysosomal hydrolases, regulation of lysosomal pH and the turnover of proteins. Interestingly, the lipid activator protein GM2a was also increased in S1P lyase deficient cells. GM2a participates in the degradation of

GM2 by forming a soluble complex and delivering the substrate to the degrading enzymes (Sandhoff & Kolter, 1998). Interestingly, deficiency of GM2a was shown to induce the storage of GM2 gangliosides, similar to the Tay-Sachs or Sandhoff diseases, also known as the AB variant of GM2 gangliosidosis (Liu et al, 1997; Sakuraba et al, 1999). In line with this, gene expression analysis of the enzymes involved in the degradation of GM2 gangliosides, GM2a, hexosaminidase A and hexosaminidase B, were reduced in S1P-lyase deficient cells (*Fig. 29B-C*). However, the accumulation of GM2a in lysosomes and the reduced mRNA levels are conflicting. Interpretation and correlation of mRNA to protein level is difficult as extensively reviewed by Vogel and Marcotte (Vogel & Marcotte, 2012). Splicing, post-translational modification, long protein half-life and transcriptional regulation can cause discrepancies between mRNA and protein levels. Altogether, the intracellular accumulation of APP together with lysosomal proteins GM2a, lamp2, and immature Cathepsin D suggests an impairment of the lysosomal activity thereby showing characteristic features of lipid storage disorders. Macroautophagy, from here on referred to autophagy, is an important cellular mechanism for the degradation of long-lived proteins into amino acids and is highly dependent on the action of lysosomes. Autophagy furthermore mediates the catabolic processing of lipids, carbohydrates and even organelles like mitochondria or lipid droplets to maintain a healthy cellular homeostasis (Singh & Cuervo, 2011). Fusion of autophagosomes with lysosomes promotes the degradation of the luminal content and provides amino acids as building blocks for new biosynthesis under conditions of starvation (Levine & Klionsky, 2004). When analyzing global protein metabolism by metabolic pulse-chase experiments, a reduced turnover of these proteins in S1P-lyase deficient cells were observed (*Fig. 24A, B*). However, induction of autophagy upon starvation was similar in WT and S1P-lyase deficient cells, as indicated by similar conversion of LC3-I to LC3-II. However, while LC3-II in WT cells was efficiently consumed, LC3-II was more stable in S1P-lyase deficient cells (*Fig. 25A*). As shown previously, persistent starvation causes an increased and unspecific breakdown of proteins for the maintenance of cellular homeostasis (Cuervo et al, 1995; Mizushima et al, 2004). In fact, nutrient depletion demonstrated a reduced catabolism of LC3-II in S1P-lyase deficient cells as compared to WT cells when starvation was persistent (*Fig. 25A*). When autophagy was induced using rapamycin, a pharmacological inhibitor of mTOR, the proportion of LC3-II in S1P-lyase deficient cells was higher

than in WT cells (*Fig. 25*). The obtained data indeed suggested a different response of WT and S1P-lyase deficient cells to rapamycin. However, the differences are small and do not allow any definite conclusions. Hypothetically, this finding would suggest a generally low conversion rate in both cell lines, which could be intensified in S1P-lyase deficient cells due to impaired lysosomal activity and less efficient consumption. Nevertheless, further experiments are needed to confirm this hypothesis.

The involvement of autophagy in the degradation of lipid droplets has only been described very recently (Singh et al, 2009). The catabolic processing of free fatty acids and triglycerides promotes the generation of ATP via  $\beta$ -oxidation thereby supplying cells with energy. Inhibition of the autophagic or lysosomal activity was shown to increase the storage of free fatty acids in lipid droplets (Singh et al, 2009). As shown in *Fig. 29*, S1P-lyase deficient cells show a pronounced accumulation of lipid droplets, further supporting a lysosomal impairment in these cells. Thus, it would be interesting to further analyze the metabolism of lipid droplets and fatty acids and the functional consequences upon modulation of the S1P metabolism.

The combined results indicate impaired lysosomal activity in S1P-lyase deficient cells. This also affects the autophagic process by decreasing final clearance of cargo in the lysosome, while induction of autophagy appears unaffected.

Determination of the overall APP-FL maturation state revealed a significant difference in the ratio of mature to immature APP (*Fig. 21A, B*). Increased maturation of APP was ruled out by cycloheximid treatment (*Fig. 21C, D*). These results demonstrate a higher stability of APP-FL<sub>m</sub>, either caused by lowered proteolytic activity or by reduced secretase activity, as discussed before (see 4.1). However, earlier studies also highlighted the role of the lysosomal activity on the APP processing secretases. BACE1 has a pH optimum of ~4.5 – 5 and elevation of the pH lowers its activity (Vassar et al, 1999; Vassar & Citron, 2000). On the other hand, BACE1 seems to be critical for the lysosomal activity as well. Pharmacological or genetic inhibition of BACE1 was shown to reduce the cathepsin D activity by ~40 % and to increase the lysosomal pH, causing an accumulation of lipofuscin in retinal pigment epithelium (Cai et al, 2012). It is difficult to link the exact interplay of BACE1 and lysosomal activity in the S1P-lyase deficient cell model. According to the previously mentioned literature, impairment of

lysosomal activity can hamper BACE1 and vice versa. However, the findings rather suggest an impairment of BACE1 caused by the storage of lipids.

Less is known about the relation of lysosomal and  $\gamma$ -secretase activity. Most studies state a predominant localization of the catalytically active  $\gamma$ -secretase complex at the PM, partially in endosomal-lysosomal compartments and to a lesser extent in the Golgi (Haass et al, 2012). An interesting study by Pasternak and colleagues demonstrated a localization of  $\gamma$ -secretase subunits at the lysosomal membrane (Pasternak et al, 2003). In contrast to other studies (Zhang et al, 2001) they were able to demonstrate a pH optimum for the  $\gamma$ -secretase activity at 4.5 in this compartment.

Thus, lowered lysosomal activity induced by changes in the pH, could partially explain the reduced  $\gamma$ -secretase and  $\beta$ -secretase activities. Nevertheless, further pH dependent  $\gamma$ -secretase or BACE1 assays would help to clarify the exact role of the lysosomal pH on the secretases and determine the conflicting results for the BACE1 activity measurements (*Fig. 14*) and the levels of secreted sAPP $\beta$  (*Fig. 15*).

#### 4.3 Potential role of S1P-lyase in vesicular trafficking.

As stated before, S1P-lyase deficient cells show a wide range of similarities with LSDs including impaired lysosomal activity. But storage of lipids have been shown to hamper membrane fluidity and subcellular trafficking as well (Pagano et al, 2000). Accumulation of GSLs was shown to disrupt the intracellular transport in a NPC1<sup>-/-</sup> mice model, probably by mistargeting annexin 2 and 6 (te Vruchte et al, 2004). Deficiency of NPC1 was furthermore shown to increase the affinity of sphingosine to endosomal or lysosomal compartments and could display a regulating mechanism for protein and lipid transport (Blom et al, 2012). Studies in retinoid cells revealed a crucial role for the dihydro-S1P to S1P ratio in the endosomal- and lysosomal trafficking of the receptor potential channels and its degradation (TRPC) (Yonamine et al, 2011). These receptors are selective ion gating channels and critical for a variety of intracellular signaling cascades (Montell, 2005). Interestingly, the members of the subfamily TRPML1 – 3 (TRP-mucopolipidosis type IV associated 1 - 3) are localized in endosomal/lysosomal membranes where they mediate the rapid release of Ca<sup>2+</sup> from these compartments (Dong et

al, 2010). Notably, lipid storage blocks the release of  $\text{Ca}^{2+}$  by inhibiting the TRPML1 and the lysosomal trafficking in NPC1 cells (Shen et al, 2012). In line with this finding, the study by Lloyd-Evans and colleagues illustrated a defective  $\text{Ca}^{2+}$  signaling in NPC1 cells due to increased sphingosine storage (Lloyd-Evans et al, 2008). Fusion of different organelles with the lysosomes and overall maturation of lysosomes is a highly  $\text{Ca}^{2+}$  dependent process (Luzio et al, 2007; Luzio et al, 2003). Moreover, fusion of lysosomal membranes with the plasma membrane during exocytosis also depends on  $\text{Ca}^{2+}$  (Bastow et al, 2012). Lysosomes are capable to store  $\text{Ca}^{2+}$  at a concentration of 400 – 600  $\mu\text{M}$  in their lumen (Burdakov et al, 2005; Christensen et al, 2002). Rapid release from these stores is crucial for the fusion of the lysosomal membrane with the target membrane (Pryor et al, 2000).

Interestingly, increasing cytosolic  $\text{Ca}^{2+}$  by inhibition of SERCA with thapsigargin or stimulation of lysosomal release with GPN resulted in an efficient reduction of APP-CTFs and partially restored their clearance in S1P-lyase deficient cells (*Fig. 31*). This result strongly indicates that efficient  $\text{Ca}^{2+}$  signaling and probably its local increase at the lysosome is important for the lysosomal function. A study on S1P-lyase deficient cells indeed showed an aberrant  $\text{Ca}^{2+}$  storage as well as a general increase in the intracellular concentration of cytosolic  $\text{Ca}^{2+}$  in S1P lyase deficient cells (Claas et al, 2010). However, experiments with pharmacological modulators reducing the intracellular  $\text{Ca}^{2+}$  concentration in S1P-lyase deficient cells have to be performed. This could help to cover the exact role of  $\text{Ca}^{2+}$  in intracellular trafficking.

Interestingly, the analysis of other subcellular compartments by immunocytochemistry revealed alterations of early Golgi compartments, the ER and early endosomes in S1P-lyase deficient cells. In particular, enlargement of giantin positive structures (*Fig. 27*) could suggest an impaired docking of COPI vesicles to the cytoplasmic site of *cis*-Golgi compartments.  $\text{Ca}^{2+}$  is crucial for the trafficking of COPI-coated vesicles since it is necessary for the efficient coating and their recycling (Ahluwalia et al, 2001). This  $\text{Ca}^{2+}$  regulated coating of the vesicles facilitates their fusion with the target golgi-membranes (Bentley et al, 2010).

S1P-lyase deficient cells also showed a higher number of tubular EEA1 positive endosomal compartments (*Fig. 28*). During the maturation of early to late endosomes scaffolding proteins are

removed from the early endosomes, causing a loss of the tubular appearance and an increase in size due to homotypic vesicle fusion (van Weering & Cullen, 2014). This action is probably mediated by a replacement of Rab5 by Rab7 (Rink et al, 2005). Interestingly, the COPI protein complex was also detected on early endosomes and seems to play an important role in their maturation. Impaired binding of COPI-coated vesicles to Golgi membranes was shown to cause tubulation and reorganization of early endosomes (Aniento et al, 1996; Lippincott-Schwartz et al, 1991; Tooze & Hollinshead, 1992). Hypothetically, the increased number of tubular endosomes in S1P-lyase deficient cells might emerge from a generally impaired maturation of the endosomes. This could cause a reduced lysosomal activity due to inefficient acidification of lysosomal compartments or a reduced delivery of proteins and enzymes. Thus, it would be interesting to further address and functionally analyze this interesting link between impaired  $\text{Ca}^{2+}$  signaling, and altered vesicular trafficking and maturation of endosomes to lysosomes in S1P deficient cells.

In general, cause for aberrant high levels of  $\text{Ca}^{2+}$  in S1P-lyase deficient cells can only be speculated. Seol and colleagues postulated that the presence of intracellular S1P induces an influx of  $\text{Ca}^{2+}$  from extracellular pools (Seol et al, 2005). Pandol and colleagues furthermore reported that high levels of sphingosine can directly impair  $\text{Ca}^{2+}$  ATPases and hamper the reuptake into intracellular  $\text{Ca}^{2+}$  stores, causing an increase of the cytosolic  $\text{Ca}^{2+}$  concentrations (Pandol et al, 1994). In general, sphingolipid metabolism appears to be tightly linked to cellular  $\text{Ca}^{2+}$  homeostasis and therefore to subcellular trafficking.

#### *4.4 Role of PKC in the processing of APP.*

$\text{Ca}^{2+}$  plays a critical role in intracellular signaling and is involved in a multitude of cellular processes. One of the major  $\text{Ca}^{2+}$  dependent enzymes involved in cellular regulation is the protein kinase C (PKC) (Mellor & Parker, 1998; Nishizuka, 1995). The classical PKC isoforms  $\alpha$ ,  $\beta_1$ ,  $\beta_{II}$  or  $\gamma$  require the second messenger molecules  $\text{Ca}^{2+}$  and also DAG for full activation (Mellor & Parker, 1998). Both second messengers are released upon activation of phospholipase C (PLC) that cleaves phosphatidylinositol 4,5-bisphosphate (PIP<sub>2</sub>) in the plasma membrane to generate DAG and IP<sub>3</sub>. The

latter activates IP<sub>3</sub>-dependent Ca<sup>2+</sup> channels in the ER leading, to increased cytosolic Ca<sup>2+</sup> concentration. DAG and Ca<sup>2+</sup> bind to the C1 and C2 domains of PKC, respectively (Ono et al, 1989). Initial binding of Ca<sup>2+</sup> to its C2 domain mediates the RACK (receptor for activated c-kinases)-dependent translocation of PKC to the plasma membrane (Haberman et al, 2011). Upon translocation to the plasma membrane, PKC binds to the membrane-bound DAG and gets activated (Ono et al, 1989). PKC was shown to promote  $\alpha$ -secretase cleavage of APP-FL, when activated by phorbol esters or other reagents (Efthimiopoulos et al, 1994). PKC stimulation causes a competition between  $\alpha$ - and  $\beta$ -secretases resulting in elevated secretion of sAPP $\alpha$  (Skovronsky et al, 2000). Furthermore, activation of PKC promoted the  $\alpha$ -secretase mediated cleavage of APP and ameliorated AD pathology in fibroblasts of AD patients and transgenic AD mice (Etcheberrigaray et al, 2004). Modulation of PKC activity might represent an interesting target for AD therapeutics.

The analysis of WT and S1P-lyase deficient cells demonstrated significant differences in the localization of PKC. Cells lacking S1P-lyase have a higher ratio of cytosolic to membrane localized PKC as compared to WT cells (*Fig. 32A, B* and *Fig. 33A, B*), suggesting a reduced activity of PKC. In an early study, sphingosine was shown to compete with DAG for the C1 domain of PKC and thereby inhibit its activation (Hannun & Bell, 1989). Moreover, in primary fibroblasts from patients with NPC1, increased levels of sphingosine were shown to impair the activation of PKC by blocking the binding to its activator PDBU (phorbol 12, 13-dibutyrate) (Rodriguez-Lafrasse et al, 1997). Thus, the elevated levels of sphingosine observed in S1P-lyase deficient cells in the present work might underlie the lower association of PKC with cellular membranes. Treatment with SKiII reduced the levels of S1P and increased the intracellular sphingosine concentration in both WT and S1P-lyase deficient cells (*Fig. 10A*). This increase in the level of sphingosine was associated with a significant increase in cytosolic localized PKC in WT cells (*Fig. 32B*). Notably, the changes in the ratio of cytosolic to membrane localized PKC were not significant in S1P-lyase deficient cells (*Fig. 32C*). Interestingly, level of membrane localized PKC were clearly elevated upon SKiII in S1P-lyase deficient cells (*Fig. 32A*).

Inhibition of PKC with the inhibitor bisindolylmaleimide I (BIM I) showed a striking reduction of cytosolic localized PKC in WT and S1P-lyase deficient cells (*Fig. 33A, C, D*). Surprisingly, this result

and would rather indicate an activation of PKC, although membrane localized PKC in WT cells decreases (*Fig. 33A*). Level of membrane localized PKC in S1P-lyase deficient cells increase upon BIM I (*Fig. 33A*). This finding indicates that the response of membrane localized PKC to BIM I as well as to SKiII (*Fig. 32A*) in S1P-lyase deficient cells is different as compared to WT cells.

The effect of BIM I on the cytosolic PKC levels remain elusive. BIM I is a competitive inhibitor for the ATP binding site of PKC and efficiently inhibits the isoforms  $\alpha$ ,  $\beta_I$ ,  $\beta_{II}$ ,  $\gamma$ ,  $\delta$  and  $\epsilon$  at low nanomolar concentrations (~20 nM) (Toullec et al, 1991). However, the concentration used in these experiments was 1  $\mu$ M. This high concentration might have caused the inhibition of other kinases like GSK3 $\beta$  or PKA cells (Hers et al, 1999) and induced offside effect.

The levels of APP-FL and APP-CTFs were strongly increased upon inhibition of PKC (*Fig. 33A*), similar to the sphingosine treatment (*Fig. 34A, B*). Both, WT and the S1P-lyase deficient cells, show a time dependent increase in APP-FL and APP-CTFs when treated with sphingosine (*Fig. 34A, B*). This increase was accompanied by a simultaneous change in the PKC localization in WT, but not in S1P-lyase deficient cells (*Fig. 34C*).

Both, BIM I and sphingosine treatment caused a decrease in the ratio of the active to the intermediate forms of Cathepsin D, indicating impaired lysosomal activity (*Fig. 33A* and *Fig. 34A*). These results support the hypothesis, that accumulation of sphingosine or other lipids can cause an inhibition of PKC, and also an impairment of lysosomal activity. However, the functional relation of PKC, lipids and lysosomal activity remains elusive. Accumulation of sphingosine was shown to inhibit PKC activity and cause a hyper phosphorylation of vimentin (Walter et al, 2009). Hyper phosphorylated vimentin shows less efficient polymerization and was shown to induce dysfunction of endosomal compartments in cells in a NPC1 model (Walter et al, 2009). Overexpression of PKC $\epsilon$  on the other hand partially overcame the phenotype in these cells and even ameliorated the hampered cholesterol transport (Tamari et al, 2013). It would therefore be interesting to analyze whether the activation of PKC by phorbol esters or the overexpression of PKC reduce the phenotype in the S1P-lyase deficient cells. Taken together, the present results lead to the conclusion that sphingosine could also induce effects on APP-FL and APP-CTFs via inhibition of PKC. These findings are in line with the previously described effects of PKC activation on the APP metabolism (Efthimiopoulos et al, 1994).



However, it remains elusive whether the aberrant  $\text{Ca}^{2+}$  signaling impairs the PKC activity or vice versa. Harper and Poole demonstrated, that inhibition of PKC with BIM I can actually negatively regulate  $\text{Ca}^{2+}$  release as well as  $\text{Ca}^{2+}$  entry (Harper & Poole, 2011). Nevertheless, the effects on the PKC localization exerted by SKiII, BIM I and sphingosine are similar, but APP-FL and APP-CTFs levels respond differently. While BIM I and sphingosine show an increase of APP-FL and APP-CTFs (*Fig. 33* and *Fig. 34*), SKiII causes a striking decrease (*Fig. 10C, D* and *Fig. 32*). It is assumed that sphingosine indeed alters the PKC localization, as shown for the treatment with SKiII and sphingosine. However, the reduced S1P concentration might promote the secretase activity in general. It would therefore be interesting to analyze, whether SKiII treatment would cause a reduction of APP-FL and APP-CTFs under conditions of PKC inhibition.

In summary, the effects of the S1P-lyase deficiency on the localization and probably the PKC activity are evident. Sphingosine, rather than S1P, might cause inhibition of PKC and could also decrease lysosomal activity. However, it cannot be explained whether the effects on APP-FL and APP-CTF accumulation are due to the lowered PKC activity or not. Sphingosine and S1P might exert dual roles. While S1P reduces secretase activities, sphingosine causes a relocation of PKC in the analyzed fractions and probably a reduction in its activity. The role of  $\text{Ca}^{2+}$  signaling on the PKC activity remains unclear. At the current state it is feasible to identify whether aberrant  $\text{Ca}^{2+}$  levels are caused by S1P (Seol et al, 2005) or caused by PKC itself (Harper & Poole, 2011).

Thus, S1P-lyase deficiency resembles phenotypes observed in other LSDs. Storage of S1P and sphingosine has far-ranging consequences on the proteolytic processing of APP by the secretases or in lysosomal compartment (*Fig. 35*).

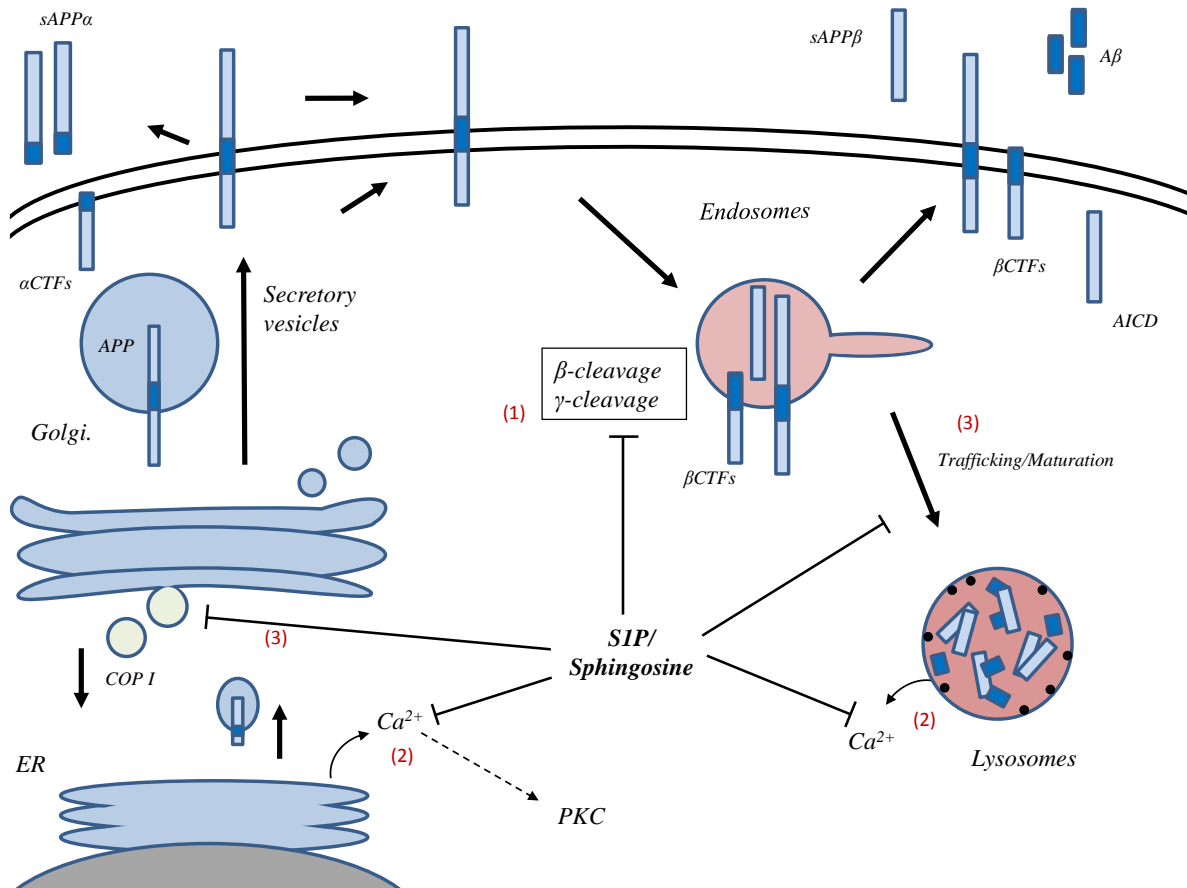


**Fig. 35: Hypothetical scheme of the effects induced by S1P-lyase deficiency.** Storage of S1P and sphingosine in S1P-lyase deficient cells impairs the proteolytic processing of APP. High levels of S1P cause a reduction of the β- and γ-secretase activities and might alter the processing of APP (1). S1P and sphingosine accumulation affect the Ca<sup>2+</sup> signaling (2) and probably hampering membrane dynamics, trafficking and maturation of vesicles (3). Inefficiently matured lysosomes could cause the elevated levels of APP-FL and APP-CTF in S1P-lyase deficient cells.

## 5. Outlook

The contribution of lipids like cholesterol and GSLs in pathogenesis of AD has been extensively investigated in past decades. However, the role of sphingoid bases like S1P or sphingosine is less clear. Deficiency of the S1P-lyase caused increased sphingosine and S1P level and provided interesting insights into the proteolytic processing of APP and general cellular mechanisms. Nevertheless, further experiments are necessary to specifically determine the pathological relevance of these findings.

Lysosomal activity was found to be reduced in the S1PL-KO model contributing to the elevated levels of APP and CTFs. The present study furthermore shows direct decreasing effects of S1P level on the  $\beta$ - and  $\gamma$ -secretases activity. The molecular mechanisms causing this impairing effect remain elusive and might be triggered by the hampered sub-cellular trafficking. Further experiments are necessary to determine whether these effects are directly linked or mediated by altered  $\text{Ca}^{2+}$  homeostasis.

Moreover, lysosomal deficiency plays a crucial role in numerous other neurodegenerative diseases like Parkinson's disease or Huntington's disease. It would be of great interest to determine the contribution of the S1P-lyase deficiency on these pathologies.

The early mortality of S1P-lyase deficient mice is a major problem for the age dependent investigation of APP. However conditional KO mice in a nestin-cre background could be useful to better understand the function of the S1P-lyase in neuronal cells. First, the effect of S1P-lyase deficiency on the cognitive ability of these mice during aging could be investigated. Later on, conditional KO mice could be crossed with transgenic AD mouse models. This could give more experimental opportunities to analyze the effect of the neuron specific S1P-lyase knockout. Future experiments could also help to determine the role of the S1P-sphingosine axis on the plaque deposition and cognitive abilities.

Although SphK1 and SphK2 have been partially analyzed in different brain regions of AD patients, the results are still conflictive and allow only little conclusions. Expression pattern analysis and genome wide association studies could help to determine potential factors contributing to the pathogenesis. Correlation studies of sphingolipid mediating enzymes or sphingolipid intermediates with the AD associated proteins would increase the probability to develop treatment strategies or promote the clinical research.

## 6. References

- Agholme L, Hallbeck M, Benedikz E, Marcusson J, Kagedal K (2012) Amyloid-beta secretion, generation, and lysosomal sequestration in response to proteasome inhibition: involvement of autophagy. *Journal of Alzheimer's disease : JAD* **31**: 343-358
- Ahluwalia JP, Topp JD, Weirather K, Zimmerman M, Stannes M (2001) A role for calcium in stabilizing transport vesicle coats. *J Biol Chem* **276**: 34148-34155
- Allende ML, Bektas M, Lee BG, Bonifacino E, Kang J, Tuymetova G, Chen W, Saba JD, Proia RL (2011) Sphingosine-1-phosphate lyase deficiency produces a pro-inflammatory response while impairing neutrophil trafficking. *J Biol Chem* **286**: 7348-7358
- Allinson TM, Parkin ET, Turner AJ, Hooper NM (2003) ADAMs family members as amyloid precursor protein alpha-secretases. *Journal of neuroscience research* **74**: 342-352
- Altan N, Chen Y, Schindler M, Simon SM (1999) Tamoxifen inhibits acidification in cells independent of the estrogen receptor. *Proceedings of the National Academy of Sciences of the United States of America* **96**: 4432-4437
- Alvarez SE, Harikumar KB, Hait NC, Allegood J, Strub GM, Kim EY, Maceyka M, Jiang H, Luo C, Kordula T, Milstien S, Spiegel S (2010) Sphingosine-1-phosphate is a missing cofactor for the E3 ubiquitin ligase TRAF2. *Nature* **465**: 1084-1088
- Andersson CX, Fernandez-Rodriguez J, Laos S, Baeckstrom D, Haass C, Hansson GC (2005) Shedding and gamma-secretase-mediated intramembrane proteolysis of the mucin-type molecule CD43. *The Biochemical journal* **387**: 377-384
- Ando K, Iijima KI, Elliott JI, Kirino Y, Suzuki T (2001) Phosphorylation-dependent regulation of the interaction of amyloid precursor protein with Fe65 affects the production of beta-amyloid. *J Biol Chem* **276**: 40353-40361
- Aniento F, Gu F, Parton RG, Gruenberg J (1996) An endosomal beta COP is involved in the pH-dependent formation of transport vesicles destined for late endosomes. *The Journal of cell biology* **133**: 29-41
- Aridor M, Hannan LA (2000) Traffic jam: a compendium of human diseases that affect intracellular transport processes. *Traffic* **1**: 836-851
- Arikawa K, Takuwa N, Yamaguchi H, Sugimoto N, Kitayama J, Nagawa H, Takehara K, Takuwa Y (2003) Ligand-dependent inhibition of B16 melanoma cell migration and invasion via endogenous S1P2 G protein-coupled receptor. Requirement of inhibition of cellular RAC activity. *J Biol Chem* **278**: 32841-32851
- Arnaiz E, Almkvist O (2003) Neuropsychological features of mild cognitive impairment and preclinical Alzheimer's disease. *Acta neurologica Scandinavica Supplementum* **179**: 34-41
- Barrett PJ, Song Y, Van Horn WD, Hustedt EJ, Schafer JM, Hadziselimovic A, Beel AJ, Sanders CR (2012) The amyloid precursor protein has a flexible transmembrane domain and binds cholesterol. *Science* **336**: 1168-1171
- Bastow ER, Last K, Golub S, Stow JL, Stanley AC, Fosang AJ (2012) Evidence for lysosomal exocytosis and release of aggrecan-degrading hydrolases from hypertrophic chondrocytes, in vitro and in vivo. *Biology open* **1**: 318-328

- Benes P, Vetvicka V, Fusek M (2008) Cathepsin D--many functions of one aspartic protease. *Critical reviews in oncology/hematology* **68**: 12-28
- Bennett BD, Denis P, Haniu M, Teplow DB, Kahn S, Louis JC, Citron M, Vassar R (2000) A furin-like convertase mediates propeptide cleavage of BACE, the Alzheimer's beta -secretase. *J Biol Chem* **275**: 37712-37717
- Bentley M, Nycz DC, Joglekar A, Fertschai I, Malli R, Graier WF, Hay JC (2010) Vesicular calcium regulates coat retention, fusogenicity, and size of pre-Golgi intermediates. *Molecular biology of the cell* **21**: 1033-1046
- Bhattacharyya R, Barren C, Kovacs DM (2013) Palmitoylation of amyloid precursor protein regulates amyloidogenic processing in lipid rafts. *The Journal of neuroscience : the official journal of the Society for Neuroscience* **33**: 11169-11183
- Blom T, Li Z, Bittman R, Somerharju P, Ikonen E (2012) Tracking sphingosine metabolism and transport in sphingolipidoses: NPC1 deficiency as a test case. *Traffic* **13**: 1234-1243
- Boland B, Smith DA, Mooney D, Jung SS, Walsh DM, Platt FM (2010) Macroautophagy is not directly involved in the metabolism of amyloid precursor protein. *J Biol Chem* **285**: 37415-37426
- Borg JP, Ooi J, Levy E, Margolis B (1996) The phosphotyrosine interaction domains of X11 and FE65 bind to distinct sites on the YENPTY motif of amyloid precursor protein. *Molecular and cellular biology* **16**: 6229-6241
- Borowsky AD, Bandhuvula P, Kumar A, Yoshinaga Y, Nefedov M, Fong LG, Zhang M, Baridon B, Dillard L, de Jong P, Young SG, West DB, Saba JD (2012) Sphingosine-1-phosphate lyase expression in embryonic and adult murine tissues. *Journal of lipid research* **53**: 1920-1931
- Braak H, Braak E (1996) Evolution of the neuropathology of Alzheimer's disease. *Acta neurologica Scandinavica Supplementum* **165**: 3-12
- Bu G (2009) Apolipoprotein E and its receptors in Alzheimer's disease: pathways, pathogenesis and therapy. *Nature reviews Neuroscience* **10**: 333-344
- Burdakov D, Petersen OH, Verkhratsky A (2005) Intraluminal calcium as a primary regulator of endoplasmic reticulum function. *Cell calcium* **38**: 303-310
- Burg VK, Grimm HS, Rothhaar TL, Grosgen S, Hundsdorfer B, Hauptenthal VJ, Zimmer VC, Mett J, Weingartner O, Laufs U, Broersen LM, Tanila H, Vanmierlo T, Lutjohann D, Hartmann T, Grimm MO (2013) Plant sterols the better cholesterol in Alzheimer's disease? A mechanistical study. *The Journal of neuroscience : the official journal of the Society for Neuroscience* **33**: 16072-16087
- Burns M, Gaynor K, Olm V, Mercken M, LaFrancois J, Wang L, Mathews PM, Noble W, Matsuoka Y, Duff K (2003) Presenilin redistribution associated with aberrant cholesterol transport enhances beta-amyloid production in vivo. *The Journal of neuroscience : the official journal of the Society for Neuroscience* **23**: 5645-5649
- Buxbaum JD, Gandy SE, Cicchetti P, Ehrlich ME, Czernik AJ, Fracasso RP, Ramabhadran TV, Unterbeck AJ, Greengard P (1990) Processing of Alzheimer beta/A4 amyloid precursor protein: modulation by agents that regulate protein phosphorylation. *Proceedings of the National Academy of Sciences of the United States of America* **87**: 6003-6006

- Cai H, Wang Y, McCarthy D, Wen H, Borchelt DR, Price DL, Wong PC (2001) BACE1 is the major beta-secretase for generation of Abeta peptides by neurons. *Nature neuroscience* **4**: 233-234
- Cai J, Qi X, Kociok N, Skosyrski S, Emilio A, Ruan Q, Han S, Liu L, Chen Z, Bowes Rickman C, Golde T, Grant MB, Saftig P, Serneels L, de Strooper B, Jousen AM, Boulton ME (2012) beta-Secretase (BACE1) inhibition causes retinal pathology by vascular dysregulation and accumulation of age pigment. *EMBO molecular medicine* **4**: 980-991
- Cai XD, Golde TE, Younkin SG (1993) Release of excess amyloid beta protein from a mutant amyloid beta protein precursor. *Science* **259**: 514-516
- Cao X, Sudhof TC (2001) A transcriptionally [correction of transcriptively] active complex of APP with Fe65 and histone acetyltransferase Tip60. *Science* **293**: 115-120
- Capell A, Steiner H, Willem M, Kaiser H, Meyer C, Walter J, Lammich S, Multhaup G, Haass C (2000) Maturation and pro-peptide cleavage of beta-secretase. *J Biol Chem* **275**: 30849-30854
- Carrera I, Etcheverria I, Fernandez-Novoa L, Lombardi V, Cacabelos R, Vigo C (2012) Vaccine Development to Treat Alzheimer's Disease Neuropathology in APP/PS1 Transgenic Mice. *International journal of Alzheimer's disease* **2012**: 376138
- Carstea ED, Morris JA, Coleman KG, Loftus SK, Zhang D, Cummings C, Gu J, Rosenfeld MA, Pavan WJ, Krizman DB, Nagle J, Polymeropoulos MH, Sturley SL, Ioannou YA, Higgins ME, Comly M, Cooney A, Brown A, Kaneski CR, Blanchette-Mackie EJ, Dwyer NK, Neufeld EB, Chang TY, Liscum L, Strauss JF, 3rd, Ohno K, Zeigler M, Carmi R, Sokol J, Markie D, O'Neill RR, van Diggelen OP, Elleder M, Patterson MC, Brady RO, Vanier MT, Pentchev PG, Tagle DA (1997) Niemann-Pick C1 disease gene: homology to mediators of cholesterol homeostasis. *Science* **277**: 228-231
- Carter DB (2005) The interaction of amyloid-beta with ApoE. *Sub-cellular biochemistry* **38**: 255-272
- Ceccom J, Loukh N, Lauwers-Cances V, Touriol C, Nicaise Y, Gentil C, Uro-Coste E, Pitson S, Maurage CA, Duyckaerts C, Cuvillier O, Delisle MB (2014) Reduced sphingosine kinase-1 and enhanced sphingosine 1-phosphate lyase expression demonstrate deregulated sphingosine 1-phosphate signaling in Alzheimer's disease. *Acta neuropathologica communications* **2**: 12
- Chang KA, Kim HS, Ha TY, Ha JW, Shin KY, Jeong YH, Lee JP, Park CH, Kim S, Baik TK, Suh YH (2006) Phosphorylation of amyloid precursor protein (APP) at Thr668 regulates the nuclear translocation of the APP intracellular domain and induces neurodegeneration. *Molecular and cellular biology* **26**: 4327-4338
- Chen F, Hasegawa H, Schmitt-Ulms G, Kawarai T, Bohm C, Katayama T, Gu Y, Sanjo N, Glista M, Rogaeva E, Wakutani Y, Pardossi-Piquard R, Ruan X, Tandon A, Checler F, Marambaud P, Hansen K, Westaway D, St George-Hyslop P, Fraser P (2006) TMP21 is a presenilin complex component that modulates gamma-secretase but not epsilon-secretase activity. *Nature* **440**: 1208-1212
- Chi H (2011) Sphingosine-1-phosphate and immune regulation: trafficking and beyond. *Trends in pharmacological sciences* **32**: 16-24
- Christensen KA, Myers JT, Swanson JA (2002) pH-dependent regulation of lysosomal calcium in macrophages. *Journal of cell science* **115**: 599-607
- Citron M, Diehl TS, Gordon G, Biere AL, Seubert P, Selkoe DJ (1996) Evidence that the 42- and 40-amino acid forms of amyloid beta protein are generated from the beta-amyloid precursor protein by different protease activities. *Proceedings of the National Academy of Sciences of the United States of America* **93**: 13170-13175

- Citron M, Oltersdorf T, Haass C, McConlogue L, Hung AY, Seubert P, Vigo-Pelfrey C, Lieberburg I, Selkoe DJ (1992) Mutation of the beta-amyloid precursor protein in familial Alzheimer's disease increases beta-protein production. *Nature* **360**: 672-674
- Claas RF, ter Braak M, Hegen B, Hardel V, Angioni C, Schmidt H, Jakobs KH, Van Veldhoven PP, zu Heringdorf DM (2010) Enhanced Ca<sup>2+</sup> storage in sphingosine-1-phosphate lyase-deficient fibroblasts. *Cellular signalling* **22**: 476-483
- Cordy JM, Hussain I, Dingwall C, Hooper NM, Turner AJ (2003) Exclusively targeting beta-secretase to lipid rafts by GPI-anchor addition up-regulates beta-site processing of the amyloid precursor protein. *Proceedings of the National Academy of Sciences of the United States of America* **100**: 11735-11740
- Couttas TA, Kain N, Daniels B, Lim XY, Shepherd C, Kril J, Pickford R, Li H, Garner B, Don AS (2014) Loss of the neuroprotective factor Sphingosine 1-phosphate early in Alzheimer's disease pathogenesis. *Acta neuropathologica communications* **2**: 9
- Cuervo AM, Knecht E, Terlecky SR, Dice JF (1995) Activation of a selective pathway of lysosomal proteolysis in rat liver by prolonged starvation. *The American journal of physiology* **269**: C1200-1208
- Cuvillier O, Ader I, Bouquerel P, Brizuela L, Malavaud B, Mazerolles C, Rischmann P (2010) Activation of sphingosine kinase-1 in cancer: implications for therapeutic targeting. *Current molecular pharmacology* **3**: 53-65
- Cuvillier O, Pirianov G, Kleuser B, Vanek PG, Coso OA, Gutkind S, Spiegel S (1996) Suppression of ceramide-mediated programmed cell death by sphingosine-1-phosphate. *Nature* **381**: 800-803
- Davies L, Fassbender K, Walter S (2013) Sphingolipids in neuroinflammation. *Handbook of experimental pharmacology*: 421-430
- Dawkins E, Small DH (2014) Insights into the physiological function of the beta-amyloid precursor protein: beyond Alzheimer's disease. *Journal of neurochemistry*
- De Strooper B (2007) Loss-of-function presenilin mutations in Alzheimer disease. *Talking Point on the role of presenilin mutations in Alzheimer disease. EMBO reports* **8**: 141-146
- De Strooper B, Iwatsubo T, Wolfe MS (2012) Presenilins and gamma-secretase: structure, function, and role in Alzheimer Disease. *Cold Spring Harbor perspectives in medicine* **2**: a006304
- De Strooper B, Saftig P, Craessaerts K, Vanderstichele H, Guhde G, Annaert W, Von Figura K, Van Leuven F (1998) Deficiency of presenilin-1 inhibits the normal cleavage of amyloid precursor protein. *Nature* **391**: 387-390
- Deng Y, Wang Z, Wang R, Zhang X, Zhang S, Wu Y, Staufenbiel M, Cai F, Song W (2013) Amyloid-beta protein (A $\beta$ ) Glu11 is the major beta-secretase site of beta-site amyloid-beta precursor protein-cleaving enzyme 1(BACE1), and shifting the cleavage site to A $\beta$  Asp1 contributes to Alzheimer pathogenesis. *The European journal of neuroscience* **37**: 1962-1969
- Desplats PA, Denny CA, Kass KE, Gilmartin T, Head SR, Sutcliffe JG, Seyfried TN, Thomas EA (2007) Glycolipid and ganglioside metabolism imbalances in Huntington's disease. *Neurobiology of disease* **27**: 265-277

- Dewachter I, Moechars D, van Dorpe J, Tesseur I, Van den Haute C, Spittaels K, Van Leuven F (2001) Modelling Alzheimer's disease in multiple transgenic mice. *Biochemical Society symposium*: 203-210
- Ding G, Sonoda H, Yu H, Kajimoto T, Goparaju SK, Jahangeer S, Okada T, Nakamura S (2007) Protein kinase D-mediated phosphorylation and nuclear export of sphingosine kinase 2. *J Biol Chem* **282**: 27493-27502
- Dominguez D, Tournoy J, Hartmann D, Huth T, Cryns K, Deforce S, Serneels L, Camacho IE, Marjaux E, Craessaerts K, Roebroek AJ, Schwake M, D'Hooge R, Bach P, Kalinke U, Moechars D, Alzheimer C, Reiss K, Saftig P, De Strooper B (2005) Phenotypic and biochemical analyses of BACE1- and BACE2-deficient mice. *J Biol Chem* **280**: 30797-30806
- Dong XP, Shen D, Wang X, Dawson T, Li X, Zhang Q, Cheng X, Zhang Y, Weisman LS, Delling M, Xu H (2010) PI(3,5)P(2) controls membrane trafficking by direct activation of mucolipin Ca(2+) release channels in the endolysosome. *Nature communications* **1**: 38
- Dries DR, Shah S, Han YH, Yu C, Yu S, Shearman MS, Yu G (2009) Glu-333 of nicastrin directly participates in gamma-secretase activity. *J Biol Chem* **284**: 29714-29724
- Dries DR, Yu G (2008) Assembly, maturation, and trafficking of the gamma-secretase complex in Alzheimer's disease. *Current Alzheimer research* **5**: 132-146
- Dudek J, Benedix J, Cappel S, Greiner M, Jalal C, Muller L, Zimmermann R (2009) Functions and pathologies of BiP and its interaction partners. *Cellular and molecular life sciences : CMLS* **66**: 1556-1569
- Efthimiopoulos S, Felsenstein KM, Sambamurti K, Robakis NK, Refolo LM (1994) Study of the phorbol ester effect on Alzheimer amyloid precursor processing: sequence requirements and involvement of a cholera toxin sensitive protein. *Journal of neuroscience research* **38**: 81-90
- Eehalt R, Michel B, De Pietri Tonelli D, Zacchetti D, Simons K, Keller P (2002) Splice variants of the beta-site APP-cleaving enzyme BACE1 in human brain and pancreas. *Biochemical and biophysical research communications* **293**: 30-37
- Esch FS, Keim PS, Beattie EC, Blacher RW, Culwell AR, Oltersdorf T, McClure D, Ward PJ (1990) Cleavage of amyloid beta peptide during constitutive processing of its precursor. *Science* **248**: 1122-1124
- Etcheberrigaray R, Tan M, Dewachter I, Kuiperi C, Van der Auwera I, Wera S, Qiao L, Bank B, Nelson TJ, Kozikowski AP, Van Leuven F, Alkon DL (2004) Therapeutic effects of PKC activators in Alzheimer's disease transgenic mice. *Proceedings of the National Academy of Sciences of the United States of America* **101**: 11141-11146
- Farzan M, Schnitzler CE, Vasilieva N, Leung D, Choe H (2000) BACE2, a beta -secretase homolog, cleaves at the beta site and within the amyloid-beta region of the amyloid-beta precursor protein. *Proceedings of the National Academy of Sciences of the United States of America* **97**: 9712-9717
- Ferri CP, Prince M, Brayne C, Brodaty H, Fratiglioni L, Ganguli M, Hall K, Hasegawa K, Hendrie H, Huang Y, Jorm A, Mathers C, Menezes PR, Rimmer E, Sczufca M (2005) Global prevalence of dementia: a Delphi consensus study. *Lancet* **366**: 2112-2117
- Fiore F, Zambrano N, Minopoli G, Donini V, Duilio A, Russo T (1995) The regions of the Fe65 protein homologous to the phosphotyrosine interaction/phosphotyrosine binding domain of Shc bind the intracellular domain of the Alzheimer's amyloid precursor protein. *J Biol Chem* **270**: 30853-30856



- Fluhrer R, Capell A, Westmeyer G, Willem M, Hartung B, Condrón MM, Teplow DB, Haass C, Walter J (2002) A non-amyloidogenic function of BACE-2 in the secretory pathway. *Journal of neurochemistry* **81**: 1011-1020
- Forstl H, Kurz A (1999) Clinical features of Alzheimer's disease. *European archives of psychiatry and clinical neuroscience* **249**: 288-290
- Francis R, McGrath G, Zhang J, Ruddy DA, Sym M, Apfeld J, Nicoll M, Maxwell M, Hai B, Ellis MC, Parks AL, Xu W, Li J, Gurney M, Myers RL, Himes CS, Hiebsch R, Ruble C, Nye JS, Curtis D (2002) *aph-1* and *pen-2* are required for Notch pathway signaling, gamma-secretase cleavage of betaAPP, and presenilin protein accumulation. *Developmental cell* **3**: 85-97
- Fukumori A, Okochi M, Tagami S, Jiang J, Itoh N, Nakayama T, Yanagida K, Ishizuka-Katsura Y, Morihara T, Kamino K, Tanaka T, Kudo T, Tanii H, Ikuta A, Haass C, Takeda M (2006) Presenilin-dependent gamma-secretase on plasma membrane and endosomes is functionally distinct. *Biochemistry* **45**: 4907-4914
- Fuller M (2010) Sphingolipids: the nexus between Gaucher disease and insulin resistance. *Lipids in health and disease* **9**: 113
- Fyrst H, Saba JD (2010) An update on sphingosine-1-phosphate and other sphingolipid mediators. *Nature chemical biology* **6**: 489-497
- Galadari S, Rahman A, Pallichankandy S, Galadari A, Thayyullathil F (2013) Role of ceramide in diabetes mellitus: evidence and mechanisms. *Lipids in health and disease* **12**: 98
- Genter MB, Van Veldhoven PP, Jegga AG, Sakthivel B, Kong S, Stanley K, Witte DP, Ebert CL, Aronow BJ (2003) Microarray-based discovery of highly expressed olfactory mucosal genes: potential roles in the various functions of the olfactory system. *Physiological genomics* **16**: 67-81
- Ghosh TK, Bian J, Gill DL (1990) Intracellular calcium release mediated by sphingosine derivatives generated in cells. *Science* **248**: 1653-1656
- Ghosh TK, Bian J, Gill DL (1994) Sphingosine 1-phosphate generated in the endoplasmic reticulum membrane activates release of stored calcium. *J Biol Chem* **269**: 22628-22635
- Gieselmann V, Hasilik A, von Figura K (1985) Processing of human cathepsin D in lysosomes in vitro. *J Biol Chem* **260**: 3215-3220
- Gieselmann V, Pohlmann R, Hasilik A, Von Figura K (1983) Biosynthesis and transport of cathepsin D in cultured human fibroblasts. *The Journal of cell biology* **97**: 1-5
- Goate A, Chartier-Harlin MC, Mullan M, Brown J, Crawford F, Fidani L, Giuffra L, Haynes A, Irving N, James L, et al. (1991) Segregation of a missense mutation in the amyloid precursor protein gene with familial Alzheimer's disease. *Nature* **349**: 704-706
- Goedert M, Klug A, Crowther RA (2006) Tau protein, the paired helical filament and Alzheimer's disease. *Journal of Alzheimer's disease : JAD* **9**: 195-207
- Goedert M, Spillantini MG (2000) Tau mutations in frontotemporal dementia FTDP-17 and their relevance for Alzheimer's disease. *Biochimica et biophysica acta* **1502**: 110-121

- Goldgaber D, Lerman MI, McBride OW, Saffiotti U, Gajdusek DC (1987) Characterization and chromosomal localization of a cDNA encoding brain amyloid of Alzheimer's disease. *Science* **235**: 877-880
- Gomez-Munoz A, Gangoiti P, Arana L, Ouro A, Rivera IG, Ordonez M, Trueba M (2013) New insights on the role of ceramide 1-phosphate in inflammation. *Biochimica et biophysica acta* **1831**: 1060-1066
- Goni FM, Alonso A (2009) Effects of ceramide and other simple sphingolipids on membrane lateral structure. *Biochimica et biophysica acta* **1788**: 169-177
- Gonzalez-Cabrera PJ, Jo E, Sanna MG, Brown S, Leaf N, Marsolais D, Schaeffer MT, Chapman J, Cameron M, Guerrero M, Roberts E, Rosen H (2008) Full pharmacological efficacy of a novel S1P1 agonist that does not require S1P-like headgroup interactions. *Molecular pharmacology* **74**: 1308-1318
- Grimm MO, Grimm HS, Hartmann T (2007) Amyloid beta as a regulator of lipid homeostasis. *Trends in molecular medicine* **13**: 337-344
- Grimm MO, Grimm HS, Patzold AJ, Zinser EG, Halonen R, Duering M, Tschape JA, De Strooper B, Muller U, Shen J, Hartmann T (2005) Regulation of cholesterol and sphingomyelin metabolism by amyloid-beta and presenilin. *Nature cell biology* **7**: 1118-1123
- Grimm MO, Hauptenthal VJ, Rothhaar TL, Zimmer VC, Grosgen S, Hundsdorfer B, Lehmann J, Grimm HS, Hartmann T (2013) Effect of Different Phospholipids on alpha-Secretase Activity in the Non-Amyloidogenic Pathway of Alzheimer's Disease. *International journal of molecular sciences* **14**: 5879-5898
- Grosgen S, Grimm MO, Friess P, Hartmann T (2010) Role of amyloid beta in lipid homeostasis. *Biochimica et biophysica acta* **1801**: 966-974
- Grundke-Iqbal I, Iqbal K, Tung YC, Quinlan M, Wisniewski HM, Binder LI (1986) Abnormal phosphorylation of the microtubule-associated protein tau (tau) in Alzheimer cytoskeletal pathology. *Proceedings of the National Academy of Sciences of the United States of America* **83**: 4913-4917
- Guerreiro R, Wojtas A, Bras J, Carrasquillo M, Rogava E, Majounie E, Cruchaga C, Sassi C, Kauwe JS, Younkin S, Hazrati L, Collinge J, Pocock J, Lashley T, Williams J, Lambert JC, Amouyel P, Goate A, Rademakers R, Morgan K, Powell J, St George-Hyslop P, Singleton A, Hardy J (2013) TREM2 variants in Alzheimer's disease. *The New England journal of medicine* **368**: 117-127
- Haass C, Hung AY, Schlossmacher MG, Teplow DB, Selkoe DJ (1993) beta-Amyloid peptide and a 3-kDa fragment are derived by distinct cellular mechanisms. *J Biol Chem* **268**: 3021-3024
- Haass C, Kaether C, Thinakaran G, Sisodia S (2012) Trafficking and proteolytic processing of APP. *Cold Spring Harbor perspectives in medicine* **2**: a006270
- Haass C, Koo EH, Capell A, Teplow DB, Selkoe DJ (1995) Polarized sorting of beta-amyloid precursor protein and its proteolytic products in MDCK cells is regulated by two independent signals. *The Journal of cell biology* **128**: 537-547
- Haass C, Koo EH, Mellon A, Hung AY, Selkoe DJ (1992a) Targeting of cell-surface beta-amyloid precursor protein to lysosomes: alternative processing into amyloid-bearing fragments. *Nature* **357**: 500-503

- Haass C, Schlossmacher MG, Hung AY, Vigo-Pelfrey C, Mellon A, Ostaszewski BL, Lieberburg I, Koo EH, Schenk D, Teplow DB, et al. (1992b) Amyloid beta-peptide is produced by cultured cells during normal metabolism. *Nature* **359**: 322-325
- Haberman Y, Alon LT, Eliyahu E, Shalgi R (2011) Receptor for activated C kinase (RACK) and protein kinase C (PKC) in egg activation. *Theriogenology* **75**: 80-89
- Hagen-Euteneuer N, Lutjohann D, Park H, Merrill AH, Jr., van Echten-Deckert G (2012) Sphingosine 1-phosphate (S1P) lyase deficiency increases sphingolipid formation via recycling at the expense of de novo biosynthesis in neurons. *J Biol Chem* **287**: 9128-9136
- Hagen N, Van Veldhoven PP, Proia RL, Park H, Merrill AH, Jr., van Echten-Deckert G (2009) Subcellular origin of sphingosine 1-phosphate is essential for its toxic effect in lyase-deficient neurons. *J Biol Chem* **284**: 11346-11353
- Hait NC, Allegood J, Maceyka M, Strub GM, Harikumar KB, Singh SK, Luo C, Marmorstein R, Kordula T, Milstien S, Spiegel S (2009) Regulation of histone acetylation in the nucleus by sphingosine-1-phosphate. *Science* **325**: 1254-1257
- Hait NC, Bellamy A, Milstien S, Kordula T, Spiegel S (2007) Sphingosine kinase type 2 activation by ERK-mediated phosphorylation. *J Biol Chem* **282**: 12058-12065
- Hanada K, Kumagai K, Tomishige N, Kawano M (2007) CERT and intracellular trafficking of ceramide. *Biochimica et biophysica acta* **1771**: 644-653
- Hannun YA, Bell RM (1989) Regulation of protein kinase C by sphingosine and lysosphingolipids. *Clinica chimica acta; international journal of clinical chemistry* **185**: 333-345
- Hannun YA, Obeid LM (2008) Principles of bioactive lipid signalling: lessons from sphingolipids. *Nature reviews Molecular cell biology* **9**: 139-150
- Hardy J, Selkoe DJ (2002) The amyloid hypothesis of Alzheimer's disease: progress and problems on the road to therapeutics. *Science* **297**: 353-356
- Harold D, Abraham R, Hollingworth P, Sims R, Gerrish A, Hamshere ML, Pahwa JS, Moskva V, Dowzell K, Williams A, Jones N, Thomas C, Stretton A, Morgan AR, Lovestone S, Powell J, Proitsi P, Lupton MK, Brayne C, Rubinsztein DC, Gill M, Lawlor B, Lynch A, Morgan K, Brown KS, Passmore PA, Craig D, McGuinness B, Todd S, Holmes C, Mann D, Smith AD, Love S, Kehoe PG, Hardy J, Mead S, Fox N, Rossor M, Collinge J, Maier W, Jessen F, Schurmann B, Heun R, van den Bussche H, Heuser I, Kornhuber J, Wiltfang J, Dichgans M, Frolich L, Hampel H, Hull M, Rujescu D, Goate AM, Kauwe JS, Cruchaga C, Nowotny P, Morris JC, Mayo K, Sleegers K, Bettens K, Engelborghs S, De Deyn PP, Van Broeckhoven C, Livingston G, Bass NJ, Gurling H, McQuillin A, Gwilliam R, Deloukas P, Al-Chalabi A, Shaw CE, Tsolaki M, Singleton AB, Guerreiro R, Muhleisen TW, Nothen MM, Moebus S, Jockel KH, Klopp N, Wichmann HE, Carrasquillo MM, Pankratz VS, Younkin SG, Holmans PA, O'Donovan M, Owen MJ, Williams J (2009) Genome-wide association study identifies variants at CLU and PICALM associated with Alzheimer's disease. *Nature genetics* **41**: 1088-1093
- Harper MT, Poole AW (2011) PKC inhibition markedly enhances Ca<sup>2+</sup> signaling and phosphatidylserine exposure downstream of protease-activated receptor-1 but not protease-activated receptor-4 in human platelets. *Journal of thrombosis and haemostasis : JTH* **9**: 1599-1607
- Harrison SM, Harper AJ, Hawkins J, Duddy G, Grau E, Pugh PL, Winter PH, Shilliam CS, Hughes ZA, Dawson LA, Gonzalez MI, Upton N, Pangalos MN, Dingwall C (2003) BACE1 (beta-secretase)

transgenic and knockout mice: identification of neurochemical deficits and behavioral changes. *Molecular and cellular neurosciences* **24**: 646-655

Hartmann D, de Strooper B, Serneels L, Craessaerts K, Herreman A, Annaert W, Umans L, Lubke T, Lena Illert A, von Figura K, Saftig P (2002) The disintegrin/metalloprotease ADAM 10 is essential for Notch signalling but not for alpha-secretase activity in fibroblasts. *Human molecular genetics* **11**: 2615-2624

Hasegawa H, Sanjo N, Chen F, Gu YJ, Shier C, Petit A, Kawarai T, Katayama T, Schmidt SD, Mathews PM, Schmitt-Ulms G, Fraser PE, St George-Hyslop P (2004) Both the sequence and length of the C terminus of PEN-2 are critical for intermolecular interactions and function of presenilin complexes. *J Biol Chem* **279**: 46455-46463

Hass MR, Yankner BA (2005) A  $\gamma$ -secretase-independent mechanism of signal transduction by the amyloid precursor protein. *J Biol Chem* **280**: 36895-36904

He G, Luo W, Li P, Remmers C, Netzer WJ, Hendrick J, Bettayeb K, Flajolet M, Gorelick F, Wennogle LP, Greengard P (2010a) Gamma-secretase activating protein is a therapeutic target for Alzheimer's disease. *Nature* **467**: 95-98

He X, Huang Y, Li B, Gong CX, Schuchman EH (2010b) Deregulation of sphingolipid metabolism in Alzheimer's disease. *Neurobiology of aging* **31**: 398-408

Hebert SS, Serneels L, Tolia A, Craessaerts K, Derks C, Filippov MA, Muller U, De Strooper B (2006) Regulated intramembrane proteolysis of amyloid precursor protein and regulation of expression of putative target genes. *EMBO reports* **7**: 739-745

Hemmati F, Dargahi L, Nasoohi S, Omidbakhsh R, Mohamed Z, Chik Z, Naidu M, Ahmadiani A (2013) Neurorestorative effect of FTY720 in a rat model of Alzheimer's disease: comparison with memantine. *Behavioural brain research* **252**: 415-421

Hemming ML, Elias JE, Gygi SP, Selkoe DJ (2008) Proteomic profiling of gamma-secretase substrates and mapping of substrate requirements. *PLoS biology* **6**: e257

Hendershot LM, Valentine VA, Lee AS, Morris SW, Shapiro DN (1994) Localization of the gene encoding human BiP/GRP78, the endoplasmic reticulum cognate of the HSP70 family, to chromosome 9q34. *Genomics* **20**: 281-284

Herreman A, Hartmann D, Annaert W, Saftig P, Craessaerts K, Serneels L, Umans L, Schrijvers V, Checler F, Vanderstichele H, Baekelandt V, Dressel R, Cupers P, Huylebroeck D, Zwijsen A, Van Leuven F, De Strooper B (1999) Presenilin 2 deficiency causes a mild pulmonary phenotype and no changes in amyloid precursor protein processing but enhances the embryonic lethal phenotype of presenilin 1 deficiency. *Proceedings of the National Academy of Sciences of the United States of America* **96**: 11872-11877

Hers I, Tavaré JM, Denton RM (1999) The protein kinase C inhibitors bisindolylmaleimide I (GF 109203x) and IX (Ro 31-8220) are potent inhibitors of glycogen synthase kinase-3 activity. *FEBS letters* **460**: 433-436

Hinkovska-Galcheva V, VanWay SM, Shanley TP, Kunkel RG (2008) The role of sphingosine-1-phosphate and ceramide-1-phosphate in calcium homeostasis. *Curr Opin Investig Drugs* **9**: 1192-1205

Hla T, Dannenberg AJ (2012) Sphingolipid signaling in metabolic disorders. *Cell metabolism* **16**: 420-434

- Hofmann LP, Ren S, Schwalm S, Pfeilschifter J, Huwiler A (2008) Sphingosine kinase 1 and 2 regulate the capacity of mesangial cells to resist apoptotic stimuli in an opposing manner. *Biological chemistry* **389**: 1399-1407
- Hollak CE, Evers L, Aerts JM, van Oers MH (1997) Elevated levels of M-CSF, sCD14 and IL8 in type 1 Gaucher disease. *Blood cells, molecules & diseases* **23**: 201-212
- Holmes O, Paturi S, Ye W, Wolfe MS, Selkoe DJ (2012) Effects of membrane lipids on the activity and processivity of purified gamma-secretase. *Biochemistry* **51**: 3565-3575
- Hong L, He X, Huang X, Chang W, Tang J (2004) Structural features of human memapsin 2 (beta-secretase) and their biological and pathological implications. *Acta biochimica et biophysica Sinica* **36**: 787-792
- Hu Y, Fortini ME (2003) Different cofactor activities in gamma-secretase assembly: evidence for a nicastrin-Aph-1 subcomplex. *The Journal of cell biology* **161**: 685-690
- Hung AY, Haass C, Nitsch RM, Qiu WQ, Citron M, Wurtman RJ, Growdon JH, Selkoe DJ (1993) Activation of protein kinase C inhibits cellular production of the amyloid beta-protein. *J Biol Chem* **268**: 22959-22962
- Hung AY, Selkoe DJ (1994) Selective ectodomain phosphorylation and regulated cleavage of beta-amyloid precursor protein. *The EMBO journal* **13**: 534-542
- Hussain I, Powell D, Howlett DR, Tew DG, Meek TD, Chapman C, Gloger IS, Murphy KE, Southan CD, Ryan DM, Smith TS, Simmons DL, Walsh FS, Dingwall C, Christie G (1999) Identification of a novel aspartic protease (Asp 2) as beta-secretase. *Mol Cell Neurosci* **14**: 419-427
- Igarashi N, Okada T, Hayashi S, Fujita T, Jahangeer S, Nakamura S (2003) Sphingosine kinase 2 is a nuclear protein and inhibits DNA synthesis. *J Biol Chem* **278**: 46832-46839
- Ikeda M, Kihara A, Igarashi Y (2004) Sphingosine-1-phosphate lyase SPL is an endoplasmic reticulum-resident, integral membrane protein with the pyridoxal 5'-phosphate binding domain exposed to the cytosol. *Biochemical and biophysical research communications* **325**: 338-343
- Ikeda M, Kihara A, Kariya Y, Lee YM, Igarashi Y (2005) Sphingolipid-to-glycerophospholipid conversion in SPL-null cells implies the existence of an alternative isozyme. *Biochemical and biophysical research communications* **329**: 474-479
- Jenne CN, Enders A, Rivera R, Watson SR, Bankovich AJ, Pereira JP, Xu Y, Roots CM, Beilke JN, Banerjee A, Reiner SL, Miller SA, Weinmann AS, Goodnow CC, Lanier LL, Cyster JG, Chun J (2009) T-bet-dependent S1P5 expression in NK cells promotes egress from lymph nodes and bone marrow. *The Journal of experimental medicine* **206**: 2469-2481
- Jesko H, Okada T, Strosznajder RP, Nakamura S (2014) Sphingosine kinases modulate the secretion of amyloid beta precursor protein from SH-SY5Y neuroblastoma cells: the role of alpha-synuclein. *Folia neuropathologica / Association of Polish Neuropathologists and Medical Research Centre, Polish Academy of Sciences* **52**: 70-78
- Jin LW, Shie FS, Maezawa I, Vincent I, Bird T (2004) Intracellular accumulation of amyloidogenic fragments of amyloid-beta precursor protein in neurons with Niemann-Pick type C defects is associated with endosomal abnormalities. *The American journal of pathology* **164**: 975-985
- Joachim CL, Morris JH, Selkoe DJ (1989) Diffuse senile plaques occur commonly in the cerebellum in Alzheimer's disease. *The American journal of pathology* **135**: 309-319

Jonsson T, Stefansson H, Steinberg S, Jonsdottir I, Jonsson PV, Snaedal J, Bjornsson S, Huttenlocher J, Levey AI, Lah JJ, Rujescu D, Hampel H, Giegling I, Andreassen OA, Engedal K, Ulstein I, Djurovic S, Ibrahim-Verbaas C, Hofman A, Ikram MA, van Duijn CM, Thorsteinsdottir U, Kong A, Stefansson K (2013) Variant of TREM2 associated with the risk of Alzheimer's disease. *The New England journal of medicine* **368**: 107-116

Kaether C, Haass C, Steiner H (2006) Assembly, trafficking and function of gamma-secretase. *Neurodegener Dis* **3**: 275-283

Kalvodova L, Kahya N, Schwille P, Eehalt R, Verkade P, Drechsel D, Simons K (2005) Lipids as modulators of proteolytic activity of BACE: involvement of cholesterol, glycosphingolipids, and anionic phospholipids in vitro. *J Biol Chem* **280**: 36815-36823

Karaca I, Tamboli IY, Glebov K, Richter J, Fell LH, Grimm MO, Haupenthal VJ, Hartmann T, Graler MH, van Echten-Deckert G, Walter J (2014) Deficiency of sphingosine-1-phosphate lyase impairs lysosomal metabolism of the amyloid precursor protein. *J Biol Chem*

Katsel P, Li C, Haroutunian V (2007) Gene expression alterations in the sphingolipid metabolism pathways during progression of dementia and Alzheimer's disease: a shift toward ceramide accumulation at the earliest recognizable stages of Alzheimer's disease? *Neurochemical research* **32**: 845-856

Kawahara A, Nishi T, Hisano Y, Fukui H, Yamaguchi A, Mochizuki N (2009) The sphingolipid transporter spns2 functions in migration of zebrafish myocardial precursors. *Science* **323**: 524-527

Keilani S, Lun Y, Stevens AC, Williams HN, Sjoberg ER, Khanna R, Valenzano KJ, Checler F, Buxbaum JD, Yanagisawa K, Lockhart DJ, Wustman BA, Gandy S (2012) Lysosomal dysfunction in a mouse model of Sandhoff disease leads to accumulation of ganglioside-bound amyloid-beta peptide. *The Journal of neuroscience : the official journal of the Society for Neuroscience* **32**: 5223-5236

Kim DY, Carey BW, Wang H, Ingano LA, Binshtok AM, Wertz MH, Pettingell WH, He P, Lee VM, Woolf CJ, Kovacs DM (2007) BACE1 regulates voltage-gated sodium channels and neuronal activity. *Nature cell biology* **9**: 755-764

Kimberly WT, Esler WP, Ye W, Ostaszewski BL, Gao J, Diehl T, Selkoe DJ, Wolfe MS (2003) Notch and the amyloid precursor protein are cleaved by similar gamma-secretase(s). *Biochemistry* **42**: 137-144

Kimberly WT, Zheng JB, Guenette SY, Selkoe DJ (2001) The intracellular domain of the beta-amyloid precursor protein is stabilized by Fe65 and translocates to the nucleus in a notch-like manner. *J Biol Chem* **276**: 40288-40292

Kins S, Lauther N, Szodorai A, Beyreuther K (2006) Subcellular trafficking of the amyloid precursor protein gene family and its pathogenic role in Alzheimer's disease. *Neurodegener Dis* **3**: 218-226

Kitazume S, Tachida Y, Oka R, Kotani N, Ogawa K, Suzuki M, Dohmae N, Takio K, Saido TC, Hashimoto Y (2003) Characterization of alpha 2,6-sialyltransferase cleavage by Alzheimer's beta -secretase (BACE1). *J Biol Chem* **278**: 14865-14871

Knops J, Suomensaari S, Lee M, McConlogue L, Seubert P, Sinha S (1995) Cell-type and amyloid precursor protein-type specific inhibition of A beta release by bafilomycin A1, a selective inhibitor of vacuolar ATPases. *J Biol Chem* **270**: 2419-2422

- Koh YH, von Arnim CA, Hyman BT, Tanzi RE, Tesco G (2005) BACE is degraded via the lysosomal pathway. *J Biol Chem* **280**: 32499-32504
- Kohama T, Olivera A, Edsall L, Nagiec MM, Dickson R, Spiegel S (1998) Molecular cloning and functional characterization of murine sphingosine kinase. *J Biol Chem* **273**: 23722-23728
- Koike M, Nakanishi H, Saftig P, Ezaki J, Isahara K, Ohsawa Y, Schulz-Schaeffer W, Watanabe T, Waguri S, Kametaka S, Shibata M, Yamamoto K, Kominami E, Peters C, von Figura K, Uchiyama Y (2000) Cathepsin D deficiency induces lysosomal storage with ceroid lipofuscin in mouse CNS neurons. *The Journal of neuroscience : the official journal of the Society for Neuroscience* **20**: 6898-6906
- Kolter T, Sandhoff K (2010) Lysosomal degradation of membrane lipids. *FEBS letters* **584**: 1700-1712
- Korkotian E, Schwarz A, Pelled D, Schwarzmann G, Segal M, Futerman AH (1999) Elevation of intracellular glucosylceramide levels results in an increase in endoplasmic reticulum density and in functional calcium stores in cultured neurons. *J Biol Chem* **274**: 21673-21678
- Kracun I, Kalanj S, Talan-Hranilovic J, Cosovic C (1992a) Cortical distribution of gangliosides in Alzheimer's disease. *Neurochemistry international* **20**: 433-438
- Kracun I, Rosner H, Drnovsek V, Vukelic Z, Cosovic C, Trbojevic-Cepe M, Kubat M (1992b) Gangliosides in the human brain development and aging. *Neurochemistry international* **20**: 421-431
- Kuhn PH, Marjaux E, Imhof A, De Strooper B, Haass C, Lichtenthaler SF (2007) Regulated intramembrane proteolysis of the interleukin-1 receptor II by alpha-, beta-, and gamma-secretase. *J Biol Chem* **282**: 11982-11995
- Kuhn PH, Wang H, Dislich B, Colombo A, Zeitschel U, Ellwart JW, Kremmer E, Rossner S, Lichtenthaler SF (2010) ADAM10 is the physiologically relevant, constitutive alpha-secretase of the amyloid precursor protein in primary neurons. *The EMBO journal* **29**: 3020-3032
- LaFerla FM, Oddo S (2005) Alzheimer's disease: Abeta, tau and synaptic dysfunction. *Trends in molecular medicine* **11**: 170-176
- Lai A, Sisodia SS, Trowbridge IS (1995) Characterization of sorting signals in the beta-amyloid precursor protein cytoplasmic domain. *J Biol Chem* **270**: 3565-3573
- LaVoie MJ, Fraering PC, Ostaszewski BL, Ye W, Kimberly WT, Wolfe MS, Selkoe DJ (2003) Assembly of the gamma-secretase complex involves early formation of an intermediate subcomplex of Aph-1 and nicastrin. *J Biol Chem* **278**: 37213-37222
- Lee HJ, Jung KM, Huang YZ, Bennett LB, Lee JS, Mei L, Kim TW (2002) Presenilin-dependent gamma-secretase-like intramembrane cleavage of ErbB4. *J Biol Chem* **277**: 6318-6323
- Levine B, Klionsky DJ (2004) Development by self-digestion: molecular mechanisms and biological functions of autophagy. *Developmental cell* **6**: 463-477
- Li H, Kim WS, Guillemin GJ, Hill AF, Evin G, Garner B (2010) Modulation of amyloid precursor protein processing by synthetic ceramide analogues. *Biochimica et biophysica acta* **1801**: 887-895
- Li Q, Sudhof TC (2004) Cleavage of amyloid-beta precursor protein and amyloid-beta precursor-like protein by BACE 1. *J Biol Chem* **279**: 10542-10550

- Liao L, Cheng D, Wang J, Duong DM, Losik TG, Gearing M, Rees HD, Lah JJ, Levey AI, Peng J (2004) Proteomic characterization of postmortem amyloid plaques isolated by laser capture microdissection. *J Biol Chem* **279**: 37061-37068
- Lichtenthaler SF, Dominguez DI, Westmeyer GG, Reiss K, Haass C, Saftig P, De Strooper B, Seed B (2003) The cell adhesion protein P-selectin glycoprotein ligand-1 is a substrate for the aspartyl protease BACE1. *J Biol Chem* **278**: 48713-48719
- Lippincott-Schwartz J, Yuan L, Tipper C, Amherdt M, Orci L, Klausner RD (1991) Brefeldin A's effects on endosomes, lysosomes, and the TGN suggest a general mechanism for regulating organelle structure and membrane traffic. *Cell* **67**: 601-616
- Liu H, Sugiura M, Nava VE, Edsall LC, Kono K, Poulton S, Milstien S, Kohama T, Spiegel S (2000) Molecular cloning and functional characterization of a novel mammalian sphingosine kinase type 2 isoform. *J Biol Chem* **275**: 19513-19520
- Liu J, Beckman BS, Foroozesh M (2013) A review of ceramide analogs as potential anticancer agents. *Future medicinal chemistry* **5**: 1405-1421
- Liu K, Doms RW, Lee VM (2002) Glu11 site cleavage and N-terminally truncated A beta production upon BACE overexpression. *Biochemistry* **41**: 3128-3136
- Liu Q, Zerbinatti CV, Zhang J, Hoe HS, Wang B, Cole SL, Herz J, Muglia L, Bu G (2007) Amyloid precursor protein regulates brain apolipoprotein E and cholesterol metabolism through lipoprotein receptor LRP1. *Neuron* **56**: 66-78
- Liu Y, Hoffmann A, Grinberg A, Westphal H, McDonald MP, Miller KM, Crawley JN, Sandhoff K, Suzuki K, Proia RL (1997) Mouse model of GM2 activator deficiency manifests cerebellar pathology and motor impairment. *Proceedings of the National Academy of Sciences of the United States of America* **94**: 8138-8143
- Lleo A, Waldron E, von Arnim CA, Herl L, Tangredi MM, Peltan ID, Strickland DK, Koo EH, Hyman BT, Pietrzik CU, Berezovska O (2005) Low density lipoprotein receptor-related protein (LRP) interacts with presenilin 1 and is a competitive substrate of the amyloid precursor protein (APP) for gamma-secretase. *J Biol Chem* **280**: 27303-27309
- Lloyd-Evans E, Morgan AJ, He X, Smith DA, Elliot-Smith E, Sillence DJ, Churchill GC, Schuchman EH, Galione A, Platt FM (2008) Niemann-Pick disease type C1 is a sphingosine storage disease that causes deregulation of lysosomal calcium. *Nature medicine* **14**: 1247-1255
- Luo Y, Bolon B, Damore MA, Fitzpatrick D, Liu H, Zhang J, Yan Q, Vassar R, Citron M (2003) BACE1 (beta-secretase) knockout mice do not acquire compensatory gene expression changes or develop neural lesions over time. *Neurobiology of disease* **14**: 81-88
- Luzio JP, Bright NA, Pryor PR (2007) The role of calcium and other ions in sorting and delivery in the late endocytic pathway. *Biochemical Society transactions* **35**: 1088-1091
- Luzio JP, Poupon V, Lindsay MR, Mullock BM, Piper RC, Pryor PR (2003) Membrane dynamics and the biogenesis of lysosomes. *Molecular membrane biology* **20**: 141-154
- Maceyka M, Sankala H, Hait NC, Le Stunff H, Liu H, Toman R, Collier C, Zhang M, Satin LS, Merrill AH, Jr., Milstien S, Spiegel S (2005) SphK1 and SphK2, sphingosine kinase isoenzymes with opposing functions in sphingolipid metabolism. *J Biol Chem* **280**: 37118-37129



- Malnar M, Kosicek M, Lisica A, Posavec M, Krolo A, Njavro J, Omerbasic D, Tahirovic S, Hecimovic S (2012) Cholesterol-depletion corrects APP and BACE1 mistrafficking in NPC1-deficient cells. *Biochimica et biophysica acta* **1822**: 1270-1283
- Mameza MG, Lockard JM, Zamora E, Hillefors M, Lavina ZS, Kaplan BB (2007) Characterization of the adaptor protein ARH expression in the brain and ARH molecular interactions. *Journal of neurochemistry* **103**: 927-941
- Marquez-Sterling NR, Lo AC, Sisodia SS, Koo EH (1997) Trafficking of cell-surface beta-amyloid precursor protein: evidence that a sorting intermediate participates in synaptic vesicle recycling. *The Journal of neuroscience : the official journal of the Society for Neuroscience* **17**: 140-151
- Masters CL, Beyreuther K (1991) Alzheimer's disease: molecular basis of structural lesions. *Brain Pathol* **1**: 226-227
- Mattson MP (1997) Cellular actions of beta-amyloid precursor protein and its soluble and fibrillogenic derivatives. *Physiological reviews* **77**: 1081-1132
- McLoughlin DM, Miller CC (2008) The FE65 proteins and Alzheimer's disease. *Journal of neuroscience research* **86**: 744-754
- Mellor H, Parker PJ (1998) The extended protein kinase C superfamily. *The Biochemical journal* **332** ( Pt 2): 281-292
- Merrill AH, Jr. (2011) Sphingolipid and glycosphingolipid metabolic pathways in the era of sphingolipidomics. *Chemical reviews* **111**: 6387-6422
- Mizugishi K, Yamashita T, Olivera A, Miller GF, Spiegel S, Proia RL (2005) Essential role for sphingosine kinases in neural and vascular development. *Molecular and cellular biology* **25**: 11113-11121
- Mizushima N, Yamamoto A, Matsui M, Yoshimori T, Ohsumi Y (2004) In vivo analysis of autophagy in response to nutrient starvation using transgenic mice expressing a fluorescent autophagosome marker. *Molecular biology of the cell* **15**: 1101-1111
- Montell C (2005) The TRP superfamily of cation channels. *Science's STKE : signal transduction knowledge environment* **2005**: re3
- Neely Kayala KM, Dickinson GD, Minassian A, Walls KC, Green KN, Laferla FM (2012) Presenilin-null cells have altered two-pore calcium channel expression and lysosomal calcium: implications for lysosomal function. *Brain research* **1489**: 8-16
- Nishizuka Y (1995) Protein kinase C and lipid signaling for sustained cellular responses. *FASEB journal : official publication of the Federation of American Societies for Experimental Biology* **9**: 484-496
- Okada T, Ding G, Sonoda H, Kajimoto T, Haga Y, Khosrowbeygi A, Gao S, Miwa N, Jahangeer S, Nakamura S (2005) Involvement of N-terminal-extended form of sphingosine kinase 2 in serum-dependent regulation of cell proliferation and apoptosis. *J Biol Chem* **280**: 36318-36325
- Olivera A, Spiegel S (1993) Sphingosine-1-phosphate as second messenger in cell proliferation induced by PDGF and FCS mitogens. *Nature* **365**: 557-560

- Ono Y, Fujii T, Igarashi K, Kuno T, Tanaka C, Kikkawa U, Nishizuka Y (1989) Phorbol ester binding to protein kinase C requires a cysteine-rich zinc-finger-like sequence. *Proceedings of the National Academy of Sciences of the United States of America* **86**: 4868-4871
- Osada M, Yatomi Y, Ohmori T, Ikeda H, Ozaki Y (2002) Enhancement of sphingosine 1-phosphate-induced migration of vascular endothelial cells and smooth muscle cells by an EDG-5 antagonist. *Biochemical and biophysical research communications* **299**: 483-487
- Osenkowski P, Ye W, Wang R, Wolfe MS, Selkoe DJ (2008) Direct and potent regulation of gamma-secretase by its lipid microenvironment. *J Biol Chem* **283**: 22529-22540
- Pagano RE, Puri V, Dominguez M, Marks DL (2000) Membrane traffic in sphingolipid storage diseases. *Traffic* **1**: 807-815
- Pandol SJ, Schoeffield-Payne MS, Gukovskaya AS, Rutherford RE (1994) Sphingosine regulates Ca(2+)-ATPase and reloading of intracellular Ca2+ stores in the pancreatic acinar cell. *Biochimica et biophysica acta* **1195**: 45-50
- Pasternak SH, Bagshaw RD, Guiral M, Zhang S, Ackerley CA, Pak BJ, Callahan JW, Mahuran DJ (2003) Presenilin-1, nicastrin, amyloid precursor protein, and gamma-secretase activity are co-localized in the lysosomal membrane. *J Biol Chem* **278**: 26687-26694
- Pastorino L, Ikin AF, Nairn AC, Pursnani A, Buxbaum JD (2002) The carboxyl-terminus of BACE contains a sorting signal that regulates BACE trafficking but not the formation of total A(beta). *Molecular and cellular neurosciences* **19**: 175-185
- Peest U, Sensken SC, Andreani P, Hanel P, Van Veldhoven PP, Graler MH (2008) S1P-lyase independent clearance of extracellular sphingosine 1-phosphate after dephosphorylation and cellular uptake. *Journal of cellular biochemistry* **104**: 756-772
- Perez RG, Soriano S, Hayes JD, Ostaszewski B, Xia W, Selkoe DJ, Chen X, Stokin GB, Koo EH (1999) Mutagenesis identifies new signals for beta-amyloid precursor protein endocytosis, turnover, and the generation of secreted fragments, including Abeta42. *J Biol Chem* **274**: 18851-18856
- Perez RG, Squazzo SL, Koo EH (1996) Enhanced release of amyloid beta-protein from codon 670/671 "Swedish" mutant beta-amyloid precursor protein occurs in both secretory and endocytic pathways. *J Biol Chem* **271**: 9100-9107
- Peschon JJ, Slack JL, Reddy P, Stocking KL, Sunnarborg SW, Lee DC, Russell WE, Castner BJ, Johnson RS, Fitzner JN, Boyce RW, Nelson N, Kozlosky CJ, Wolfson MF, Rauch CT, Cerretti DP, Paxton RJ, March CJ, Black RA (1998) An essential role for ectodomain shedding in mammalian development. *Science* **282**: 1281-1284
- Piccinini M, Scandroglio F, Prioni S, Buccinna B, Loberto N, Aureli M, Chigorno V, Lupino E, DeMarco G, Lomartire A, Rinaudo MT, Sonnino S, Prinetti A (2010) Deregulated sphingolipid metabolism and membrane organization in neurodegenerative disorders. *Molecular neurobiology* **41**: 314-340
- Pitman MR, Pitson SM (2010) Inhibitors of the sphingosine kinase pathway as potential therapeutics. *Current cancer drug targets* **10**: 354-367
- Pitson SM (2011) Regulation of sphingosine kinase and sphingolipid signaling. *Trends in biochemical sciences* **36**: 97-107

- Pitson SM, Moretti PA, Zebol JR, Lynn HE, Xia P, Vadas MA, Wattenberg BW (2003) Activation of sphingosine kinase 1 by ERK1/2-mediated phosphorylation. *The EMBO journal* **22**: 5491-5500
- Prokop S, Shirotani K, Edbauer D, Haass C, Steiner H (2004) Requirement of PEN-2 for stabilization of the presenilin N-/C-terminal fragment heterodimer within the gamma-secretase complex. *J Biol Chem* **279**: 23255-23261
- Pryor PR, Mullock BM, Bright NA, Gray SR, Luzio JP (2000) The role of intraorganellar Ca(2+) in late endosome-lysosome heterotypic fusion and in the reformation of lysosomes from hybrid organelles. *The Journal of cell biology* **149**: 1053-1062
- Puglielli L, Ellis BC, Saunders AJ, Kovacs DM (2003) Ceramide stabilizes beta-site amyloid precursor protein-cleaving enzyme 1 and promotes amyloid beta-peptide biogenesis. *J Biol Chem* **278**: 19777-19783
- Pyne NJ, Pyne S (2010) Sphingosine 1-phosphate and cancer. *Nature reviews Cancer* **10**: 489-503
- Pyne S, Pyne NJ (2000) Sphingosine 1-phosphate signalling in mammalian cells. *The Biochemical journal* **349**: 385-402
- Reiss U, Oskouian B, Zhou J, Gupta V, Sooriyakumaran P, Kelly S, Wang E, Merrill AH, Jr., Saba JD (2004) Sphingosine-phosphate lyase enhances stress-induced ceramide generation and apoptosis. *J Biol Chem* **279**: 1281-1290
- Riddell DR, Christie G, Hussain I, Dingwall C (2001) Compartmentalization of beta-secretase (Asp2) into low-buoyant density, noncaveolar lipid rafts. *Current biology* : CB **11**: 1288-1293
- Rink J, Ghigo E, Kalaidzidis Y, Zerial M (2005) Rab conversion as a mechanism of progression from early to late endosomes. *Cell* **122**: 735-749
- Roberds SL, Anderson J, Basi G, Bienkowski MJ, Branstetter DG, Chen KS, Freedman SB, Frigon NL, Games D, Hu K, Johnson-Wood K, Kappenman KE, Kawabe TT, Kola I, Kuehn R, Lee M, Liu W, Motter R, Nichols NF, Power M, Robertson DW, Schenk D, Schoor M, Shopp GM, Shuck ME, Sinha S, Svensson KA, Tatsuno G, Tintrup H, Wijsman J, Wright S, McConlogue L (2001) BACE knockout mice are healthy despite lacking the primary beta-secretase activity in brain: implications for Alzheimer's disease therapeutics. *Human molecular genetics* **10**: 1317-1324
- Rodriguez-Lafrasse C, Rousson R, Valla S, Antignac P, Louisot P, Vanier MT (1997) Modulation of protein kinase C by endogenous sphingosine: inhibition of phorbol dibutyrate binding in Niemann-Pick C fibroblasts. *The Biochemical journal* **325 ( Pt 3)**: 787-791
- Rogelj B, Mitchell JC, Miller CC, McLoughlin DM (2006) The X11/Mint family of adaptor proteins. *Brain research reviews* **52**: 305-315
- Rossjohn J, Cappai R, Feil SC, Henry A, McKinsty WJ, Galatis D, Hesse L, Multhaup G, Beyreuther K, Masters CL, Parker MW (1999) Crystal structure of the N-terminal, growth factor-like domain of Alzheimer amyloid precursor protein. *Nature structural biology* **6**: 327-331
- Sakuraba H, Itoh K, Shimmoto M, Utsumi K, Kase R, Hashimoto Y, Ozawa T, Ohwada Y, Imataka G, Eguchi M, Furukawa T, Schepers U, Sandhoff K (1999) GM2 gangliosidosis AB variant: clinical and biochemical studies of a Japanese patient. *Neurology* **52**: 372-377
- Samarel AM, Ferguson AG, Decker RS, Lesch M (1989) Effects of cysteine protease inhibitors on rabbit cathepsin D maturation. *The American journal of physiology* **257**: C1069-1079

- Sandhoff K, Kolter T (1998) Processing of sphingolipid activator proteins and the topology of lysosomal digestion. *Acta biochimica Polonica* **45**: 373-384
- Sanna MG, Wang SK, Gonzalez-Cabrera PJ, Don A, Marsolais D, Matheu MP, Wei SH, Parker I, Jo E, Cheng WC, Cahalan MD, Wong CH, Rosen H (2006) Enhancement of capillary leakage and restoration of lymphocyte egress by a chiral S1P1 antagonist in vivo. *Nature chemical biology* **2**: 434-441
- Sastre M, Steiner H, Fuchs K, Capell A, Multhaup G, Condron MM, Teplow DB, Haass C (2001) Presenilin-dependent gamma-secretase processing of beta-amyloid precursor protein at a site corresponding to the S3 cleavage of Notch. *EMBO reports* **2**: 835-841
- Sawamura N, Ko M, Yu W, Zou K, Hanada K, Suzuki T, Gong JS, Yanagisawa K, Michikawa M (2004) Modulation of amyloid precursor protein cleavage by cellular sphingolipids. *J Biol Chem* **279**: 11984-11991
- Schengrund CL (2010) Lipid rafts: keys to neurodegeneration. *Brain research bulletin* **82**: 7-17
- Schwab SR, Cyster JG (2007) Finding a way out: lymphocyte egress from lymphoid organs. *Nature immunology* **8**: 1295-1301
- Schwab SR, Pereira JP, Matloubian M, Xu Y, Huang Y, Cyster JG (2005) Lymphocyte sequestration through S1P lyase inhibition and disruption of S1P gradients. *Science* **309**: 1735-1739
- Seals DF, Courtneidge SA (2003) The ADAMs family of metalloproteases: multidomain proteins with multiple functions. *Genes & development* **17**: 7-30
- Selkoe DJ (2001a) Alzheimer's disease results from the cerebral accumulation and cytotoxicity of amyloid beta-protein. *Journal of Alzheimer's disease : JAD* **3**: 75-80
- Selkoe DJ (2001b) Alzheimer's disease: genes, proteins, and therapy. *Physiol Rev* **81**: 741-766
- Senechal Y, Kelly PH, Dev KK (2008) Amyloid precursor protein knockout mice show age-dependent deficits in passive avoidance learning. *Behavioural brain research* **186**: 126-132
- Seol GH, Kim MY, Liang GH, Kim JA, Kim YJ, Oh S, Suh SH (2005) Sphingosine-1-phosphate-induced intracellular Ca<sup>2+</sup> mobilization in human endothelial cells. *Endothelium : journal of endothelial cell research* **12**: 263-269
- Serra M, Saba JD (2010) Sphingosine 1-phosphate lyase, a key regulator of sphingosine 1-phosphate signaling and function. *Advances in enzyme regulation* **50**: 349-362
- Shah S, Lee SF, Tabuchi K, Hao YH, Yu C, LaPlant Q, Ball H, Dann CE, 3rd, Sudhof T, Yu G (2005) Nicastrin functions as a gamma-secretase-substrate receptor. *Cell* **122**: 435-447
- Shen D, Wang X, Li X, Zhang X, Yao Z, Dibble S, Dong XP, Yu T, Lieberman AP, Showalter HD, Xu H (2012) Lipid storage disorders block lysosomal trafficking by inhibiting a TRP channel and lysosomal calcium release. *Nature communications* **3**: 731
- Shen J, Bronson RT, Chen DF, Xia W, Selkoe DJ, Tonegawa S (1997) Skeletal and CNS defects in Presenilin-1-deficient mice. *Cell* **89**: 629-639
- Singh R, Cuervo AM (2011) Autophagy in the cellular energetic balance. *Cell metabolism* **13**: 495-504

- Singh R, Kaushik S, Wang Y, Xiang Y, Novak I, Komatsu M, Tanaka K, Cuervo AM, Czaja MJ (2009) Autophagy regulates lipid metabolism. *Nature* **458**: 1131-1135
- Sinha S, Anderson JP, Barbour R, Basi GS, Caccavello R, Davis D, Doan M, Dovey HF, Frigon N, Hong J, Jacobson-Croak K, Jewett N, Keim P, Knops J, Lieberburg I, Power M, Tan H, Tatsuno G, Tung J, Schenk D, Seubert P, Suomensari SM, Wang S, Walker D, Zhao J, McConlogue L, John V (1999) Purification and cloning of amyloid precursor protein beta-secretase from human brain. *Nature* **402**: 537-540
- Sisodia SS (1992a) Beta-amyloid precursor protein cleavage by a membrane-bound protease. *Proceedings of the National Academy of Sciences of the United States of America* **89**: 6075-6079
- Sisodia SS (1992b) Secretion of the beta-amyloid precursor protein. *Annals of the New York Academy of Sciences* **674**: 53-57
- Sisodia SS, Koo EH, Beyreuther K, Unterbeck A, Price DL (1990) Evidence that beta-amyloid protein in Alzheimer's disease is not derived by normal processing. *Science* **248**: 492-495
- Skovronsky DM, Moore DB, Milla ME, Doms RW, Lee VM (2000) Protein kinase C-dependent alpha-secretase competes with beta-secretase for cleavage of amyloid-beta precursor protein in the trans-golgi network. *J Biol Chem* **275**: 2568-2575
- Small DH, Nurcombe V, Moir R, Michaelson S, Monard D, Beyreuther K, Masters CL (1992) Association and release of the amyloid protein precursor of Alzheimer's disease from chick brain extracellular matrix. *The Journal of neuroscience : the official journal of the Society for Neuroscience* **12**: 4143-4150
- Smith PK, Krohn RI, Hermanson GT, Mallia AK, Gartner FH, Provenzano MD, Fujimoto EK, Goeke NM, Olson BJ, Klenk DC (1985) Measurement of protein using bicinchoninic acid. *Analytical biochemistry* **150**: 76-85
- Sonnino S, Chigorno V (2000) Ganglioside molecular species containing C18- and C20-sphingosine in mammalian nervous tissues and neuronal cell cultures. *Biochimica et biophysica acta* **1469**: 63-77
- Spandl J, White DJ, Peychl J, Thiele C (2009) Live cell multicolor imaging of lipid droplets with a new dye, LD540. *Traffic* **10**: 1579-1584
- Spiegel S, Milstien S (2003) Sphingosine-1-phosphate: an enigmatic signalling lipid. *Nature reviews Molecular cell biology* **4**: 397-407
- Spiegel S, Milstien S (2011) The outs and the ins of sphingosine-1-phosphate in immunity. *Nature reviews Immunology* **11**: 403-415
- Stahelin RV, Hwang JH, Kim JH, Park ZY, Johnson KR, Obeid LM, Cho W (2005) The mechanism of membrane targeting of human sphingosine kinase 1. *J Biol Chem* **280**: 43030-43038
- Stanford PM, Halliday GM, Brooks WS, Kwok JB, Storey CE, Creasey H, Morris JG, Fulham MJ, Schofield PR (2000) Progressive supranuclear palsy pathology caused by a novel silent mutation in exon 10 of the tau gene: expansion of the disease phenotype caused by tau gene mutations. *Brain : a journal of neurology* **123** ( Pt 5): 880-893
- Strittmatter WJ, Saunders AM, Schmechel D, Pericak-Vance M, Enghild J, Salvesen GS, Roses AD (1993) Apolipoprotein E: high-avidity binding to beta-amyloid and increased frequency of type 4 allele in late-onset familial Alzheimer disease. *Proceedings of the National Academy of Sciences of the United States of America* **90**: 1977-1981

- Suzuki N, Cheung TT, Cai XD, Odaka A, Otvos L, Jr., Eckman C, Golde TE, Younkin SG (1994) An increased percentage of long amyloid beta protein secreted by familial amyloid beta protein precursor (beta APP717) mutants. *Science* **264**: 1336-1340
- Svennerholm L, Bostrom K, Fredman P, Mansson JE, Rosengren B, Rynmark BM (1989) Human brain gangliosides: developmental changes from early fetal stage to advanced age. *Biochimica et biophysica acta* **1005**: 109-117
- Svennerholm L, Bostrom K, Jungbjer B, Olsson L (1994) Membrane lipids of adult human brain: lipid composition of frontal and temporal lobe in subjects of age 20 to 100 years. *Journal of neurochemistry* **63**: 1802-1811
- Swan M, Saunders-Pullman R (2013) The association between ss-glucocerebrosidase mutations and parkinsonism. *Current neurology and neuroscience reports* **13**: 368
- Tagliavini F, Giaccone G, Frangione B, Bugiani O (1988) Preamyloid deposits in the cerebral cortex of patients with Alzheimer's disease and nondemented individuals. *Neuroscience letters* **93**: 191-196
- Takabe K, Kim RH, Allegood JC, Mitra P, Ramachandran S, Nagahashi M, Harikumar KB, Hait NC, Milstien S, Spiegel S (2010) Estradiol induces export of sphingosine 1-phosphate from breast cancer cells via ABCC1 and ABCG2. *J Biol Chem* **285**: 10477-10486
- Takasugi N, Sasaki T, Ebinuma I, Osawa S, Isshiki H, Takeo K, Tomita T, Iwatsubo T (2013) FTY720/fingolimod, a sphingosine analogue, reduces amyloid-beta production in neurons. *PloS one* **8**: e64050
- Takasugi N, Sasaki T, Suzuki K, Osawa S, Isshiki H, Hori Y, Shimada N, Higo T, Yokoshima S, Fukuyama T, Lee VM, Trojanowski JQ, Tomita T, Iwatsubo T (2011) BACE1 activity is modulated by cell-associated sphingosine-1-phosphate. *The Journal of neuroscience : the official journal of the Society for Neuroscience* **31**: 6850-6857
- Tamari F, Chen FW, Li C, Chaudhari J, Ioannou YA (2013) PKC activation in Niemann pick C1 cells restores subcellular cholesterol transport. *PloS one* **8**: e74169
- Tamboli DA, Harris MA, Hogg JP, Realini T, Sivak-Callcott JA (2011a) Computed tomography dimensions of the lacrimal gland in normal Caucasian orbits. *Ophthalmic plastic and reconstructive surgery* **27**: 453-456
- Tamboli IY, Hampel H, Tien NT, Tolksdorf K, Breiden B, Mathews PM, Saftig P, Sandhoff K, Walter J (2011b) Sphingolipid storage affects autophagic metabolism of the amyloid precursor protein and promotes A $\beta$  generation. *The Journal of neuroscience : the official journal of the Society for Neuroscience* **31**: 1837-1849
- Tamboli IY, Prager K, Barth E, Heneka M, Sandhoff K, Walter J (2005) Inhibition of glycosphingolipid biosynthesis reduces secretion of the beta-amyloid precursor protein and amyloid beta-peptide. *J Biol Chem* **280**: 28110-28117
- Tamboli IY, Prager K, Thal DR, Thelen KM, Dewachter I, Pietrzik CU, St George-Hyslop P, Sisodia SS, De Strooper B, Heneka MT, Filippov MA, Muller U, van Leuven F, Lutjohann D, Walter J (2008) Loss of gamma-secretase function impairs endocytosis of lipoprotein particles and membrane cholesterol homeostasis. *The Journal of neuroscience : the official journal of the Society for Neuroscience* **28**: 12097-12106

- Tamboli IY, Tien NT, Walter J (2011c) Sphingolipid storage impairs autophagic clearance of Alzheimer-associated proteins. *Autophagy* **7**: 645-646
- Tanzi RE, Bertram L (2001) New frontiers in Alzheimer's disease genetics. *Neuron* **32**: 181-184
- Tanzi RE, Bertram L (2005) Twenty years of the Alzheimer's disease amyloid hypothesis: a genetic perspective. *Cell* **120**: 545-555
- te Vruchte D, Lloyd-Evans E, Veldman RJ, Neville DC, Dwek RA, Platt FM, van Blitterswijk WJ, Sillence DJ (2004) Accumulation of glycosphingolipids in Niemann-Pick C disease disrupts endosomal transport. *J Biol Chem* **279**: 26167-26175
- Tesco G, Koh YH, Kang EL, Cameron AN, Das S, Sena-Esteves M, Hiltunen M, Yang SH, Zhong Z, Shen Y, Simpkins JW, Tanzi RE (2007) Depletion of GGA3 stabilizes BACE and enhances beta-secretase activity. *Neuron* **54**: 721-737
- Thal DR, Rub U, Orantes M, Braak H (2002) Phases of A beta-deposition in the human brain and its relevance for the development of AD. *Neurology* **58**: 1791-1800
- Thinakaran G, Borchelt DR, Lee MK, Slunt HH, Spitzer L, Kim G, Ratovitsky T, Davenport F, Nordstedt C, Seeger M, Hardy J, Levey AI, Gandy SE, Jenkins NA, Copeland NG, Price DL, Sisodia SS (1996) Endoproteolysis of presenilin 1 and accumulation of processed derivatives in vivo. *Neuron* **17**: 181-190
- Toimela T, Tahti H, Salminen L (1995) Retinal pigment epithelium cell culture as a model for evaluation of the toxicity of tamoxifen and chloroquine. *Ophthalmic research* **27 Suppl 1**: 150-153
- Tomita S, Kirino Y, Suzuki T (1998) Cleavage of Alzheimer's amyloid precursor protein (APP) by secretases occurs after O-glycosylation of APP in the protein secretory pathway. Identification of intracellular compartments in which APP cleavage occurs without using toxic agents that interfere with protein metabolism. *J Biol Chem* **273**: 6277-6284
- Tomita T, Tanaka S, Morohashi Y, Iwatsubo T (2006) Presenilin-dependent intramembrane cleavage of ephrin-B1. *Molecular neurodegeneration* **1**: 2
- Tooze J, Hollinshead M (1992) Evidence that globular Golgi clusters in mitotic HeLa cells are clustered tubular endosomes. *European journal of cell biology* **58**: 228-242
- Tornquist K (2012) Sphingosine 1-phosphate, sphingosine kinase and autocrine calcium signalling in thyroid cells. *Acta Physiol (Oxf)* **204**: 151-157
- Toullec D, Pianetti P, Coste H, Bellevergue P, Grand-Perret T, Ajakane M, Baudet V, Boissin P, Boursier E, Loriolle F, et al. (1991) The bisindolylmaleimide GF 109203X is a potent and selective inhibitor of protein kinase C. *J Biol Chem* **266**: 15771-15781
- Treiman M, Caspersen C, Christensen SB (1998) A tool coming of age: thapsigargin as an inhibitor of sarco-endoplasmic reticulum Ca(2+)-ATPases. *Trends in pharmacological sciences* **19**: 131-135
- Ulrich JD, Finn MB, Wang Y, Shen A, Mahan TE, Jiang H, Stewart FR, Piccio L, Colonna M, Holtzman DM (2014) Altered microglial response to Aβ plaques in APPS1-21 mice heterozygous for TREM2. *Molecular neurodegeneration* **9**: 20
- van Echten-Deckert G, Herget T (2006) Sphingolipid metabolism in neural cells. *Biochimica et biophysica acta* **1758**: 1978-1994

- van Echten-Deckert G, Walter J (2012a) Sphingolipids: Critical players in Alzheimer's disease. *Progress in lipid research* **51**: 378-393
- van Echten-Deckert G, Walter J (2012b) Sphingolipids: critical players in Alzheimer's disease. *Progress in lipid research* **51**: 378-393
- Van Nostrand WE, Schmaier AH, Farrow JS, Cines DB, Cunningham DD (1991) Protease nexin-2/amyloid beta-protein precursor in blood is a platelet-specific protein. *Biochemical and biophysical research communications* **175**: 15-21
- Van Veldhoven PP (2000) Sphingosine-1-phosphate lyase. *Methods in enzymology* **311**: 244-254
- Van Veldhoven PP, Mannaerts GP (1991) Subcellular localization and membrane topology of sphingosine-1-phosphate lyase in rat liver. *J Biol Chem* **266**: 12502-12507
- van Veldhoven PP, Mannaerts GP (1993) Sphingosine-phosphate lyase. *Advances in lipid research* **26**: 69-98
- van Weering JR, Cullen PJ (2014) Membrane-associated cargo recycling by tubule-based endosomal sorting. *Seminars in cell & developmental biology* **31C**: 40-47
- Vassar R, Bennett BD, Babu-Khan S, Kahn S, Mendiaz EA, Denis P, Teplow DB, Ross S, Amarante P, Loeloff R, Luo Y, Fisher S, Fuller J, Edenson S, Lile J, Jarosinski MA, Biere AL, Curran E, Burgess T, Louis JC, Collins F, Treanor J, Rogers G, Citron M (1999) Beta-secretase cleavage of Alzheimer's amyloid precursor protein by the transmembrane aspartic protease BACE. *Science* **286**: 735-741
- Vassar R, Citron M (2000) Abeta-generating enzymes: recent advances in beta- and gamma-secretase research. *Neuron* **27**: 419-422
- Vogel C, Marcotte EM (2012) Insights into the regulation of protein abundance from proteomic and transcriptomic analyses. *Nature reviews Genetics* **13**: 227-232
- von Arnim CA, Kinoshita A, Peltan ID, Tangredi MM, Herl L, Lee BM, Spoelgen R, Hshieh TT, Ranganathan S, Battey FD, Liu CX, Bacskai BJ, Sever S, Irizarry MC, Strickland DK, Hyman BT (2005) The low density lipoprotein receptor-related protein (LRP) is a novel beta-secretase (BACE1) substrate. *J Biol Chem* **280**: 17777-17785
- von Arnim CA, Spoelgen R, Peltan ID, Deng M, Courchesne S, Koker M, Matsui T, Kowa H, Lichtenthaler SF, Irizarry MC, Hyman BT (2006) GGA1 acts as a spatial switch altering amyloid precursor protein trafficking and processing. *The Journal of neuroscience : the official journal of the Society for Neuroscience* **26**: 9913-9922
- von Rotz RC, Kohli BM, Bosset J, Meier M, Suzuki T, Nitsch RM, Konietzko U (2004) The APP intracellular domain forms nuclear multiprotein complexes and regulates the transcription of its own precursor. *Journal of cell science* **117**: 4435-4448
- Wahle T, Prager K, Raffler N, Haass C, Famulok M, Walter J (2005) GGA proteins regulate retrograde transport of BACE1 from endosomes to the trans-Golgi network. *Molecular and cellular neurosciences* **29**: 453-461
- Wahle T, Thal DR, Sastre M, Rentmeister A, Bogdanovic N, Famulok M, Heneka MT, Walter J (2006) GGA1 is expressed in the human brain and affects the generation of amyloid beta-peptide. *J Neurosci* **26**: 12838-12846



- Walkley SU (2003) Neurobiology and cellular pathogenesis of glycolipid storage diseases. *Philosophical transactions of the Royal Society of London Series B, Biological sciences* **358**: 893-904
- Walkley SU, Vanier MT (2009) Secondary lipid accumulation in lysosomal disease. *Biochimica et biophysica acta* **1793**: 726-736
- Walter J (2012) gamma-Secretase, apolipoprotein E and cellular cholesterol metabolism. *Current Alzheimer research* **9**: 189-199
- Walter J, Capell A, Grunberg J, Pesold B, Schindzielorz A, Prior R, Podlisny MB, Fraser P, Hyslop PS, Selkoe DJ, Haass C (1996) The Alzheimer's disease-associated presenilins are differentially phosphorylated proteins located predominantly within the endoplasmic reticulum. *Mol Med* **2**: 673-691
- Walter J, Capell A, Hung AY, Langen H, Schnolzer M, Thinakaran G, Sisodia SS, Selkoe DJ, Haass C (1997a) Ectodomain phosphorylation of beta-amyloid precursor protein at two distinct cellular locations. *J Biol Chem* **272**: 1896-1903
- Walter J, Fluhrer R, Hartung B, Willem M, Kaether C, Capell A, Lammich S, Multhaup G, Haass C (2001) Phosphorylation regulates intracellular trafficking of beta-secretase. *J Biol Chem* **276**: 14634-14641
- Walter J, Grunberg J, Capell A, Pesold B, Schindzielorz A, Citron M, Mendla K, George-Hyslop PS, Multhaup G, Selkoe DJ, Haass C (1997b) Proteolytic processing of the Alzheimer disease-associated presenilin-1 generates an in vivo substrate for protein kinase C. *Proceedings of the National Academy of Sciences of the United States of America* **94**: 5349-5354
- Walter J, Haass C (2000) Posttranslational modifications of amyloid precursor protein : ectodomain phosphorylation and sulfation. *Methods in molecular medicine* **32**: 149-168
- Walter M, Chen FW, Tamari F, Wang R, Ioannou YA (2009) Endosomal lipid accumulation in NPC1 leads to inhibition of PKC, hypophosphorylation of vimentin and Rab9 entrapment. *Biology of the cell / under the auspices of the European Cell Biology Organization* **101**: 141-152
- Wang R, Meschia JF, Cotter RJ, Sisodia SS (1991) Secretion of the beta/A4 amyloid precursor protein. Identification of a cleavage site in cultured mammalian cells. *J Biol Chem* **266**: 16960-16964
- Weidemann A, Konig G, Bunke D, Fischer P, Salbaum JM, Masters CL, Beyreuther K (1989) Identification, biogenesis, and localization of precursors of Alzheimer's disease A4 amyloid protein. *Cell* **57**: 115-126
- Willem M, Garratt AN, Novak B, Citron M, Kaufmann S, Rittger A, DeStrooper B, Saftig P, Birchmeier C, Haass C (2006) Control of peripheral nerve myelination by the beta-secretase BACE1. *Science* **314**: 664-666
- Williamson R, Sutherland C (2011) Neuronal membranes are key to the pathogenesis of Alzheimer's disease: the role of both raft and non-raft membrane domains. *Current Alzheimer research* **8**: 213-221
- Wiltfang J, Esselmann H, Bibl M, Smirnov A, Otto M, Paul S, Schmidt B, Klafki HW, Maler M, Dyrks T, Bienert M, Beyermann M, Ruther E, Kornhuber J (2002) Highly conserved and disease-specific patterns of carboxyterminally truncated Abeta peptides 1-37/38/39 in addition to 1-40/42 in Alzheimer's disease and in patients with chronic neuroinflammation. *Journal of neurochemistry* **81**: 481-496

- Winkler E, Hobson S, Fukumori A, Dumpelfeld B, Luebbers T, Baumann K, Haass C, Hopf C, Steiner H (2009) Purification, pharmacological modulation, and biochemical characterization of interactors of endogenous human gamma-secretase. *Biochemistry* **48**: 1183-1197
- Winkler E, Kamp F, Scheuring J, Ebke A, Fukumori A, Steiner H (2012) Generation of Alzheimer disease-associated amyloid beta42/43 peptide by gamma-secretase can be inhibited directly by modulation of membrane thickness. *J Biol Chem* **287**: 21326-21334
- Wolfe MS, Xia W, Ostaszewski BL, Diehl TS, Kimberly WT, Selkoe DJ (1999) Two transmembrane aspartates in presenilin-1 required for presenilin endoproteolysis and gamma-secretase activity. *Nature* **398**: 513-517
- Wunderlich P, Glebov K, Kemmerling N, Tien NT, Neumann H, Walter J (2013) Sequential proteolytic processing of the triggering receptor expressed on myeloid cells-2 (TREM2) protein by ectodomain shedding and gamma-secretase-dependent intramembranous cleavage. *J Biol Chem* **288**: 33027-33036
- Xu F, Previti ML, Nieman MT, Davis J, Schmaier AH, Van Nostrand WE (2009) AbetaPP/APLP2 family of Kunitz serine proteinase inhibitors regulate cerebral thrombosis. *The Journal of neuroscience : the official journal of the Society for Neuroscience* **29**: 5666-5670
- Yamaguchi H, Hirai S, Morimatsu M, Shoji M, Ihara Y (1988) A variety of cerebral amyloid deposits in the brains of the Alzheimer-type dementia demonstrated by beta protein immunostaining. *Acta neuropathologica* **76**: 541-549
- Yan R, Bienkowski MJ, Shuck ME, Miao H, Tory MC, Pauley AM, Brashier JR, Stratman NC, Mathews WR, Buhl AE, Carter DB, Tomasselli AG, Parodi LA, Heinrikson RL, Gurney ME (1999) Membrane-anchored aspartyl protease with Alzheimer's disease beta-secretase activity. *Nature* **402**: 533-537
- Yanagawa M, Tsukuba T, Nishioku T, Okamoto Y, Okamoto K, Takii R, Terada Y, Nakayama KI, Kadowaki T, Yamamoto K (2007) Cathepsin E deficiency induces a novel form of lysosomal storage disorder showing the accumulation of lysosomal membrane sialoglycoproteins and the elevation of lysosomal pH in macrophages. *J Biol Chem* **282**: 1851-1862
- Yang Y, Wang M, Lv B, Ma R, Hu J, Dun Y, Sun S, Li G (2014) Sphingosine Kinase-1 Protects Differentiated N2a Cells Against Beta-Amyloid25-35-Induced Neurotoxicity Via the Mitochondrial Pathway. *Neurochemical research*
- Yang Z, Cool BH, Martin GM, Hu Q (2006) A dominant role for FE65 (APBB1) in nuclear signaling. *J Biol Chem* **281**: 4207-4214
- Yonamine I, Bamba T, Nirala NK, Jesmin N, Kosakowska-Cholody T, Nagashima K, Fukusaki E, Acharya JK, Acharya U (2011) Sphingosine kinases and their metabolites modulate endolysosomal trafficking in photoreceptors. *The Journal of cell biology* **192**: 557-567
- Yu G, Nishimura M, Arawaka S, Levitan D, Zhang L, Tandon A, Song YQ, Rogaeva E, Chen F, Kawarai T, Supala A, Levesque L, Yu H, Yang DS, Holmes E, Milman P, Liang Y, Zhang DM, Xu DH, Sato C, Rogaev E, Smith M, Janus C, Zhang Y, Aebersold R, Farrer LS, Sorbi S, Bruni A, Fraser P, St George-Hyslop P (2000) Nicastrin modulates presenilin-mediated notch/glp-1 signal transduction and betaAPP processing. *Nature* **407**: 48-54
- Zha Q, Ruan Y, Hartmann T, Beyreuther K, Zhang D (2004) GM1 ganglioside regulates the proteolysis of amyloid precursor protein. *Molecular psychiatry* **9**: 946-952

- Zhang L, Song L, Terracina G, Liu Y, Pramanik B, Parker E (2001) Biochemical characterization of the gamma-secretase activity that produces beta-amyloid peptides. *Biochemistry* **40**: 5049-5055
- Zhang Y, Li X, Becker KA, Gulbins E (2009) Ceramide-enriched membrane domains--structure and function. *Biochimica et biophysica acta* **1788**: 178-183
- Zhang Y, Yu Q, Lai TB, Yang Y, Li G, Sun SG (2013) Effects of small interfering RNA targeting sphingosine kinase-1 gene on the animal model of Alzheimer's disease. *Journal of Huazhong University of Science and Technology Medical sciences = Hua zhong ke ji da xue xue bao Yi xue Ying De wen ban = Huazhong keji daxue xuebao Yixue Yingdewen ban* **33**: 427-432
- Zheng H, Jiang M, Trumbauer ME, Hopkins R, Sirinathsinghji DJ, Stevens KA, Conner MW, Slunt HH, Sisodia SS, Chen HY, Van der Ploeg LH (1996) Mice deficient for the amyloid precursor protein gene. *Annals of the New York Academy of Sciences* **777**: 421-426
- Zheng H, Koo EH (2006) The amyloid precursor protein: beyond amyloid. *Molecular neurodegeneration* **1**: 5
- Zhou J, Zhu P, Jiang JL, Zhang Q, Wu ZB, Yao XY, Tang H, Lu N, Yang Y, Chen ZN (2005) Involvement of CD147 in overexpression of MMP-2 and MMP-9 and enhancement of invasive potential of PMA-differentiated THP-1. *BMC cell biology* **6**: 25

## 7. Acknowledgment

First of all, I would like to thank Prof. Dr. Jochen Walter for giving me the opportunity to carry out this project under his guidance and supervision. I am grateful for his support, all the valuable discussions and the motivation during this project. It truly broadened my horizon and helped me to think out of the box.

I would like to thank Prof. Dr. Jörg Höhfeld for his acceptance and his willingness to examine my thesis. I also thank Prof. Dr. Peter Dörmann for his valuable time. I would like to thank PD Gerhild van Echten-Deckert not only for her valuable time as a member of my thesis committee, but also for long and deep discussions on the enigmatic role of SIP and other sphingolipids.

I would also like to thank all my co-operation partners Prof. Dr. Tobias Hartmann, Dr. Marcus Grimm and Viola Hauptenthal for measuring secretase activities. In addition I am grateful to Prof. Dr. Markus Gräler who has measured SIP and sphingosine levels in his lab.

Very special thanks go to all current and former members of the lab. Especially Dr. Patrick Wunderlich, who was not only willing to proofread my thesis, but also like a drop-in center when experiments didn't work or when I was at my wit's end. I also thank Dr. Konstantin Glebov for his support with experimental troubles and his help with the analysis. I thank Dr. Sathish Kumar for all the discussions and supports. Furthermore I would like to thank Dr. Irfan Tamboli, who initiated this project and helped me in the beginning. I am very thankful to all members of the lab Sandra, Josi, Nadja, Esteban and Marie, as well as the former members Tien and Angela. For all your help, but also for being more than only colleagues. I enjoy every day in the lab with you. I thank all the members from the neurobiology: Anne, Berndt, Dominik, Hassan, Ina, Laura, Peter, Sabine and Vishwas.

I cannot describe how thankful I am to my parents and my sister. For their support, their help and their faith in me. I would not have achieved this without you!

At the end I want to thank the most important person in my life, Natalie. With whom I share the good and the bad. Words cannot describe how important you are and how thankful I am that we walk the same path! Your faith and love supported and motivated me more than anything!

## 8. Curriculum Vitae

---

### Ilker Karaca

Birthplace : Viersen, Germany  
Family status : unmarried, no children  
Nationality : German

---

### Publications

**Karaca I**, Tamboli IY, Glebov K, Richter J, Fell LH, Grimm MO, Haupenthal VJ, Hartmann T, Graler MH, van Echten-Deckert G, Walter J (2014) Deficiency of Sphingosine-1-phosphate Lyase Impairs Lysosomal Metabolism of the Amyloid Precursor Protein. *J Biol Chem* **289**: 16761-16772

van Echten-Deckert G, Hagen-Euteneuer N, **Karaca I**, Walter J (2014) Sphingosine-1-phosphate: boon and bane for the brain. *Cellular physiology and biochemistry : international journal of experimental cellular physiology, biochemistry, and pharmacology* **34**: 148-157